Forsmark 1 & 2 Boiling Water Reactor Stability Benchmark

Time Series Analysis Methods for Oscillation during BWR Operation

Final Report

G. Verdú (UPV/Dpto. IQMN)
D. Ginestar (UPV/Dpto. IQMN)
J.L. Muñoz-Cobo (UPV/Dpto. IQMN)
J. Navarro (UPV/Dpto. IQMN)
Mª.J. Palomo (UPV/Dpto. IQMN)
P. Lansaker (Vattenfall-AB)
J.M. Conde, M. Recio (CSN)
E. Sartori (OECD/NEA)

June 2001

NUCLEAR ENERGY AGENCY
ORGANISATION FOR ECONOMIC CO-OPERATION AND DEVELOPMENT

ORGANISATION FOR ECONOMIC CO-OPERATION AND DEVELOPMENT

Pursuant to Article 1 of the Convention signed in Paris on 14th December 1960, and which came into force on 30th September 1961, the Organisation for Economic Co-operation and Development (OECD) shall promote policies designed:

- to achieve the highest sustainable economic growth and employment and a rising standard of living in Member countries, while maintaining financial stability, and thus to contribute to the development of the world economy;
- to contribute to sound economic expansion in Member as well as non-member countries in the process of economic development; and
- to contribute to the expansion of world trade on a multilateral, non-discriminatory basis in accordance with international obligations.

The original Member countries of the OECD are Austria, Belgium, Canada, Denmark, France, Germany, Greece, Iceland, Ireland, Italy, Luxembourg, the Netherlands, Norway, Portugal, Spain, Sweden, Switzerland, Turkey, the United Kingdom and the United States. The following countries became Members subsequently through accession at the dates indicated hereafter: Japan (28th April 1964), Finland (28th January 1969), Australia (7th June 1971), New Zealand (29th May 1973), Mexico (18th May 1994), the Czech Republic (21st December 1995), Hungary (7th May 1996), Poland (22nd November 1996), Korea (12th December 1996) and the Slovak Republic (14 December 2000). The Commission of the European Communities takes part in the work of the OECD (Article 13 of the OECD Convention).

NUCLEAR ENERGY AGENCY

The OECD Nuclear Energy Agency (NEA) was established on 1st February 1958 under the name of the OEEC European Nuclear Energy Agency. It received its present designation on 20th April 1972, when Japan became its first non-European full Member. NEA membership today consists of 27 OECD Member countries: Australia, Austria, Belgium, Canada, Czech Republic, Denmark, Finland, France, Germany, Greece, Hungary, Iceland, Ireland, Italy, Japan, Luxembourg, Mexico, the Netherlands, Norway, Portugal, Republic of Korea, Spain, Sweden, Switzerland, Turkey, the United Kingdom and the United States. The Commission of the European Communities also takes part in the work of the Agency.

The mission of the NEA is:

- to assist its Member countries in maintaining and further developing, through international co-operation, the scientific, technological and legal bases required for a safe, environmentally friendly and economical use of nuclear energy for peaceful purposes, as well as
- to provide authoritative assessments and to forge common understandings on key issues, as input to government decisions on nuclear energy policy and to broader OECD policy analyses in areas such as energy and sustainable development.

Specific areas of competence of the NEA include safety and regulation of nuclear activities, radioactive waste management, radiological protection, nuclear science, economic and technical analyses of the nuclear fuel cycle, nuclear law and liability, and public information. The NEA Data Bank provides nuclear data and computer program services for participating countries.

In these and related tasks, the NEA works in close collaboration with the International Atomic Energy Agency in Vienna, with which it has a Co-operation Agreement, as well as with other international organisations in the nuclear field.

FOREWORD

This is the second in a series of benchmarks based on data from operating, Swedish boiling water reactors (BWRs). The first benchmark concerned measurements made in Cycles 14, 15, 16 and 17 at Ringhals 1 and addressed the validation of the predictive capability of the codes and models for stability analysis in BWRs. Part of the data was disclosed only after participants had provided their results. This work was co-ordinated by Tomas Lefvert from Vattenfall AB with the help of the team at Ringhals 1. The results were published in the report NEA/NSC/DOC(96)22 (November 1996).

It was emphasised during the benchmark meeting of May 1995 that there was much more to be said about the evaluation of time series data. Several different approaches were possible and used in the past, but the results obtained with these approaches were at times very different.

A recommendation of the Ringhals 1 benchmark was to study the different time series analysis methods in order to obtain a unified methodology to detect and suppress the oscillations during reactor operation, as well as better qualification of the applied noise analysis methods. A follow-up benchmark was thus proposed, dedicated to the analysis of time series data and including the evaluation of both global and regional stability.

Tomas Lefvert, with the help of Paer Lansaker, Forsmarks Kraftgrupp AB, identified six interesting cases for the purpose of this study, all measured at Forsmark 1 and 2. The proposal was presented to the NEA Nuclear Science Committee, which approved it.

José Manuel Conde and Manuel Recio from the Consejo de Seguridad Nuclear, Madrid, agreed to obtain the necessary support to arrange the co-ordination of this benchmark through the team of Professor Gumersindo Verdú of the Polytechnical University of Valencia.

Practically all countries operating boiling water reactors participated in this study. The different solutions submitted were discussed during a workshop hosted by the Consejo de Seguridad Nuclear, Madrid, Spain on 18-19 February 1999. Results of the study were also presented and discussed at different international conferences, in particular at M&C'99 Madrid, held on 27-30 September 2000.

Acknowledgements

The authors would first like to thank the personnel at the Forsmark 1 & 2 nuclear power plants for preparing the data and for their collaboration with the benchmark.

Also, without the effort and generous contribution of the participants this study would not have been possible. We wish to thank them here for their time and enthusiasm, and above all for their willingness to share their know-how and competence.

TABLE OF CONTENTS

Foreword 3

Executive Summary 7

Contributors to the Benchmark Study 9

Chapter 1 INTRODUCTION 11

Chapter 2 TEST PROBLEMS CONSIDERED 13

Case 1 13

Case 2 14

Case 3 14

Case 4 15

Case 5 16

Case 6 16

Chapter 3 METHODS FOR THE ESTIMATION OF THE DECAY RATIO AND THE FUNDAMENTAL FREQUENCY USED BY THE PARTICIPANTS 19

Chapter 4 RESULTS 21

Chapter 5 SUMMARY AND CONCLUSIONS 31

Annex 1 – List of participants 33

Annex 2 – Methodologies and results presented by UPV-CSN 37

Annex 3 – Methodologies and results presented by PSU 57

Annex 4 – Methodologies and results presented by TSUKUBA 67

Annex 5 – Methodologies and results presented by PSI 73

Annex 6 – Methodologies and results presented by JAERI 81

Annex 7 – Methodologies and results presented by SIEMENS 93

Annex 8 – Methodologies and results presented by TOSHIBA 101

Annex 9 – Methodologies and results presented by TU DELFT 139

Annex 10 – Methodologies and results presented by CSNNS 143

EXECUTIVE SUMMARY

The purpose of this benchmark is the intercomparison of different time series analysis methods applied to the study of BWR stability. It is focused on the analysis of time series data by means of noise analysis techniques, in the time domain.

The primary goal was to elucidate if it is possible to determine the main stability parameters from the neutronic signals time series with sufficient reliability and accuracy. Typically, the main stability parameters are assumed to be the decay ratio (DR) and the frequency of the oscillation. However, there are other parameters that provide interesting information. Two kinds of power oscillations have been observed in BWRs: in-phase (core-wide) oscillations, where all the core oscillations are in phase, and out-of-phase, where half of the core oscillates out of phase with the other part. The oscillations are studied using LPRM and APRM signals. Thus, the oscillation detection algorithms are important to detect the instabilities from the neutronic power signal.

The benchmark is based on data from several measurements performed in the Swedish BWR reactors Forsmark 1 and 2, in the period 1989 to 1997. This data is divided into six cases, and the sampling rate of all the time series is 25 Hz, decimated to 12.5 Hz.

These cases cover or address:

1. Neutron flux signals measured during several tests ranging from stable to quasi-unstable conditions, i.e. standard measurements with no distortions.

2. Study of the importance of the time duration of measured data, i.e. the variability of the decay ratio and oscillation frequency with the measurement time duration.

3. APRM data containing more than one natural frequency of the core, also containing peaks of other frequencies due to the actuation of the pressure controller, a case with two frequencies close to each other and measurements contaminated with influences from the plant control systems.

4. Data with a mixture between a global oscillation mode and a regional (half core) oscillation for addressing the interrelations between APRM and LPRM signals.

5. Analysis of two APRM signals obtained during a small plant transient that resulted in a bad behaviour of the signals; analysis of the first dominant poles of the transfer function obtained from the time series. It is a non-stationary case for which the auto-regressive methods have a limited validity.

6. Test with local (channel) oscillations with data containing APRM and LPRM signals from two tests that were performed close to each other, both in time and in the operating conditions, one of which with local oscillations.

In all, fifteen solutions were submitted by participants from eight countries representing ten organisations. The following methods were used for the analysis:

- Auto-regressive methods and dominant poles.
- Auto-regressive methods and impulse response.
- Auto-correlation.
- Recursive auto-correlation.
- ARMA (plateau method).
- Power spectrum estimation.

The following conclusions were reached:

- For noise analysis the decay ratio is associated with the least stable or dominant pole. The definition is clear for a second order system.
- For determination of decay ratios the asymptotic part of the transformation function should be used.
- The decay ratio can be determined automatically, without filtering, if expert tuning to the plant is carried out.
- The time duration required for determining the decay ratio is about inversely proportional to the value of the decay ratio.
- The decay ratio of out-of-phase oscillations can be determined for values up to 0.7 ± 0.1 and if enough LPRM signals per plane are provided. This requires the expertise of the analyst, or the sophistication of the monitoring algorithm.
- A sufficiently accurate limit to the stable behaviour of the reactor core can be determined using codes in the frequency domain. They are efficient but not sufficient. The real margin should be determined on power. The “decay ratio” is a measure of linear stability and should therefore not be used as the only indicator of BWR stability.

It was verified that the different methods consistently provide the same answer to a good degree. The applicability and reliability of the different methods were investigated. The six cases chosen are relatively difficult and are really addressing the limits of the methods. The use of a fuller set of data could be the subject of a different study involving reactor physics.

CONTRIBUTORS TO THE BENCHMARK STUDY

Original proposal made by:	Tomas Lefvert, Vattenfall AB, Sweden
Preparation and release of data:	Pär Lansaker, Vattenfall AB, Sweden
Specification prepared by:	Gumersindo Verdú, Polytechnic University of Valencia, Spain Maria.José Palomo, Polytechnic University of Valencia, Spain A. Escrivá, Polytechnic University of Valencia, Spain Damian Ginestar, Polytechnic University of Valencia, Spain
Benchmark co-ordinators and sponsors:	Gumersindo Verdú, Polytechnic University of Valencia, Spain José Manuel Conde, CSN, Spain Manuel Recio, CSN, Spain
Participants in the benchmark:	Soma Mojumder, Siemens/KWU, Germany Hidetoshi Konno, University of Tohoku, Japan Graciela Beatriz Roston, University of Tohoku, Japan Tomoaki Suzudo, JAERI, Japan Yutaka Takeuchi TOSHIBA, Japan Alejandro Nuñez-Carrera, CNSNSMEX, Mexico Willy J.M. de Kruijf, IRI, The Netherlands Damian Ginestar, Polytechnic University of Valencia, Spain J.L. Muñoz-Cobo, Polytechnic University of Valencia, Spain Joaquin Navarro, Polytechnic University of Valencia, Spain Maria José Palomo Polytechnic University of Valencia, Spain Gumersindo Verdú, Polytechnic University of Valencia, Spain Dieter Hennig, PSI, Switzerland Miguel Ceceñas-Falcon PSU, USA Yousef M. Farawila, Siemens Power Corporation, USA
Secretariat:	Enrico Sartori, OECD/NEA, France
Editing of final report:	Amanda Costa, OECD/NEA, France

Chapter 1
INTRODUCTION

Events involving unnoticed power oscillations have occurred at different BWR reactors in the past, and have led to the implementation of interim corrective actions to avoid repetition. Despite these corrections, however, power oscillations continued to occur. In response to that situation, a great deal of research and analytical activities have been carried out to improve the knowledge of the underlying phenomenology, and to define final solutions to handle this type of event. Two kinds of power oscillations have been observed in BWRs (sometimes overlapping), the in-phase (core wide) oscillation, where all the fuel bundles in the core oscillate in phase, and the out-of-phase or regional mode, where one-half of the core oscillates out of phase with respect to the other ha1f. According to the General Design Criteria (GDC12) the BWR operator may either prove that oscillations will not occur, or that if they do, they can be detected and suppressed in a safe manner. Detection and suppression systems rely on the recognition of oscillations by monitoring the LPRM signals. Thus, the oscillation detection algorithms are important to assure the early detection of instabilities. For the experimental study of the BWR oscillations, several stability tests have been performed at the Caorso, LaSalle, Forsmark 1 and 2, Oskarshamn 3 and Ringhals 1 plants.

The Forsmark 1 & 2 BWR Stability Benchmark is the second in a series of benchmarks based on data from Swedish BWRs. The first benchmark was based in measurements made in Cycles 14, 15, 16 and 17 at Ringhals 1 and addressed the predictive power of the analytical tools used in BWR stability analysis. Part of the data was disclosed only after participants had provided their results. This work was co-ordinated by Tomas Lefvert of Vattenfall AB with the help of the team at Ringhals 1. The results were published in the report NEA/NSC/DOC96(22), November 1996. It was recognised in this report that there is a need for a better qualification of the noise analysis methods applied in BWR stability studies. A follow-up benchmark was thus proposed dedicated to the analysis of time series data and including the evaluation of both global and regional stability. With the help of Par Lansaker (Forsmark Kraftgrupp AB), Tomas Lefvert identified six interesting cases for this purpose, measured at Forsmark 1 & 2. He presented a proposal to the NEA Nuclear Science Committee, who accorded its approval. José Manuel Conde and Manuel Recio from the Consejo de Seguridad Nuclear, Madrid, agreed to find the necessary support to arrange the co-ordination of this benchmark through the team of Dr. Gumersindo Verdú of the Polytechnic University of Valencia.

The purpose of this benchmark is the comparison among the different time series analysis methods that can be applied to the study of BWR stability. While the Ringhals 1 stability benchmark included both time domain and frequency domain calculation models to predict stability parameters, the new activity has been focused on the analysis of time series data by means of noise analysis techniques in the time domain.

The first goal is to elucidate if it is possible to determine the main stability parameters from the neutronic signals time series with sufficient reliability and accuracy. Typically, the main stability parameters are assumed to be the decay ratio (DR) and the frequency of the oscillation. However,

there are other parameters that provide valuab1e information, such us the Lyapunov exponents associated to the time series, or the Haussdorff dimension. In fact, the Lyapunov exponents are also a measure of the stability of the neutronic time series.

For the purpose of analysing the effects of all these parameters, the participants in this benchmark have been asked to provide a short description of the methodology used for the analysis of the time series, as well as information on the codes used with enough detail to identify the sources of discrepancies. The participants' descriptions of their experience with the analysis of the benchmark data and other information provided has been very interesting and has helped the global analysis of the results, thus facilitating the drawing of conclusions.

Chapter 2
TEST PROBLEMS CONSIDERED

Two kinds of power oscillations have been observed in BWRs: in-phase (core-wide) oscillations, where all the core oscillations are in-phase, and out-of-phase, where one-half of the core oscillates out of phase of the other part. The oscillations are studied using LPRM and APRM signals. Thus, the oscillation detection algorithms are important to detect and classify the instabilities of the neutronic power signal.

The database is divided into six cases, the sampling rate of all the time series being 25 Hz, decimated to 12.5 Hz. No filter was applied to the signals and the DC component has not been subtracted.

Case 1

This case contains the neutron flux signals measured during several tests. The objective of the case is to study several signals ranging from stable to quasi-unstable reactor conditions. The signals are standard measurements with no distortions, and were considered fairly easy to evaluate. The data provided contains measured average power range monitor (APRM) signals from stability tests.

The results for this case are the DRs and oscillation frequencies associated with the APRM signals taken during 14 different tests. The APRM signals are shown in Table 1.

Table 1. APRM signals for Case 1

N°	Name*	Date	Power %	Core flow [kg/s]
1	f1_boc_13_3	1993-07-28	64.3	4 385
2	f1_boc_13_4	1993-07-28	65.1	4 044
3	f1_boc_14_1	1994-09-02	59.9	4 383
4	f1_boc_14_3	1994-09-02	64.8	4 313
5	f1_boc_14_4	1994-09-02	64.7	4 014
6	f1_moc_14_4	1994-11-19	64.3	4 092
7	f1_boc_15	1995-08-16	64.1	4 027
8	f1_moc_16	1997-01-31	64.4	4 416
9	f1_moc_13	1995-02-05	64.3	3 940
10	f2_uppst_14	1995-07-28	65.1	4 028
11	f2_boc_14	1995-09-25	65.0	4 026
12	f2_moc_14	1995-12-18	63.3	3 850
13	f2_uppst_15	1996-09-01	64.0	3 791
14	f2_moc_15	1997-02-15	67.3	4 234

** f1 – Forsmarks 1, f2 – Forsmarks 2*

Each time series has about 4 000 points, the range of DR being from 0.4-0.8. The objective of this case is the comparison among the different methods applied to obtain the stability parameters.

Input

The files provided have the following structure in ASCII format: *c1_aprm.i (i=1,14)*, corresponding to the information shown in Table 1.

Output

The participants will provide the following results:

Case Nº	Name of the time series	DR	DR uncertainty	Frequency	Frequency uncertainty

Case 2

This case addresses the importance of the time duration of measured data.

The objective of this case is to study the variability of the DR and the oscillation frequency with the measurement time duration. There are two long time series to analyse, l1 and l2. Each one has about 14 000 points, and will be divided into blocks of approximately 4 000 and 2 000 points. The results for the short time series have to be compared with the original long series results.

Input

The files provided have the following structure in ASCII format:

c2_test.Li, c2_test.Sli, c2_test.S2i, c2_test.S3i, c2_test.S4i (i=1,2)

where *L* is long; *S1, S2, S3* and *S4* are the subseries of the original series, and *i* is the number of the time series.

Output

The participants will provide the following results:

Case Nº	Name of the time series	DR	DR uncertainty	Frequency	Frequency uncertainty

Case 3

APRM data for this case contain more than one natural frequency of the core. The data also contain peaks of other frequencies due to the actuation of the pressure controller. One case has two frequencies close to each other. Cases with more than one natural frequency make the analysis much more difficult.

This case contains five measurements contaminated with influences from the plant control systems. In this case, the time series have a bad behaviour, and consequently the standard stability parameters are not clear.

Input

The files provided have the following structure in ASCII format:

c3_test.1, c3_test.2, c3_test.3, c3_test.4, c3_test.5

Output

The participants will provide the following results:

Case Nº	Name of the time series	DR	DR uncertainty	Frequency	Frequency uncertainty	Real and imaginary parts of the first four dominant poles

Case 4

This case contains a mixture between a global oscillation mode and a regional (half core) oscillation. The case consists of APRM and LPRM (local PRM) signals coming from one test.

The case consists of APRM and LPRM (local PRM) signals coming from one test. The LPRM positions in the core are the following ones:

The time series have a good behaviour. In this case, it is interesting to study the interrelations between APRM and LPRM signals.

Input

The files provided have the following structure in ASCII format:

c4_aprm, c4_lprm.i,(i=1,22)

Output

The participants will provide the following results:

Case Nº	Name of the time series	DR	DR uncertainty	Frequency	Frequency uncertainty

Furthermore, it remains at the discretion of the participants to analyse the interaction between the signals, for example, the coherence and the phase delay among them.

Case 5

This case is focused on the analysis of two APRM signals obtained during a small plant transient that resulted in a bad behaviour of the signals. In this case, it is important to analyse the first dominant poles of the transfer function obtained from the time series. Note that this is a non-stationary case and the auto-regressive methods have a limited validity.

Input

The files provided have the following structure in ASCII format:

c5_aprm.1, c5_aprm.2

Output

The participants will provide the following results:

Case Nº	Name of the time series	DR	DR uncertainty	Frequency	Frequency uncertainty	Real and imaginary parts of the first four dominant poles

Case 6

This test shows local (channel) oscillations. The data contain APRM and LPRM signals from two tests that were performed close to each other, both in time and in operating conditions.

Test Nº	Power	Core flow
1	64.4%	4 416 kg/s
2	63.3%	4 298 kg/s

The LPRM positions in the core for Case 6 are as displayed in the following figures.

CASE 6-1

Number	*Position*	*Level*
1	23	1
2	23	4
3	26	1
4	26	4
5	11	1
6	11	4
7	6	1
8	6	4
9	34	1
10	34	4
11	20	1
12	20	4
13	31	1
14	31	2
15	24	3
16	24	4
17	29	1
18	29	2

LEVEL 1

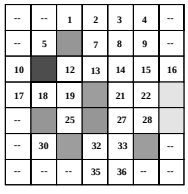

LEVEL 4

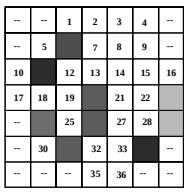

CASE 6-2

Number	*Position*	*Level*
1	23	1
2	23	4
3	26	1
4	26	4
5	11	1
6	11	4
7	6	1
8	6	4
9	34	1
10	34	4
11	20	1
12	20	4
13	31	1
14	31	2
15	24	3
16	24	4
17	29	1
18	29	2

LEVEL 1

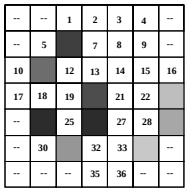

LEVEL 4

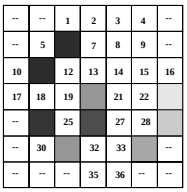

The data contain APRM and LPRM signals from two tests that were performed close to each other, both in time and in the operating conditions.

Test 1 (Case 6.1) is the same as Case 1.8, and the measurement is taken from Forsmark 1. The second test (Case 6.2) clearly shows local oscillations.

Input

The files provided have the following structure in ASCII format:

c6_aprm.i, c6_lprm..i,(i=1,2;j1,18)

Output

The participants will provide the following results:

Case Nº	Name of the time series	DR	DR uncertainty	Frequency	Frequency uncertainty

Additional results such as coherence and phase delay will contribute to increase the understanding of the mechanism of in-phase and out-of-phase oscillations.

Chapter 3

METHODS FOR THE ESTIMATION OF THE DECAY RATIO AND THE FUNDAMENTAL FREQUENCY USED BY THE PARTICIPANTS

The methods used to obtain the provided results of the different participants are shown in Table 2.

Table 2. Methods used in the solutions provided

Method	Organisation	Country
Auto-regressive methods and dominant poles	PSI UPV/CSN SIEMENS	Switzerland Spain Germany/USA
Auto-regressive methods and impulse response	TOSHIBA JAERI IRI/TU-Delft PSU	Japan Japan The Netherlands USA
Auto-correlation	TOSHIBA	Japan
Recursive auto-correlation	SIEMENS	Germany/USA
ARMA (plateau method)	PSI	Switzerland
Power spectrum estimation	CSNNS	Mexico
LAPUR (frequency domain)	PSU	USA

Chapter 4
RESULTS

Case 1

The results provided for the DR and the fundamental frequency for this case are shown in Tables 2 and 3. Taking the mean values as a reference, the following conclusions can be obtained:

- The UPV-CSN-AR methodology is dependent on the model order. AR methodologies based on an average among different orders or the plateau methodology are more stable.
- The UPV-Dynamics reconstruction method generally overestimates the DR.
- For the methods based on a fit for the impulse response it was found that JAERI's group method has a stable behaviour and the method used by TU DELFT gives deviating DRs for some of the cases.
- The PSU group and the Tsukuba University group use AR methods that generally underestimate the DR.
- The Reduced-order Method, based on the LAPUR code, provides results different from the other contributors. This could be due to the lack of an accurate input model for the Forsmark reactor.

As the main conclusion for this case we determine that Case 1 corresponds to a stable configuration of the reactor. The results for the fundamental frequency are quite uniform, and there is some dispersion for the DR values. These values range from 0.4-0.8 and they have a standard deviation of about 0.15.

Table 3. Results for the DR – Case 1

	M1	M2	M3	M4	M5	M6	M7	M8	M9	M10	M11	M12	M13	M14	M15	Mean	SD
aprm.1	0.460	0.423	0.576	0.640	0.42	0.580	0.330	0.500	0.420	0.422	0.460	0.420	0.512	0.57	0.566	0.487	0.09
aprm.2	0.656	0.654	0.702	0.824	0.52	0.500	0.420	0.510	0.510	0.523	0.613	0.650	0.577	0.46	0.454	0.572	0.11
aprm.3	0.576	0.582	0.558	0.735	0.30	0.250	0.300	0.500	0.630	0.511	0.537	0.520	0.499	0.60	0.516	0.508	0.13
aprm.4	0.515	0.514	0.525	0.634	0.39	0.260	0.230	0.530	0.420	0.549	0.528	0.510	0.558	0.78	0.516	0.497	0.14
aprm.5	0.581	0.573	0.523	0.702	0.49	0.700	0.200	0.510	0.510	0.534	0.517	0.470	0.532	0.36	0.523	0.515	0.12
aprm.6	0.540	0.549	0.521	0.659	0.44	0.100	0.420	0.550	0.510	0.559	0.526	0.550	0.587	0.53	0.764	0.520	0.14
aprm.7	0.695	0.700	0.694	0.624	0.51	0.370	0.150	0.590	0.680	0.657	0.669	0.660	0.630	0.66	0.572	0.591	0.15
aprm.8	0.533	0.542	0.503	0.577	0.27	0.220	0.370	0.450	0.460	0.495	0.483	0.440	0.445	0.57	0.519	0.458	0.10
aprm.9	0.573	0.547	0.458	0.503	0.55	0.340	0.430	0.500	0.530	0.487	0.530	0.470	0.561	0.50	0.642	0.508	0.07
aprm.10	0.611	0.635	0.631	0.545	0.45	0.520	0.300	0.450	0.490	0.482	0.585	0.470	0.537	0.32	0.764	0.519	0.12
aprm.11	0.599	0.601	0.598	0.644	0.36	0.230	0.180	0.500	0.560	0.440	0.551	0.390	0.469	0.29	0.772	0.479	0.17
aprm.12	0.812	0.809	0.828	0.751	0.68	0.430	0.560	0.780	0.780	0.757	0.792	0.780	0.740	0.66	0.559	0.715	0.12
aprm.13	0.535	0.562	0.556	0.777	0.43	0.260	0.370	0.450	0.460	0.383	0.532	0.590	0.610	0.51	0.445	0.498	0.12
aprm.14	0.722	0.715	0.704	0.782	0.56	0.270	0.380	0.650	0.710	0.658	0.698	0.660	0.662	0.71	0.130	0.600	0.19

Table 4. Results for the fundamental frequency – Case 1

	M1	M2	M3	M4	M5	M6	M7	M8	M9	M10	M11	M12	M13	M14	M15	Mean	SD
aprm.1	0.483	0.452	0.487	0.467	0.45	0.350	0.450	0.460	0.460	0.464	0.459	0.459	0.448	0.47	0.458	0.455	0.03
aprm.2	0.473	0.476	0.470	0.464	0.45	0.330	0.450	0.460	0.460	0.458	0.470	0.470	0.456	0.48	0.459	0.455	0.04
aprm.3	0.483	0.482	0.481	0.480	0.46	0.270	0.450	0.480	0.490	0.497	0.483	0.483	0.482	0.51	0.476	0.467	0.06
aprm.4	0.489	0.490	0.487	0.481	0.48	0.280	0.470	0.490	0.460	0.480	0.490	0.490	0.518	0.51	0.490	0.474	0.06
aprm.5	0.509	0.509	0.507	0.492	0.47	0.370	0.480	0.490	0.490	0.479	0.501	0.501	0.496	0.51	0.494	0.487	0.03
aprm.6	0.484	0.483	0.471	0.487	0.51	0.320	0.470	0.490	0.490	0.477	0.477	0.477	0.477	0.48	0.486	0.472	0.04
aprm.7	0.535	0.535	0.535	0.510	0.50	0.290	0.510	0.520	0.530	0.524	0.530	0.530	0.517	0.55	0.521	0.509	0.06
aprm.8	0.525	0.527	0.531	0.506	0.40	0.270	0.500	0.520	0.530	0.537	0.526	0.526	0.518	0.53	0.479	0.495	0.07
aprm.9	0.430	0.429	0.385	0.409	0.43	0.290	0.490	0.400	0.400	0.403	0.422	0.422	0.401	0.41	0.402	0.408	0.04
aprm.10	0.460	0.460	0.462	0.424	0.43	0.330	0.440	0.440	0.440	0.455	0.454	0.454	0.433	0.45	0.424	0.437	0.03
aprm.11	0.473	0.472	0.476	0.454	0.43	0.270	0.470	0.460	0.460	0.484	0.472	0.472	0.443	0.47	0.424	0.449	0.05
aprm.12	0.466	0.466	0.467	0.400	0.45	0.300	0.450	0.460	0.460	0.467	0.465	0.465	0.459	0.47	0.452	0.446	0.04
aprm.13	0.405	0.405	0.404	0.478	0.40	0.270	0.400	0.400	0.400	0.416	0.403	0.403	0.401	0.42	0.408	0.401	0.04
aprm.14	0.489	0.490	0.487	0.489	0.48	0.280	0.480	0.480	0.490	0.492	0.493	0.493	0.496	0.49	0.469	0.473	0.05

Case 2

The results provided for this case are shown in Tables 5 and 6. From these results the following conclusions can be drawn:

- For Signals L1 and L2 the fundamental frequency values are approximately constant for the different segments.
- For Signal L1 the DR values depend on the segment of the signal analysed. The first part of the signal (S1) corresponds to a more stable configuration than the other segments (S2, S3, S4).
- For Signal L2 the DR values remain approximately constant along all the segments.
- Signal L1 presents a slow transient and the results provided for this signal have larger dispersion than the ones provided for Signal L2, which is practically stationary.
- It is clear that at least for Signal L1 the DR is time dependent.
- Also, we observe some dispersion for the DR values and a slight dispersion for the fundamental frequency values.

Table 5. Results for the DR – Case 2

	M1	M2	M3	M4	M5	M7	M8	M9	M10	M11	M12	M13	M14	M15	Mean	SD
test.l1	0.395	0.394	0.469	0.432	0.350	0.160	0.350	0.550	0.339	0.360	0.270	0.386	0.23	0.393	0.363	0.10
test.s11	0.287	0.268	0.312	0.355	0.360	0.100	0.200	0.200	0.113	0.168	0.150	0.416	0.34	0.580	0.275	0.13
test.s21	0.431	0.460	0.457	0.649	0.490	0.210	0.450	0.410	0.476	0.479	0.400	0.525	0.40	0.444	0.449	0.09
test.s31	0.338	0.384	0.475	0.646	0.360	0.190	0.400	0.470	0.323	0.359	0.270	0.416	0.27	0.243	0.367	0.12
test.s41	0.457	0.467	0.469	0.368	0.370	0.180	0.400	0.390	0.263	0.416	0.390	0.406	0.14	0.311	0.359	0.10
test.l2	0.640	0.640	0.634	0.620	0.570	0.340	0.630	0.600	0.622	0.576	0.570	0.576	0.54	0.534	0.578	0.08
test.s12	0.680	0.688	0.654	0.617	0.610	0.320	0.600	0.640	0.625	0.523	0.640	0.523	0.52	0.493	0.581	0.10
test.s22	0.675	0.676	0.690	0.656	0.590	0.330	0.600	0.550	0.656	0.601	0.620	0.601	0.56	0.594	0.600	0.09
test.s32	0.599	0.598	0.597	0.641	0.540	0.220	0.530	0.450	0.539	0.523	0.520	0.523	0.44	0.502	0.516	0.10
test.s42	0.577	0.542	0.516	0.564	0.420	0.330	0.580	0.420	0.500	0.537	0.510	0.537	0.49	0.506	0.502	0.07

Table 6. Results for the fundamental frequency – Case 2

	M1	M2	M3	M4	M5	M7	M8	M9	M10	M11	M12	M13	M14	M15	Mean	SD
test.l1	0.454	0.453	0.453	0.472	0.440	0.430	0.450	0.460	0.457	0.444	0.444	0.441	0.45	0.442	0.449	0.010
test.s11	0.442	0.440	0.435	0.471	0.410	0.490	0.440	0.420	0.361	0.424	0.424	0.478	0.45	0.444	0.438	0.03
test.s21	0.467	0.468	0.438	0.439	0.410	0.430	0.460	0.430	0.451	0.449	0.449	0.510	0.45	0.448	0.450	0.02
test.s31	0.443	0.440	0.437	0.427	0.430	0.410	0.460	0.480	0.482	0.453	0.453	0.478	0.45	0.441	0.449	0.02
test.s41	0.443	0.461	0.419	0.409	0.430	0.380	0.460	0.410	0.442	0.433	0.433	0.430	0.45	0.428	0.431	0.02
test.l2	0.533	0.533	0.519	0.534	0.500	0.520	0.530	0.510	0.537	0.516	0.516	0.516	0.54	0.516	0.523	0.012
test.s12	0.539	0.539	0.537	0.529	0.520	0.530	0.540	0.530	0.529	0.510	0.510	0.510	0.54	0.520	0.527	0.012
test.s22	0.529	0.533	0.534	0.530	0.490	0.510	0.520	0.510	0.524	0.517	0.517	0.517	0.54	0.516	0.520	0.013
test.s32	0.532	0.532	0.532	0.523	0.510	0.520	0.530	0.510	0.512	0.510	0.510	0.510	0.55	0.516	0.521	0.012
test.s42	0.507	0.505	0.515	0.527	0.480	0.480	0.510	0.500	0.502	0.515	0.515	0.515	0.50	0.509	0.506	0.013

Case 3

The results provided for this case are shown in Tables 7 and 8. From these results the following conclusions can be obtained:

- For this case the UPV-CSN group has found some problems to determine the fundamental harmonic of the oscillation.
- The other contributors give homogenous results for the frequency of the neutronic signals.
- The typical dispersion for the values of the DR appear. For example, the values provided for the DR in Test 3 range from 0.1-0.6.
- The signal conditions can play an important role to resolve the stability information. Further discussions about the signal conditioning can be found in Annex 2.

Table 7. Results for the DR – Case 3

	M1			M2			M3		
test.1	0.382	0.291	0.488	0.376	0.273	0.506	0.370	0.310	0.514
test.2	0.236	0.372-0.441	0.442-0.584	0.249	0.316-0.422	0.446-0.581	0.453	0.318	0.453
test.3	0.414	0.587	0.320-0.613	0.424	0.592	0.619	0.388	0.363	0.489
test.4	0.514	0.614	0.707	0.528	0.629	0.720	0.516	0.580	0.748

	M4	M5	M7	M8	M10	M11	M12	M13	M14	M15
test.1	0.552	0.27	0.17	0.400	0.287	0.409	0.360	0.435	0.30	0.600
test.2	0.621	0.29	0.21	0.310	0.345	0.330	0.370	0.495	0.39	0.882
test.3	0.516	0.23	0.10	0.400	0.177	0.395	0.330	0.373	0.20	0.632
test.4	0.676	0.34	0.24	0.420	0.744	0.517	0.550	0.520	0.36	0.551

Table 8. Results for the fundamental frequency – Case 3

	M1			M2			M3		
test.1	0.397	0.344	0.439	0.400	0.342	0.440	0.385	0.331	0.434
test.2	0.406	0.331-0.475	0.307-0.447	0.416	0.334-0.471	0.307-0.447	0.430	0.360	0.313
test.3	0.461	0.477	0.301-0.470	0.461	0.476	0.470	0.474	0.304	0.467
test.4	0.481	0.483	0.475	0.480	0.483	0.474	0.484	0.485	0.478

	M4	M5	M7	M8	M10	M11	M12	M13	M14	M15
test.1	0.420	0.391	0.380	0.420	0.417	0.408	0.408	0.392	0.45	0.404
test.2	0.431	0.391	0.330	0.430	0.422	0.411	0.411	0.397	0.40	0.312
test.3	0.465	0.422	0.450	0.460	0.434	0.455	0.455	0.450	0.46	0.263
test.4	0.437	0.467	0.470	0.480	0.489	0.480	0.480	0.473	0.48	0.260

Case 4

The results for this case are shown in Tables 9 and 10. From these tables the following conclusions are obtained:

- There is not a large dispersion for the values of the DR in this case because the configuration of the reactor is more unstable, that is the DR is high (≅ 0.8).

- There is a half of the reactor (locations 23 and 9) where the DR is high and the other half (locations 31 and 11) where the DR is lower. The upper part of the reactor seems to be more stable than the lower part.

- Spectral analysis of the signals indicates that there is a phase shift between the LPRM at radial locations 23 and 11, and locations 23 and 31, but the out-of-phase oscillation is not totally developed.

- To establish a more accurate regional analysis more information is needed, e.g. more LPRM signals, the operating conditions for this case and the nuclear cross-sections. Nevertheless, for this case the SIEMENS group provides regional decay ratio calculations obtained from diagonal LPRMs. These results can be found in Annex 7.

Table 9. Results for the DR – Case 4

	M1	M2	M3	M4	M5	M6	M7	M8	M9	M10	M11	M12	M13	M14	M15
aprm	0.797	0.788	0.699	0.806	0.813	0.900	0.850	0.850	0.850	0.768	0.763	0.710	0.450	0.78	0.459
lprm.1	0.877	0.877	0.874	0.889	0.906	0.900	0.890	0.900	0.900	0.834	0.876	0.830	0.918		0.527
lprm.2	0.899	0.901	0.901	0.918	0.907	0.900	0.900	0.900	0.900	0.829	0.898	0.860	0.919		0.567
lprm.3	0.910	0.910	0.910	0.914	0.916	0.910	0.900	0.900	0.950	0.845	0.901	0.880	0.917		0.514
lprm.4	0.901	0.901	0.898	0.854	0.868	0.910	0.850	0.880	0.880	0.859	0.894	0.900	0.903		0.502
lprm.5	0.814	0.818	0.814	0.830	0.852	0.910	0.820	0.860	0.850	0.774	0.811	0.750	0.860		0.546
lprm.6	0.808	0.800	0.803	0.869	0.852	0.890	0.810	0.850	0.850	0.768	0.803	0.750	0.846		0.464
lprm.7	0.782	0.786	0.786	0.826	0.782	0.860	0.770	0.800	0.760	0.765	0.787	0.740	0.805		0.518
lprm.8	0.703	0.705	0.694	0.733	0.688	0.740	0.620	0.760	0.710	0.729	0.760	0.700	0.733		0.403
lprm.9	0.744	0.749	0.761	0.848	0.808	0.850	0.780	0.800	0.810	0.703	0.758	0.690	0.792		0.465
lprm.10	0.703	0.707	0.711	0.757	0.712	0.500	0.670	0.750	0.730	0.749	0.751	0.710	0.756		0.565
lprm.11	0.634	0.635	0.650	0.749	0.767	0.880	0.710	0.770	0.760	0.714	0.678	0.670	0.788		0.486
lprm.12	0.709	0.709	0.733	0.787	0.517	0.270	0.450	0.580	0.560	0.677	0.677	0.710	0.654		0.530
lprm.13	0.767	0.771	0.771	0.835	0.821	0.870	0.770	0.810	0.830	0.737	0.787	0.700	0.833		0.422
lprm.14	0.739	0.742	0.740	0.817	0.813	0.880	0.750	0.810	0.800	0.728	0.767	0.700	0.823		0.517
lprm.15	0.646	0.657	0.657	0.691	0.788	0.870	0.760	0.800	0.800	0.790	0.740	0.690	0.783		0.552
lprm.16	0.675	0.668	0.670	0.699	0.801	0.880	0.800	0.800	0.810	0.796	0.690	0.680	0.771		0.547
lprm.17	0.833	0.834	0.836	0.838	0.861	0.900	0.830	0.850	0.860	0.854	0.838	0.810	0.862		0.478
lprm.18	0.819	0.817	0.821	0.877	0.843	0.880	0.820	0.850	0.850	0.845	0.829	0.810	0.857		0.489
lprm.19	0.813	0.814	0.813	0.886	0.628	0.850	0.450	0.800	0.790	0.785	0.812	0.800	0.787		0.495
lprm.20	0.721	0.720	0.701	0.757	0.695	0.840	0.670	0.750	0.740	0.756	0.767	0.700	0.769		0.500
lprm.21	0.666	0.672	0.661	0.771	0.766	0.880	0.670	0.770	0.760	0.770	0.738	0.670	0.791		0.496
lprm.22	0.583	0.569	0.569	0.702	0.360	0.860	0.380	0.390	0.360	0.422	0.517	0.490	0.447		0.582

Table 10. Results for the fundamental frequency – Case 4

	M1	M2	M3	M4	M5	M6	M7	M8	M9	M10	M11	M12	M13	M14	M15
aprm	0.486	0.485	0.492	0.490	0.508	0.480	0.495	0.510	0.480	0.508	0.491	0.491	0.522	0.51	0.512
lprm.1	0.482	0.482	0.481	0.495	0.492	0.480	0.495	0.490	0.490	0.494	0.486	0.486	0.493		0.503
lprm.2	0.482	0.482	0.481	0.491	0.492	0.480	0.495	0.490	0.490	0.495	0.486	0.486	0.491		0.497
lprm.3	0.482	0.481	0.482	0.488	0.489	0.490	0.495	0.490	0.480	0.494	0.485	0.485	0.489		0.494
lprm.4	0.485	0.485	0.485	0.485	0.492	0.490	0.495	0.490	0.490	0.489	0.488	0.488	0.490		0.493
lprm.5	0.486	0.486	0.485	0.515	0.500	0.490	0.495	0.500	0.500	0.498	0.493	0.493	0.500		0.512
lprm.6	0.488	0.491	0.488	0.510	0.500	0.470	0.495	0.500	0.500	0.498	0.495	0.495	0.500		0.512
lprm.7	0.492	0.489	0.492	0.494	0.500	0.450	0.495	0.500	0.500	0.502	0.499	0.499	0.500		0.512
lprm.8	0.509	0.510	0.507	0.478	0.508	0.400	0.495	0.500	0.510	0.504	0.507	0.507	0.507		0.514
lprm.9	0.492	0.492	0.490	0.491	0.508	0.450	0.495	0.510	0.500	0.504	0.499	0.499	0.506		0.520
lprm.10	0.527	0.526	0.520	0.522	0.530	0.360	0.495	0.530	0.530	0.527	0.526	0.526	0.529		0.530
lprm.11	0.524	0.523	0.523	0.518	0.521	0.470	0.520	0.520	0.520	0.522	0.514	0.514	0.519		0.532
lprm.12	0.541	0.540	0.540	0.542	0.534	0.290	0.495	0.530	0.530	0.531	0.536	0.536	0.497		0.542
lprm.13	0.491	0.490	0.490	0.505	0.508	0.460	0.520	0.510	0.510	0.504	0.498	0.498	0.506		0.518
lprm.14	0.492	0.493	0.493	0.506	0.508	0.470	0.495	0.510	0.510	0.505	0.501	0.501	0.508		0.520
lprm.15	0.503	0.502	0.502	0.497	0.513	0.460	0.495	0.510	0.510	0.513	0.506	0.506	0.507		0.518
lprm.16	0.496	0.496	0.501	0.522	0.517	0.470	0.495	0.520	0.520	0.520	0.504	0.504	0.516		0.520
lprm.17	0.485	0.485	0.485	0.500	0.496	0.480	0.495	0.490	0.490	0.494	0.490	0.490	0.494		0.506
lprm.18	0.486	0.486	0.486	0.487	0.492	0.460	0.495	0.490	0.490	0.495	0.490	0.490	0.494		0.505
lprm.19	0.492	0.492	0.492	0.499	0.496	0.450	0.495	0.500	0.500	0.497	0.495	0.495	0.497		0.507
lprm.20	0.497	0.497	0.495	0.478	0.508	0.440	0.495	0.500	0.500	0.500	0.502	0.502	0.516		0.512
lprm.21	0.502	0.501	0.500	0.518	0.513	0.470	0.495	0.510	0.510	0.511	0.507	0.507	0.510		0.533
lprm.22	0.530	0.531	0.530	0.557	0.540	0.450	0.495	0.530	0.550	0.512	0.526	0.526	0.523		0.548

Case 5

The results for this case are shown in Tables 11 and 12. For this case the following conclusions can be obtained:

- For APRM 1 signal considered as a whole, the results are quite uniform, the DR is near 1, and the results for the frequency are near 0.5 Hz.

- If the signal is divided into two or three records, the first part corresponds to a limit cycle, and the second part is more stable.

- For the APRM 2 the results of all the contributors are quite similar. The signal can also be divided in two or three parts, the first part of the signal being more stable than the second.

- We can assume that when the DR is high the methodology seems to work even for small power transients.

- For cases with a mild plant transient, the transient portion of the signal, which must correspond to a time-varying decay ratio, was shown to have an averaged decay ratio. This confirms the validity of the methods used to obtain the stability parameters in mild transient conditions.

Table 11. Results for the DR – Case 5

	M1	M2	M3	M4	M5	M7	M8	M9	M10	M11	M12	M13			M14	M15
aprm.1	0.951	0.949	0.948	0.98	0.98	0.980			1.020			0.918	0.955	0.961	0.85	0.143
	1.000	1.000	1.000				1.000			0.998	0.990					
	0.679	0.811	0.818				0.940			0.699	0.690					
aprm.2	0.650	0.647	0.671	0.717	0.59	0.470			0.823			0.589	0.881	0.933	0.80	0.748
	0.688	0.692	0.764				0.670			0.620	0.660					
	0.574	0.580	0.536				0.470			0.659	0.670					
										0.515	0.550					

Table 12. Results for the fundamental frequency – Case 5

	M1	M2	M3	M4	M5	M7	M8	M10	M11	M12	M13			M14	M15
aprm.1	0.534	0.534	0.534	0.53	0.53	0.520		0.526	0.524	0.524	0.529	0.525	0.527	0.53	0.535
	0.569	0.426	0.441				0.530		0.556	0.556					
	0.536	0.553	0.552				0.540								
aprm.2	0.514	0.514	0.510	0.494	0.54	0.500		0.520	0.500	0.500	0.516	0.513	0.509	0.52	0.505
	0.514	0.514	0.514				0.490		0.516	0.516					
	0.513	0.513	0.509				0.500		0.504	0.504					

Case 6

The preliminary results for this case are shown in Tables 13, 14, 15 and 16. The following conclusions can be obtained:

Case 6.1

- This is a stable case where the typical dispersion for the values provided for the DR are observed while the results for the frequency are more accurate.
- The LPRM signal at location 11 has a higher DR than the one corresponding to the APRM signal.

Case 6.2

- The APRM signal corresponds to an almost unstable situation (DR > 0.9) and the results from the different benchmark contributors are quite similar.
- It is observed that half of the reactor is oscillating while the other half is stable.
- The channels with radial locations 26, 11, 6, 24 are almost unstable. It seems that half of the reactor is oscillating and the other half is stable.
- There is a kind of local oscillation but there is no phase shift between the LPRMs signals. Clearly this case is not an out-of-phase oscillation
- Case 6.2 corresponds to a “strange” oscillation where some channels oscillate and other channels are stable. Dr. Hennig has proposed a possible explanation of this case based on the assumption of unseated channels in the core.

Table 13. Results for the DR – Case 6.1

	M1	M2	M3	M4	M5	M6	M7	M8	M10	M11	M12	M13	M14	M15
aprm.1	0.523	0.523	0.490	0.589	0.290	0.220	0.160	0.35	0.503	0.474	0.520	0.459	0.39	0.563
lprm.11	0.377	0.372	0.405	0.518	0.085	0.410	0.090	0.15	0.382	0.358	0.450	0.267		0.373
lprm.12	0.276	0.297	0.297	0.295	0.080	0.200	0.100	0.22	0.552	0.170	0.240	0.261		0.439
lprm.13	0.547	0.549	0.577	0.689	0.238	0.260	0.120	0.42	0.296	0.473	0.640	0.373		0.556
lprm.14	0.395	0.469	0.402	0.664	0.226	0.150	0.200	0.20	(0.321)	0.405	0.370	0.413		0.506
lprm.15	0.654	0.583	0.663	0.639	0.270	0.270	0.130	0.58	0.589	0.603	0.700	0.449		0.516
lprm.16	0.803	0.804	0.801	0.818	0.559	0.170	0.420	0.80	(.721)	0.758	0.790	0.664		0.441
lprm.17	0.564	0.563	0.583	0.533	0.254	0.240	0.150	0.50	0.477	0.529	0.560	0.421		0.542
lprm.18	0.638	0.635	0.643	0.686	0.499	0.140	0.570	0.50		0.565	0.490	0.517		0.287
lprm.19	0.339	0.340	0.390	0.460	0.100	0.280	0.030	0.32	0.266	0.349	0.330	0.339		0.808
lprm.110	0.241	0.248	0.302	0.491	0.148	0.170	0.130	0.20		0.204	0.160	0.290		0.068
lprm.111	0.392	0.391	0.382	0.461	0.105	0.280	0.110	0.23	0.277	0.361	0.400	0.344		0.907
lprm.112	0.413	0.413	0.439	0.362	**	0.150	0.230	0.20	(.545)	0.333	0.320	0.292		0.071
lprm.113	0.378	0.375	0.361	0.308	0.098	0.290	0.040	0.20	0.239	0.341	0.380	0.330		0.784
lprm.114	0.419	0.423	0.441	0.474	0.275	0.160	0.280	0.35		0.379	0.430	0.408		0.813
lprm.115	0.560	0.562	0.549	0.516	0.241	0.270	0.120	0.44	0.296	0.478	0.660	0.402		0.553
lprm.116	0.565	0.567	0.574	0.703	0.261	0.250	0.130	0.43	0.318	0.482	0.660	0.395		0.531
lprm.117	0.296	0.289	0.319	0.661	0.092	0.330	0.080	0.19	0.733	0.610	0.310	0.306		0.401
lprm.118	0.312	0.304	0.296	0.222	**	0.150	0.210	0.20		0.267	0.160	0.411		0.383

Table 14. Results for the fundamental frequency – Case 6.1

	M1	M2	M3	M4	M5	M6	M7	M8	M10	M11	M12	M13	M14	M15
aprm.1	0.522	0.523	0.528	0.505	0.490	0.270	0.520	0.49	0.532	0.523	0.523	0.510	0.51	0.497
lprm.11	0.502	0.503	0.513	0.481	0.427	0.310	0.500	0.46	0.526	0.498	0.498	0.481		0.552
lprm.12	0.517	0.514	0.491	0.512	0.504	0.260	0.500	0.49	0.464	0.472	0.472	0.475		0.516
lprm.13	0.524	0.524	0.526	0.511	0.500	0.270	0.510	0.52	0.489	0.524	0.524	0.525		0.523
lprm.14	0.519	0.523	0.502	0.548	0.510	0.250	0.500	0.51	(.512)	0.522	0.522	0.506		0.476
lprm.15	0.529	0.526	0.530	0.509	0.504	0.280	0.510	0.52	0.525	0.525	0.525	0.519		0.526
lprm.16	0.529	0.529	0.529	0.536	0.517	0.250	0.510	0.52	(.528)	0.528	0.528	0.516		0.519
lprm.17	0.522	0.522	0.556	0.502	0.492	0.270	0.510	0.51	0.522	0.517	0.517	0.514		0.513
lprm.18	0.529	0.529	0.529	0.482	0.528	0.250	0.510	0.50		0.527	0.527	0.517		0.510
lprm.19	0.543	0.543	0.548	0.468	0.463	0.280	0.530	0.52	0.669	0.526	0.526	0.524		0.520
lprm.110	0.520	0.518	0.467	0.502	0.500	0.250	0.520	0.52		0.534	0.534	0.556		0.476
lprm.111	0.505	0.506	0.506	0.457	0.463	0.280	0.510	0.53	0.558	0.504	0.504	0.529		0.529
lprm.112	0.541	0.542	0.545	0.492		0.250	0.520	0.53	(.520)	0.535	0.535	0.517		0.488
lprm.113	0.504	0.504	0.494	0.429	0.463	0.280	0.500	0.51	0.586	0.509	0.509	0.524		0.527
lprm.114	0.495	0.496	0.491	0.467	0.532	0.250	0.490	0.50		0.509	0.509	0.553		0.505
lprm.115	0.522	0.523	0.522	0.525	0.504	0.280	0.510	0.52	0.494	0.525	0.525	0.522		0.530
lprm.116	0.523	0.524	0.524	0.514	0.504	0.270	0.510	0.52	0.492	0.525	0.525	0.524		0.525
lprm.117	0.522	0.489	0.487	0.519	0.435	0.290	0.44-0.53	0.47	0.394	0.496	0.496	0.502		0.523
lprm.118	0.533	0.533	0.484	0.443		0.250	0.480	0.50		0.508	0.508	0.472		0.478

Table 15. Results for the DR – Case 6.2

	M1	M2	M3	M4	M5	M6	M7	M8	M9	M10	M11	M12	M13	M14	M15
aprm.2	0.929	0.928	0.926	0.923	0.840	0.720	0.700	0.900		(.965)	0.915	0.960	0.886	0.88	0.379
lprm.21	0.601	0.596	0.601	0.735	0.205	0.680	0.210			0.575	0.546	0.700	0.470		0.533
lprm.22	0.384	0.390	0.397	0.589	0.233	0.710	0.200	0.250	0.250	0.332	0.293	0.400	0.357		0.391
lprm.23	0.959	0.959	0.961	0.966	0.875	0.770	0.800	0.950	0.98	0.986	0.950	0.990	0.928		0.524
lprm.24	0.891	0.888	0.882	0.935	0.701	0.750	0.630	0.950	0.980	(.959)	0.858	0.920	0.807		0.085
lprm.25	0.948	0.971	0.968	0.964	0.904	0.790	0.800	0.980	0.94	0.981	0.961	0.990	0.934		0.515
lprm.26	0.985	0.986	0.986	0.963	0.956	0.920	0.920	0.980		1.006	0.983	1.000	0.960		0.484
lprm.27	0.938	0.938	0.937	0.937	0.828	0.790	0.710	0.970		0.986	0.923	0.980	0.890		0.500
lprm.28	0.960	0.962	0.963	0.981	0.889	0.210	0.870	0.950	0.93	(.981)	0.951	0.970	0.919		0.377
lprm.29	0.719	0.710	0.726	0.752	0.366	0.670	0.300	0.650	0.50	0.300	0.674	0.830	0.560		0.517
lprm.210	0.593	0.594	0.601	0.672	0.302	0.680	0.320	0.510	0.570	(.709)	0.513	0.160	0.535		0.473
lprm.211	0.889	0.889	0.890	0.870	0.611	0.450	0.500	0.980	0.950	0.966	0.858	0.950	0.768		0.456
lprm.212	0.879	0.879	0.874	0.884	0.590	0.200	0.530	0.830	0.900	(.952)	0.837	0.950	0.747		0.398
lprm.213	0.897	0.898	0.906	0.876	0.720	0.760	0.530	0.950	0.940	0.935	0.878	0.950	0.836		0.501
lprm.214	0.894	0.896	0.895	0.919	0.766	0.870	0.680	0.820	0.930	(.965)	0.877	0.950	0.832		0.425
lprm.215	0.963	0.973	0.964	0.966	0.877	0.870	0.780	0.950		0.988	0.954	0.990	0.922		0.495
lprm.216	0.963	0.963	0.963	0.966	0.888	0.860	0.820	0.950		0.983	0.955	0.660	0.928		0.490
lprm.217	0.641	0.640	0.651	0.678	0.282	0.690	0.200	0.580	0.410	0.603	0.591	0.730	0.500		0.478
lprm.218	0.547	0.549	0.550	0.700	0.330	0.190	0.420	0.510		(.507)	0.503	0.470	0.518		0.590

Table 16. Results for the fundamental frequency – Case 6.2

	M1	M2	M3	M4	M5	M6	M7	M8	M9	M10	M11	M12	M13	M14	M15
aprm.2	0.521	0.522	0.522	0.518	0.520	0.400	0.510	0.520		(.523)	0.520	0.520	0.519	0.52	0.520
lprm.21	0.510	0.510	0.509	0.519	0.513	0.380	0.500			0.499	0.509	0.509	0.506		0.564
lprm.22	0.519	0.520	0.504	0.528	0.513	0.390	0.510	0.510	0.530	0.471	0.517	0.517	0.513		0.519
lprm.23	0.521	0.521	0.521	0.520	0.521	0.420	0.510	0.520	0.520	0.524	0.521	0.521	0.521		0.525
lprm.24	0.517	0.521	0.521	0.518	0.517	0.410	0.510	0.520	0.520	(.523)	0.520	0.520	0.518		0.516
lprm.25	0.521	0.522	0.522	0.521	0.521	0.430	0.510	0.520	0.520	0.524	0.521	0.521	0.521		0.525
lprm.26	0.522	0.522	0.522	0.521	0.521	0.530	0.510	0.520		0.520	0.522	0.522	0.521		0.522
lprm.27	0.521	0.521	0.521	0.519	0.521	0.430	0.510	0.52		0.524	0.520	0.520	0.521		0.523
lprm.28	0.522	0.522	0.522	0.521	0.521	0.260	0.510	0.520	0.520	(.523)	0.521	0.521	0.521		0.520
lprm.29	0.514	0.514	0.514	0.517	0.521	0.380	0.510	0.510	0.510	0.528	0.511	0.511	0.502		0.539
lprm.210	0.511	0.512	0.513	0.506	0.496	0.380	0.500	0.500	0.510	(.516)	0.501	0.501	0.485		0.494
lprm.211	0.521	0.521	0.521	0.518	0.525	0.310	0.510	0.520	0.520	0.523	0.521	0.521	0.519		0.535
lprm.212	0.521	0.521	0.521	0.516	0.517	0.260	0.510	0.520	0.520	(.521)	0.519	0.519	0.516		0.516
lprm.213	0.521	0.522	0.522	0.519	0.525	0.420	0.510	0.520	0.520	0.524	0.521	0.521	0.520		0.530
lprm.214	0.522	0.522	0.521	0.522	0.511	0.480	0.510	0.520	0.520	(.523)	0.521	0.521	0.521		0.523
lprm.215	0.521	0.521	0.522	0.520	0.521	0.480	0.510	0.520		0.524	0.521	0.521	0.521		0.525
lprm.216	0.521	0.521	0.521	0.520	0.521	0.480	0.510	0.520		0.524	0.521	0.521	0.521		0.525
lprm.217	0.510	0.510	0.514	0.507	0.520	0.390	0.510	0.520	0.510	0.503	0.506	0.506	0.494		0.542
lprm.218	0.513	0.514	0.514	0.511	0.510	0.250	0.500	0.510		(.498)	0.507	0.507	0.454		0.504

In Tables 2-16 above, we have used the following notation:

M1	UPV standard AR
M2	UPV Full SVD AR
M3	UPV Truncated SVD
M4	UPV Dynamics reconstruction
M5	Pennsylvania State University: AR
M6	Pennsylvania State University: LAPUR code
M7	University of Tsukuba
M8	PSI: ARMA model (Plateau method)
M9	PSI: AR-AIC
M10	JAERI
M11	SIEMENS AR
M12	SIEMENS RAC
M13	TOSHIBA
M14	TU DELFT
M15	CSNNS Mexico

Also, we note that the method M6 (LAPUR code) is not a signal analysis method. Furthermore some participants also provided standard deviation estimates. This is an important aspect of the benchmark; these results will be presented in a final report.

Additional results

Partial additional results for the benchmark signals have been provided by Dr. Behringer. He has used a method based on a multi-parametric fit of the auto-correlation function (ACF) which is calculated from the filtered power spectral density. These results are shown in Table 16.

Table 17. Additional results (ACF)

Signal	DR	FR
c1_aprm3	0.582	0.483
c1_aprm4	0.555	0.485
c1_aprm12	0.723	0.462
c2_test.L1	0.224	0.458
c2_test.L2	0.583	0.525
c2_test.s42	0.451	0.504
c3_test.1	0.377	0.415
c3_test.2	0.312	0.400
c3_test.3	0.347	0.425
c3_test.4	0.619	0.472
c4_lprm.8	0.717	0.507
c4_lprm.12	0.704	0.536
c4_lprm.22	0.569	0.532
c6_lprm.22	0.567	0.522
c6_lprm.210	0.547	0.512
c6_lprm.211	0.976	0.523
c6_lprm.212	0.884	0.521
c6_lprm.213	0.993	0.524
c6_lprm.214	0.983	0.523
c6_lprm.215	0.997	0.523

Chapter 5
SUMMARY AND CONCLUSIONS

Lessons learned on the performance of the different approaches and the issue of the determination of uncertainties were debated in a meeting and they can be summarised in the following questions and answers.

1. What is the best definition of decay ratio (DR)?

For noise analysis it is the decay ratio associated with the least stable or dominant pole. The definition is clear for a second order system.

2. What are the best methods for calculating the DR?

Several methods were used in this study: AR method, AR method plus Impulse Response, Auto-correlation, Recursive Auto-correlation methods, ARMA, LAPUR, Power Spectrum Estimation. At the Forsmark NPP stability monitors have been used for over 10 years and the uncertainty in the DR range 0.5-0.6 is smaller than 0.1. Obviously experience of the operator in using such a monitor at the plant is required. In other ranges the uncertainty can be higher. Measurements in a steady state condition, extracting signals for a given time interval and analysing them, leads to small uncertainties. The methodology for determining the uncertainty has to be defined and the model order should be known (but this is not always certain). What really matters is the DR after manoeuvring and the amplitude of the oscillation. Often oscillations are not stationary, the "decay ratio" for these signals is not well defined but the determination of frequency (Fourier analysis) is quite accurate. For the determination of decay ratios the asymptotic part of the transformation function should be used. This is a suggested pragmatic approach.

3. Is it possible to have reliable methods for determining DR automatically, independently of the analyst?

It is possible. This has been demonstrated at Forsmark where the same method is used and compared in the monitoring and off-line. The Siemens experience also affirms this answer. No filtering is required and once experience has been gained it works well. Signal conditioning has to be plant dependent. The experts tune it to the plant, then it can be run automatically.

4. What is the influence of the time duration in the estimation of DR?

An accurate auto-correlation function is required first based on the AR model. A heuristic type of algorithm is normally used. The duration depends on the value of DR (about inversely proportional to it). For power spectral density between 4 000 and 10 000 points are required.

5. Is it of interest to determine the DR in a transient? Is the calculation reliable?

It is of interest – because the method follows the trend and makes the DR derived acceptable.

6. **What happens if the signal contains more than one natural frequency? Which DR is the true one?**

   The interesting information for the operator is: oscillations driven by a noise source, disturbances in the system. Oscillations by themselves do not imply instability if driven by an external source. The stability characteristics of the reactor need to be known; the amplitudes are easy to extract.

7. **Is it possible to determine DR of an out-of-phase oscillation?**

   This is possible for DR up to 0.7 ± 0.1 and only if enough LPRM signals per plane are provided. Because there are many ways of doing it wrong and only a few to do it right, it depends on the expertise of the analyst, or on the sophistication of the monitoring algorithm.

8. **Can we provide an accurate limit to the stable behaviour of the reactor core?**

   This depends on the uncertainty. The real margin should be determined on power. Frequency domain codes can determine it; they are efficient but not sufficient. The “decay ratio” is a measure of linear stability and should therefore not be used as the only indicator of BWR stability.

Annex 1

LIST OF PARTICIPANTS

GERMANY

MOJUMDER, Soma
SIEMENS AG/KWU
KWU NBTT
Postfach 3220
D-91050 Erlangen

Tel: +49 (9131) 18 7536
Fax: +49 (9131) 18 5243
Eml: Soma.Mojumder@erl19.Siemens.de

POHLUS, Joachim
Institut fur Sicherheits-technologie
(ISTec) GmbH
Abteilung Diagnose
Forschungsgelaende
D-85748 Garching

Tel: +49 (089) 3200 4542
Fax: +49 (089) 3200 4300
Eml: poh@istecmuc.grs.de

JAPAN

KONNO, Hidetoshi
Inst. of Information Sciences & Electronics
University of Tsukuba
Ibaraki-ken 305-8573

Tel: +81 (298) 53 5016
Fax: +81 (298) 53 6471
Eml: hkonno@sakura.cc.tsukuba.ac.jp

* ROSTON, Graciela Beatriz
Quantum Science & Energy Engineering
Tohoku University
Aramaki-Aza, Aoba, Aoba-ku
Sendai 980-77

Tel: +81 22 217 7907
Fax: +81 22 217 7907
Eml: graciela@luke.qse.tohoku.ac.jp

* SUZUDO, Tomoaki
Control and AI Laboratory
Dept. of Reactor Engineering, JAERI
Shirakata Shirane 2-4, Tokai-mura
Naka-gun, Ibaraki-ken 319-1195

Tel: +81 (29) 282 6077
Fax: +81 (29) 282 6122
Eml: suzudo@clsu3a0.tokai.jaeri.go.jp

TAKEUCHI, Yutaka
TOSHIBA Corporation
Nuclear Engineering Laboratory
Systems Analysis & Mech. Eng.
4-1 Ukishima-cho, Kawasaki-ku
Kawasaki 210

Tel: +81 44 288 8131
Fax: +81 44 270 1808
Eml: takeuchi@postman.sag.nel.rdc.toshiba.co.jp

MEXICO

NUÑEZ-CARRERA, Alejandro
Comision Nacional de Seguridad Nuclear
y Salvaguardias
Dr. Barragan Num. 779
Col. Narvarte C.P. 03020
MEXICO D.F.

Tel: +52 2 590 8113
Fax: +52 5 590 6103
Eml: cnsns1@servidor.unam.mx

THE NETHERLANDS

DE KRUIJF, Willy J.M.
Interfaculty Reactor Institute
Reactor Physics Department
Mekelweg 15
2629 JB Delft

Tel: +31 15 278 6594
Fax: +31 15 278 6422
Eml: W.J.M.deKruijf@iri.tudelft.nl

SPAIN

CONDE LOPEZ, José M.
Head, Nuclear Engineering D.
Consejo de Seguridad Nuclear
Justo Dorado, 11
E-28040 Madrid

Tel: +34 91 346 02 53
Fax: +34 91 346 05 88
Eml: jmcl@csn.es

GINESTAR, Damian
Universidad Politecnica de Valencia
Dept. Ingenieria Quimic y Nuclear
Camino Devera, 14
P.O. Box 22012
E-46022 Valencia

Tel: +34 96 387 7635/7630
Fax: +34 96 387 7639
Eml: dginesta@pleione.upv.es

NAVARRO, Joaquin
Departamento de Ingenieria Quimica y Nucl
Universidad Politecnica
Campus Camiro de Vera
P.O. Box 22012
E-46071 Valencia

Tel:
Fax: +34 96 387 76 39
Eml:

* PALOMO, Maria José
Departamento de Ingenieria
Quimica y Nuclear
Universidad Politecnica
P.O. Box 22012
E-46071 Valencia

Tel:
Fax: +34 (6) 387 76 39
Eml:

RECIO SANTAMARIA, Manuel
Nuclear Engineering Dept.
Consejo de Seguridad Nuclear
Justo Dorado, 11
E-28040 Madrid

Tel: +34 91 346 02 10
Fax: +34 91 346 05 88
Eml: mrs@csn.es

REY GAYO, Jose Maria
Nuclear Engineering Dept.
Consejo de Seguridad Nuclear
Justo Dorado, 11
E-28040 Madrid

Tel: +34 91 346 02 15
Fax: +34 91 346 05 88
Eml: jmrg@csn.es

VERDÚ, Gumersindo
Departamento de Ingenieria Quimica
y Nuclear
Universidad Politecnica
Campus Camiro de Vera
P.O. Box 22012
E-46071 Valencia

Tel: +34 96 387 76 30
Fax: +34 96 387 76 39
Eml: gverdu@pleiades.upv.es

SWEDEN

LANSAKER, Pär
Vattenfall
Forsmarksverket
S-74203 Oesthammar

Tel: +46 173 81543
Fax: +46 173 81697
Eml: Eml: p1k@forsmark.vattenfall.se

SWITZERLAND

HENNIG, Dieter
Systems Engineering
Paul Scherrer Institut
CH-5232 Villingen PSI

Tel: +41 (56) 310 41 67
Fax: +41 (56) 310 23 22
Eml: Dieter.Hennig@psi.ch

UNITED STATES OF AMERICA

CECEÑAS-FALCON, Miguel
Nuclear Engineering
The Pennsylvania State University
231 Sackett Building
University Park, PA 16802

Tel: +1 814 231 0581
Fax: +1 814 865 8499
Eml: mxc209@psu.edu

FARAWILA, Yousef M.
Siemens Power Corporation
Nuclear Division
SPC
2101 Horn Rapids Road
RICHLAND, WA 99352-0130

Tel: +1 (509) 375 8720
Fax: +1 (509) 375 8402
Eml: yousef_farawila@nfuel.com

* MARCH-LEUBA, Jose A.
Oak Ridge National Laboratory
P.O. Box 2008 MS6010
Oak Ridge, TN 37831-6010

Tel: +1 423 574 5571
Fax: +1 423 576 8380
Eml: marchleubaja@ornl.gov

INTERNATIONAL ORGANISATIONS

SARTORI, Enrico
OECD/NEA Data Bank
Le Seine-Saint Germain
12, boulevard des Iles
F-92130 Issy-les-Moulineaux

Tel: +33 (0)1 45 24 10 72
Fax: +33 (0)1 45 24 11 10
Eml: sartori@nea.fr

* *Regrets having been unable to attend.*

Annex 2

METHODOLOGIES AND RESULTS PRESENTED BY UPV-CSN*

Introduction

The methodologies used by the group of the Universidad Politécnica de Valencia and the Consejo de Seguridad Nuclear are based on the methods exposed in Ref. [1]. We provide here a summary of the different methods used and the results obtained for the different signals of the Forsmark benchmark.

In all cases we will use the decay ratio (DR) and the fundamental oscillation frequency as parameters to compare the performance of the different methods. It should be noted that the DR is a parameter defined for pure second order systems, being only in this case a stable measurement of the damping of the system. For higher order systems like nuclear reactors, this concept is not clearly defined, and many different definitions currently exist [2].

The main idea of the different methods is to start from a neutronic signal, $x(t)$, and calculate the complex conjugate dominant poles, λ and λ^*, associated with the main oscillation present in the signal. From these poles we obtain the linear stability parameters:

$$DR = \exp\left(2\pi \frac{\mathrm{Re}(\lambda)}{\left|\mathrm{Im}(\lambda)\right|}\right), \quad Freq = \left|\mathrm{Im}(\lambda)\right| \tag{1}$$

We have used the following methods based on an auto-regressive model for the signal: a standard AR method, which has been denoted by M1, a full SVD-AR model (M2) and a truncated SVD-AR model (M3). The last method we used is based on a reconstruction of the dynamics associated with the neutronic signal (M4).

A singular system analysis methodology [3] has been applied to analyse some signals of the benchmark. The results obtained are also presented.

Auto-regressive model methods

These methods start from the sampled neutronic signal, $x(n)$, and assume that it can be modelled using an order p AR process, that is:

$$x(n) + \sum_{k=1}^{p} a_k x(n-k) = b_0 \varepsilon(n) \tag{2}$$

* Universidad Politécnica de Valencia
Consejo de Seguridad Nuclear
SPAIN

where ε(*n*) is a normalised white-noise process. The auto-correlation function of the process is:

$$r_x(m) = \lim_{M\to\infty} \frac{1}{2M+1} \sum_{k=-M}^{M} x(k-m)x(k)^* \tag{3}$$

In practice, as we know, only a finite number of points for the signal are available. Thus the auto-correlation sequence must be estimated with the finite data. Assuming *N* data samples, a discrete time auto-correlation estimate for the signal *x*(*n*) will have the following form:

$$r_x(m) = \frac{1}{N-m} \sum_{k=1}^{N-m} x(k-m)x(k)^* \qquad 0 \le m \le N-1 \tag{4}$$

where $r_x(-m) = r_x(m)$.

It is easy to achieve the following relationship among the AR(*p*) auto-correlation elements [4]:

$$r_x(n) + \sum_{k=1}^{p} a_k r_x(n-k) = \begin{cases} |b_0|^2 & , n = 0 \\ 0 & , n \ge 1 \end{cases} \tag{5}$$

using the matrix notation:

$$\begin{bmatrix} r_x(0) \\ r_x(1) \\ \cdot \\ r_x(p) \end{bmatrix} + \begin{bmatrix} r_x(-1) & r_x(-2) & \cdot & r_x(-p) \\ r_x(0) & r_x(-1) & \cdot & r_x(1-p) \\ \cdot & \cdot & \cdot & \cdot \\ r_x(p-1) & r_x(p-2) & \cdot & r_x(0) \end{bmatrix} \cdot \begin{bmatrix} 1 \\ a_1 \\ \cdot \\ a_p \end{bmatrix} = \begin{bmatrix} |b_0|^2 \\ 0 \\ \cdot \\ 0 \end{bmatrix}$$

and eliminating the first row of this system, we find that:

$$\begin{bmatrix} r_x(0) & r_x(1) & \cdot & r_x(1-p) \\ r_x(1) & r_x(0) & \cdot & r_x(2-p) \\ \cdot & \cdot & \cdot & \cdot \\ r_x(p-1) & r_x(p-2) & \cdot & r_x(0) \end{bmatrix} \cdot \begin{bmatrix} a_1 \\ a_2 \\ \cdot \\ a_p \end{bmatrix} = -\begin{bmatrix} r_x(1) \\ r_x(2) \\ \cdot \\ r_x(p) \end{bmatrix} \tag{6}$$

or more compactly:

$$R \cdot a = -r \tag{7}$$

the solution of which is:

$$a = -\left(R^{-1}\right)r$$

Once the AR(*p*) model associated with the signal has been obtained, we have a transfer function of the AR model:

$$H(z) = \frac{1}{z^{-p}\left(a_p + a_{p-1}z + \ldots + z^p\right)}$$

The next step will be to compute the roots of the equation:

$$z^p + a_1 z^{p-1} + \ldots + a_p = 0$$

choosing the two complex conjugate dominant roots, β and β^*, and transforming them into the s-plane by means of the following expressions:

$$\lambda = \frac{1}{T}\ln(\beta), \quad \lambda^* = \frac{1}{T}\ln(\beta^*)$$

where T is the sampling time of the neutronic signal. With these poles we obtain the DR and the frequency of the oscillation using Eq. (1). This method is what we have called the standard AR method.

On the other hand, to obtain the solution of Eq. (6) we assume that matrix R can be inverted and we calculate R^{-1}. Although this could be the case, matrix R can be ill conditioned and this method of solving the system would not provide accurate results. Thus, we use a k order pseudo inverse of the matrix R to solve Eq. (6). That is, we begin selecting an order p for the AR model which is large enough to assure that the real AR model order is smaller than the chosen p, and we calculate the singular value decomposition of the auto-correlation matrix, R [5]:

$$R = U_R \Sigma_R V_R^T \tag{8}$$

where:

$$U_R = V_R = \left[v_1, v_2, \ldots, v_p\right] \in \Re^{pxp}$$
$$\Sigma_R = diag\left(\sigma_1, \sigma_2, \ldots, \sigma_p\right) \in \Re^{pxp}$$

We will assume there are k dominant singular values, and knowing that R is a real symmetric matrix with $U_R = V_R$, we construct a k order pseudo-inverse of matrix R in the following way:

$$\left(R^{(k)}\right)^{\#} = \sum_{i=1}^{k} \sigma_i^{-1} v_i v_i^T \tag{9}$$

computing the parameters vector a as:

$$a = -\left(R^{(k)}\right)^{\#} r \tag{10}$$

Once we have selected the order p of the AR model, we must choose the order k of the auto-correlation matrix pseudo-inverse. In order to do this, the auto-correlation matrix is decomposed in singular values such as in Eq. (8), and the ratios between every two consecutive singular values are calculated in the following way:

$$ratio_i = \frac{\sigma_{i-1}}{\sigma_i}, \quad i = 2,3,\ldots,p$$

In Figures 1 and 2 we have plotted the singular values and the *ratios* versus *i*, respectively, for an experimental neutronic power signal. It can be observed that the last singular values are much smaller than the first ones. Therefore if a consistent solution to Eq. (7) is to found, the largest singular values should be chosen as the dominant ones. But, where must we stop? In Figure 2, we observe that starting at $i = p$ and going to decreasing values of i the *ratios* remain almost constant, producing values of the *ratio* near 1, and when we arrive to the smallest values of i we observe that these *ratios* grow above 2. The established truncation criterion is to select the first value of i where $ratio_i$ is higher than 2. In this way, the truncated SVD-AR method is quite independent of the initial order p selected for the auto-regressive model.

Figure 1. Spectrum of the auto-correlation matrix, R, singular values

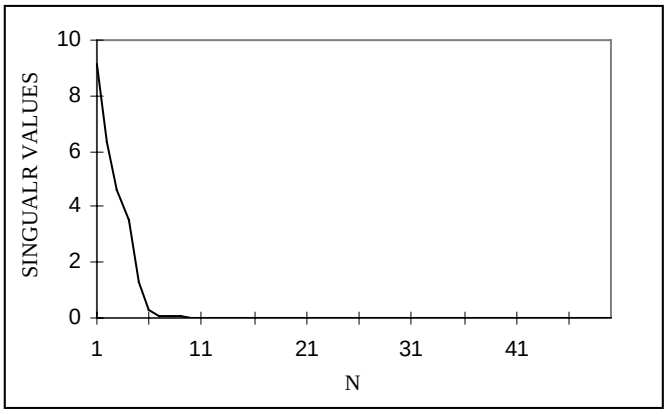

Figure 2. Ratios between every two consecutive singular values of the R

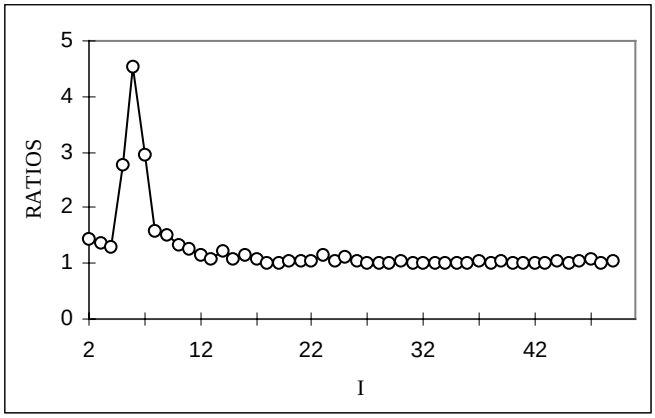

Dynamics reconstruction method

This method is based on the reconstruction of the phase space of the dynamical system associated with the neutronic signal $x(n)$, $n = 1,\ldots,N$. This reconstructed space is known as the embedding space of the signal.

The first step consists on the construction of an information matrix A, whose rows are built with the application of an n_w-window to the time series, $x(n)$, of N data, resulting in a matrix of the form [6]:

$$A \equiv \begin{bmatrix} x(1) & x(2) & \cdot & \cdot & x(n_w) \\ x(2) & x(3) & \cdot & \cdot & x(n_w+1) \\ \cdot & \cdot & \cdot & \cdot & \cdot \\ \cdot & \cdot & \cdot & \cdot & \cdot \\ x\big(N(n_w-1)\big) & x(N-n_w) & \cdot & \cdot & x(N) \end{bmatrix} \tag{11}$$

where the length of the window, n_w, is a parameter to be chosen. The embedding space is achieved by a projection of the information matrix onto a subspace, whose basis and dimension also must be selected.

In order to select the basis for the projection, we will use the singular value decomposition as main tool. The information matrix, *A*, admits a decomposition of the form:

$$A = U \cdot \Sigma \cdot V^T \tag{12}$$

where:

$$U = \left[u_1, u_2, \ldots, u_q\right] \in \Re^{pxp}$$
$$V = \left[v_1, v_2, \ldots, u_{n_w}\right] \in \Re^{n_w x n_w}$$
$$\Sigma = diag\left(\sigma_1, \sigma_2, \ldots, \sigma_{n_w}\right) \in \Re^{qxn_w}$$

where q is $N - n_w + 1$, σ_i is the singular values of *A*, u_i and v_i are the *i*-th left and *i*-th right singular vectors associated with the singular value σ_i.

Here, we select the number of significant singular values as the dimension of the projection subspace, the basis of this subspace being the corresponding singular vectors. In absence of noise the dimension of the subspace containing the embedded manifold would be the rank of the covariance matrix, defined as $\Xi = A^T A$ [6]. However, due to the noise present in the measurements, Ξ is a full rank matrix. We must note that the singular values of the information matrix, *A*, are the positive square roots of the covariance matrix singular values. Thus, the noise causes all the singular values of the information matrix to be non-zero, and we need a method to distinguish the fundamental information subspace from the noise subspace.

In the simple case of white noise, the existence of a non-zero constant background or noise floor is a notable characteristic which can be used to determine the fundamental component of the signal. But in experimental observations we will find more difficulties. Therefore in practice we have to face the selection of the fundamental subspace dimension in order to avoid the subspace associated with the noise and to obtain a good embedding space. Moreover, the above-mentioned problem of choosing the window length, n_w, of the information matrix *A* still remains.

Choosing the window length (n_w)

The criterion used in this paper to choose the window length of the information matrix *A* is based on the analysis of the singular value ratio (SVR) spectrum. Thus, we define a new matrix from the time series data, $x(n)$, in the following form:

$$Y \equiv \begin{bmatrix} x(1) & x(2) & \cdot & \cdot & x(n_w) \\ x(n_w+1) & x(n_w+2) & \cdot & \cdot & x(2n_w) \\ \cdot & \cdot & \cdot & \cdot & \cdot \\ \cdot & \cdot & \cdot & \cdot & \cdot \\ x((k-1)n_w+1) & x((k-1)n_w+2) & \cdot & \cdot & x(N) \end{bmatrix}$$

k being the integer part of the ratio N/n_w.

We also define the parameter *r*, called SVR, as the ratio between the two largest singular values of the data matrix, *Y*, σ_1/σ_2. This parameter has been used for detecting the periodic components of periodic or almost periodic signals, occurring high values of *r* at the actual period length as well as its higher multiples [7].

We will use a similar methodology, taking advantage of the SVR spectrum. In this way, we will construct the data matrix *Y* with window lengths of $n_w = 2,3,...$, drawing the SVR spectrum (SVR vs. n_w), and choosing the window length of the information matrix, n_w, as the n_w where *r* takes the first significant maximum, discarding the initial range where the SVR decreases monotonically (see Figure 3). Multiplied by τ_s, n_w can be defined as the effective period length of the signal. In Figure 3, the window length taken was 26. It should be noted that in some signals we have found difficulties in selecting this maximum because of the irregular shape of the spectrum produced by this type of signal, but in general the election of the appropriate window length it is quite clear.

Figure 3. SVR spectrum

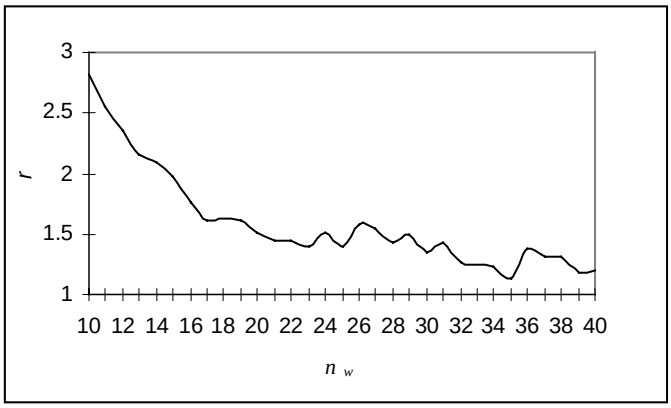

Choosing the projection subspace dimension

We deal with experimental neutronic power signals with a great amount of noise, and low signal to noise ratios (SNR). In this way, the noise masks the signal component useful for the stability analysis. Thus in choosing the appropriate dimension we mainly achieve the extraction of the subspace associated with the fundamental information of the signal.

There is not a clear criterion for the selection of that dimension. There are some criteria which suppose that the smallest singular value could be identified as noise dominated, even when the noise is not white.

The criterion proposed here is based on the selection of the dominant or significant singular values of the information matrix constructed with the appropriate window length. The smallest singular values are non-significant versus the first ones, so in order to select the dominant singular values associated to the fundamental information, we propose a criterion based on the ratio between every two consecutive singular values, σ_i/σ_{i+1}, taking as dimension d the value of i where this ratio produces a value higher than 2, starting at the end of the spectrum (see Figure 4).

Figure 4. Spectrum of ratios of every two consecutive singular values of *A* from APRM3 signal (taking the appropriate window length)

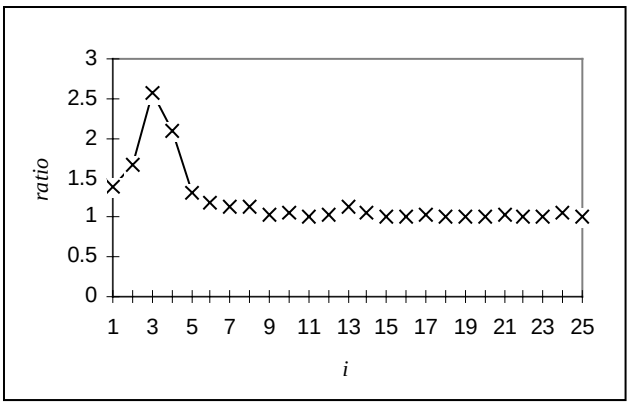

Once we have chosen the values of the two parameters n_w and d, we achieve the singular system approach using the following projection:

$$A^d = \sum_{k=1}^{d} u_k \cdot \sigma_k \cdot v_k^T \tag{13}$$

selecting as embedding space the first d columns of the matrix A^d obtained.

Global fit by means of orthonormal polynomials – Lyapunov exponents

We assume that the dynamics of a given system can be approximated by a discrete map:

$$\vec{x}(n+1) = \vec{F}\left(\vec{x}(n)\right) \tag{14}$$

We want to find the global complex Lyapunov exponents of the system [8] in order to obtain the fundamental oscillation frequency and the DR parameter as:

$$DR = \exp\left(2\pi \frac{\mathrm{Re}(\lambda)}{\left|\mathrm{Im}(\lambda)\right|}\right)$$

where λ is the dominant complex Lyapunov exponent of the system.

We will suppose that the map for Eq. (14) is unknown but, nevertheless, the function $\vec{F}$ can be approximately reconstructed as an expansion in terms of orthogonal polynomials on the attractor of the

system [9,10,11]. Denoting the orthonormal polynomials by $\pi^{(I)}$, we approximate each component of the map function, as:

$$F_j = \sum_{i_1,\ldots,i_d=0}^{np_1,\ldots,np_d} f_{(I)}^{j} \pi^{(I)} \tag{15}$$

where np_j is the maximum degree in x_j considered for the polynomials.

Thus, knowing the reconstruction of the phase space of the dynamical system and the orthonormal polynomials on the attractor, it is possible to obtain an approximation for the discrete dynamical system (14). So, from the approximation of each component of the discrete map, F_j, on each point of the attractor we obtain the Jacobian matrix of the function at point $\vec{x}(n)$.

In order to obtain the global complex Lyapunov exponents, we recover an effective linear system associated with the signal and calculate the complex Lyapunov exponents of the system as the Neperian logarithms of the dominant eigenvalues of the Jacobian matrix.

Numerical results

The results obtained for the different cases are presented in the following tables. For methods M1, M2 and M2 we show the results obtained selecting an AR model order of 40, 50 and 60, respectively.

Table 1. DR results for Case 1

	M1			**M2**			**M3**			**M4**
c1_aprm.1	0.456	0.405	0.517	0.454	0.314	0.500	0.629	0.481	0.619	0.640
c1_aprm.2	0.639	0.623	0.707	0.633	0.621	0.707	0.700	0.670	0.735	0.824
c1_aprm.3	0.531	0.577	0.620	0.538	0.583	0.625	0.446	0.592	0.636	0.735
c1_aprm.4	0.515	0.503	0.527	0.511	0.500	0.530	0.483	0.528	0.565	0.634
c1_aprm.5	0.531	0.591	0.621	0.521	0.584	0.614	0.403	0.555	0.612	0.702
c1_aprm.6	0.544	0.482	0.594	0.560	0.492	0.594	0.503	0.424	0.636	0.659
c1_aprm.7	0.680	0.704	0.702	0.684	0.708	0.707	0.684	0.671	0.726	0.624
c1_aprm.8	0.501	0.532	0.567	0.506	0.545	0.576	0.479	0.479	0.552	0.577
c1_aprm.9	0.542	0.599	0.578	0.497	0.581	0.562	0.312	0.638	0.425	0.503
c1_aprm.10	0.548	0.616	0.670	0.581	0.644	0.681	0.673	0.506	0.713	0.545
c1_aprm.11	0.535	0.645	0.618	0.538	0.644	0.622	0.542	0.625	0.626	0.644
c1_aprm.12	0.807	0.810	0.819	0.802	0.808	0.818	0.804	0.847	0.832	0.751
c1_aprm.13	0.523	0.491	0.591	0.515	0.582	0.588	0.514	0.609	0.546	0.777
c1_aprm.14	0.725	0.739	0.702	0.715	0.733	0.698	0.717	0.748	0.646	0.782

Table 2. Fundamental frequency results for Case 1

	M1			M2			M3			M4
c1_aprm.1	0.459	0.503	0.487	0.457	0.412	0.486	0.472	0.493	0.495	0.467
c1_aprm.2	0.472	0.480	0.468	0.471	0.470	0.487	0.472	0.476	0.463	0.464
c1_aprm.3	0.485	0.475	0.489	0.484	0.475	0.487	0.475	0.478	0.489	0.480
c1_aprm.4	0.482	0.499	0.487	0.483	0.500	0.488	0.479	0.500	0.481	0.481
c1_aprm.5	0.504	0.509	0.513	0.505	0.510	0.514	0.504	0.507	0.511	0.492
c1_aprm.6	0.480	0.489	0.482	0.480	0.488	0.481	0.473	0.467	0.474	0.487
c1_aprm.7	0.534	0.531	0.540	0.534	0.532	0.540	0.534	0.532	0.539	0.510
c1_aprm.8	0.523	0.533	0.518	0.526	0.535	0.520	0.536	0.553	0.503	0.506
c1_aprm.9	0.428	0.432	0.431	0.426	0.430	0.431	0.370	0.434	0.352	0.409
c1_aprm.10	0.460	0.464	0.457	0.459	0.464	0.458	0.452	0.471	0.462	0.424
c1_aprm.11	0.474	0.480	0.466	0.473	0.479	0.465	0.481	0.483	0.464	0.454
c1_aprm.12	0.466	0.467	0.465	0.466	0.467	0.465	0.465	0.468	0.467	0.400
c1_aprm.13	0.402	0.404	0.407	0.403	0.405	0.408	0.402	0.403	0.407	0.478
c1_aprm.14	0.492	0.492	0.484	0.492	0.493	0.485	0.490	0.491	0.480	0.489

Table 3. DR results for Case 2

	M1			M2			M3			M4
c2_test.l1	0.322	0.478	0.387	0.318	0.476	0.390	0.497	0.484	0.427	0.432
c2_test.s11	0.171	0.350	0.339	0.169	0.329	0.307	0.181	0.352	0.405	0.355
c2_test.s21	0.429	0.483	0.382	0.444	0.512	0.424	0.464	0.504	0.401	0.649
c2_test.s31	0.306	0.350	0.359	0.300	0.494	0.360	0.537	0.511	0.377	0.646
c2_test.s41	0.462	0.455	0.455	0.466	0.497	0.439	0.479	0.491	0.438	0.368
c2_test.l2	0.621	0.648	0.650	0.620	0.648	0.650	0.653	0.644	0.605	0.620
c2_test.s12	0.672	0.672	0.695	0.674	0.685	0.705	0.696	0.645	0.621	0.617
c2_test.s22	0.661	0.676	0.689	0.665	0.678	0.685	0.680	0.669	0.720	0.656
c2_test.s32	0.524	0.634	0.638	0.527	0.629	0.640	0.478	0.657	0.655	0.641
c2_test.s42	0.530	0.572	0.629	0.469	0.554	0.603	0.494	0.426	0.630	0.564

Table 4. Fundamental frequency results for Case 2

	M1			M2			M3			M4
c2_test.l1	0.483	0.455	0.423	0.481	0.455	0.423	0.476	0.457	0.427	0.472
c2_test.s11	0.424	0.451	0.452	0.427	0.448	0.446	0.427	0.436	0.442	0.471
c2_test.s21	0.450	0.471	0.481	0.452	0.472	0.480	0.457	0.472	0.384	0.439
c2_test.s31	0.460	0.451	0.418	0.461	0.441	0.419	0.474	0.437	0.400	0.427
c2_test.s41	0.462	0.434	0.434	0.464	0.484	0.435	0.465	0.412	0.380	0.409
c2_test.l2	0.532	0.530	0.538	0.531	0.530	0.538	0.529	0.530	0.498	0.534
c2_test.s12	0.538	0.536	0.544	0.537	0.535	0.545	0.534	0.538	0.539	0.529
c2_test.s22	0.524	0.532	0.530	0.535	0.534	0.530	0.525	0.535	0.543	0.530
c2_test.s32	0.523	0.539	0.533	0.524	0.539	0.533	0.529	0.537	0.529	0.523
c2_test.s42	0.497	0.515	0.509	0.491	0.518	0.506	0.496	0.515	0.533	0.527

Table 5. DR results for Case 3

	M1			M2			M3			M4
c3_test.1	0.382	0.291	0.488	0.376	0.273	0.506	0.370	0.310	0.514	0.552
c3_test.2	0.236	0.372-0.441	0.442-0.584	0.249	0.316-0.422	0.446-0.581	0.453	0.318	0.453	0.621
c3_test.3	0.414	0.587	0.320-0.613	0.424	0.592	0.619	0.388	0.363	0.489	0.516
c3_test.4	0.514	0.614	0.707	0.528	0.629	0.720	0.516	0.580	0.748	0.676

Table 6. Fundamental frequency results for Case 3

	M1			M2			M3			M4
c3_test.1	0.397	0.344	0.439	0.400	0.342	0.440	0.385	0.331	0.434	0.420
c3_test.2	0.406	0.331-0.475	0.307-0.447	0.416	0.334-0.471	0.307-0.447	0.430	0.360	0.313	0.431
c3_test.3	0.461	0.477	0.301-0.470	0.461	0.476	0.470	0.474	0.304	0.467	0.465
c3_test.4	0.481	0.483	0.475	0.480	0.483	0.474	0.484	0.485	0.478	0.437

Table 7. DR results for Case 4

	M1			M2			M3			M4
c4_aprm	0.784	0.770	0.838	0.784	0.761	0.820	0.777	0.495	0.825	0.806
c4_lprm.1	0.834	0.893	0.905	0.835	0.893	0.902	0.827	0.892	0.903	0.889
c4_lprm.2	0.867	0.908	0.923	0.872	0.909	0.922	0.869	0.909	0.926	0.918
c4_lprm.3	0.882	0.914	0.934	0.884	0.914	0.933	0.884	0.914	0.933	0.914
c4_lprm.4	0.897	0.900	0.906	0.897	0.900	0.905	0.896	0.897	0.902	0.854
c4_lprm.5	0.770	0.820	0.851	0.777	0.823	0.853	0.753	0.825	0.863	0.830
c4_lprm.6	0.785	0.794	0.847	0.786	0.768	0.845	0.770	0.796	0.843	0.869
c4_lprm.7	0.790	0.774	0.783	0.788	0.795	0.776	0.789	0.787	0.782	0.826
c4_lprm.8	0.757	0.740	0.612	0.761	0.737	0.618	0.772	0.737	0.574	0.733
c4_lprm.9	0.724	0.734	0.773	0.740	0.734	0.771	0.751	0.740	0.791	0.848
c4_lprm.10	0.751	0.733	0.625	0.750	0.738	0.634	0.753	0.735	0.644	0.757
c4_lprm.11	0.666	0.586	0.650	0.664	0.587	0.653	0.667	0.651	0.633	0.749
c4_lprm.12	0.695	0.720	0.713	0.691	0.720	0.716	0.700	0.764	0.735	0.787
c4_lprm.13	0.744	0.762	0.796	0.752	0.766	0.796	0.756	0.765	0.793	0.835
c4_lprm.14	0.743	0.705	0.769	0.747	0.710	0.770	0.744	0.706	0.769	0.817
c4_lprm.15	0.730	0.571	0.638	0.739	0.596	0.637	0.741	0.566	0.665	0.691
c4_lprm.16	0.663	0.652	0.709	0.672	0.636	0.697	0.652	0.639	0.718	0.699
c4_lprm.17	0.821	0.830	0.849	0.823	0.830	0.849	0.834	0.828	0.847	0.838
c4_lprm.18	0.819	0.807	0.832	0.820	0.804	0.829	0.827	0.807	0.830	0.877
c4_lprm.19	0.819	0.807	0.811	0.824	0.808	0.809	0.826	0.808	0.806	0.886
c4_lprm.20	0.764	0.750	0.650	0.766	0.751	0.643	0.756	0.750	0.598	0.757
c4_lprm.21	0.707	0.631	0.659	0.716	0.635	0.665	0.707	0.603	0.674	0.771
c4_lprm.22	0.557	0.613	0.579	0.537	0.604	0.568	0.562	0.603	0.541	0.702

Table 8. Fundamental frequency results for Case 4

	M1			M2			M3			M4
c4_aprm	0.491	0.486	0.480	0.491	0.485	0.480	0.493	0.503	0.481	0.490
c4_lprm.1	0.485	0.482	0.480	0.484	0.482	0.479	0.484	0.481	0.479	0.495
c4_lprm.2	0.484	0.482	0.480	0.484	0.482	0.480	0.484	0.481	0.479	0.491
c4_lprm.3	0.486	0.482	0.480	0.485	0.482	0.475	0.485	0.481	0.480	0.488
c4_lprm.4	0.488	0.485	0.482	0.488	0.485	0.482	0.487	0.485	0.482	0.485
c4_lprm.5	0.494	0.484	0.481	0.494	0.484	0.481	0.494	0.482	0.480	0.515
c4_lprm.6	0.496	0.487	0.483	0.496	0.496	0.482	0.497	0.486	0.482	0.510
c4_lprm.7	0.499	0.493	0.483	0.499	0.486	0.483	0.498	0.493	0.485	0.494
c4_lprm.8	0.506	0.505	0.516	0.506	0.505	0.519	0.507	0.505	0.510	0.478
c4_lprm.9	0.501	0.492	0.483	0.500	0.492	0.483	0.499	0.492	0.480	0.491
c4_lprm.10	0.527	0.524	0.530	0.527	0.523	0.528	0.527	0.523	0.511	0.522
c4_lprm.11	0.522	0.505	0.544	0.521	0.506	0.542	0.522	0.507	0.540	0.518
c4_lprm.12	0.540	0.542	0.541	0.538	0.541	0.541	0.538	0.541	0.542	0.542
c4_lprm.13	0.501	0.488	0.483	0.500	0.488	0.483	0.500	0.487	0.483	0.505
c4_lprm.14	0.504	0.490	0.483	0.505	0.491	0.483	0.506	0.490	0.483	0.506
c4_lprm.15	0.508	0.517	0.483	0.508	0.516	0.482	0.508	0.509	0.488	0.497
c4_lprm.16	0.506	0.493	0.490	0.504	0.495	0.490	0.498	0.516	0.490	0.522
c4_lprm.17	0.490	0.485	0.482	0.490	0.485	0.482	0.489	0.484	0.482	0.500
c4_lprm.18	0.491	0.484	0.482	0.491	0.484	0.482	0.490	0.484	0.483	0.487
c4_lprm.19	0.495	0.492	0.489	0.495	0.492	0.490	0.495	0.492	0.489	0.499
c4_lprm.20	0.503	0.502	0.487	0.503	0.501	0.487	0.502	0.500	0.483	0.478
c4_lprm.21	0.510	0.503	0.492	0.510	0.503	0.491	0.510	0.501	0.489	0.518
c4_lprm.22	0.529	0.525	0.537	0.529	0.525	0.539	0.530	0.525	0.536	0.557

Table 9. DR results for Case 5

	M1			M2			M3			M4
c5_aprm.1	0.954	0.946	0.953	0.951	0.941	0.954	0.950	0.942	0.953	0.98
	1.000	1.000	1.000	1.000	1.000	1.000	1.000	1.000	1.000	
	0.818	0.835	0.384	0.798	0.777	0.859	0.800	0.797	0.856	
c5_aprm.2	0.612	0.653	0.686	0.609	0.647	0.684	0.743	0.630	0.641	0.717
	0.645	0.689	0.730	0.657	0.697	0.724	0.790	0.699	0.804	
	0.525	0.542	0.654	0.542	0.542	0.655	0.446	0.495	0.666	

Table 10. Fundamental frequency results for Case 5

	M1			M2			M3			M4
c5_aprm.1	0.533	0.535	0.535	0.533	0.534	0.535	0.533	0.534	0.534	0.53
	0.542	0.577	0.587	0.422	0.435	0.422	0.421	0.439	0.463	
	0.548	0.559	0.501	0.551	0.554	0.556	0.551	0.548	0.557	
c5_aprm.2	0.520	0.507	0.516	0.519	0.507	0.516	0.514	0.506	0.509	0.494
	0.519	0.508	0.516	0.520	0.506	0.516	0.513	0.509	0.520	
	0.512	0.513	0.515	0.512	0.512	0.515	0.509	0.502	0.516	

Table 11. DR results for Case 6.1

	M1			M2			M3			M4
c6_aprm.1	0.489	0.531	0.550	0.489	0.535	0.545	0.454	0.461	0.555	0.589
c6_lprm.11	0.383	0.275	0.473	0.379	0.268	0.468	0.388	0.376	0.452	0.518
c6_lprm.12	0.225	0.286	0.317	0.221	0.312	0.356	0.147	0.383	0.360	0.295
c6_lprm.13	0.436	0.536	0.668	0.438	0.542	0.667	0.457	0.577	0.699	0.689
c6_lprm.14	0.388	0.473	0.323	0.593	0.469	0.345	0.402	0.484	0.320	0.664
c6_lprm.15	0.595	0.660	0.706	0.387	0.658	0.704	0.590	0.665	0.735	0.639
c6_lprm.16	0.784	0.810	0.814	0.788	0.809	0.814	0.780	0.809	0.816	0.818
c6_lprm.17	0.504	0.573	0.614	0.506	0.572	0.613	0.499	0.607	0.643	0.533
c6_lprm.18	0.595	0.649	0.669	0.592	0.645	0.669	0.585	0.640	0.705	0.686
c6_lprm.19	0.335	0.326	0.355	0.335	0.336	0.349	0.262	0.286	0.621	0.460
c6_lprm.110	0.205	0.150	0.368	0.203	0.174	0.368	0.301	0.257	0.347	0.491
c6_lprm.111	0.340	0.359	0.479	0.337	0.359	0.478	0.290	0.380	0.475	0.461
c6_lprm.112	0.321	0.416	0.500	0.325	0.417	0.498	0.348	0.422	0.548	0.362
c6_lprm.113	0.341	0.342	0.450	0.340	0.334	0.452	0.266	0.365	0.451	0.308
c6_lprm.114	0.372	0.414	0.469	0.369	0.427	0.474	0.414	0.406	0.504	0.474
c6_lprm.115	0.438	0.562	0.68	0.442	0.565	0.679	0.388	0.558	0.702	0.516
c6_lprm.116	0.444	0.569	0.681	0.448	0.572	0.680	0.450	0.557	0.714	0.703
c6_lprm.117	0.330	0.238	0.320	0.321	0.227	0.319	0.327	0.236	0.396	0.661
c6_lprm.118	0.276	0.297	0.364	0.270	0.287	0.357	0.303	0.3783	0.207	0.222

Table 12. Fundamental frequency results for Case 6.1

	M1			M2			M3			M4
c6_aprm.1	0.520	0.531	0.515	0.522	0.531	0.516	0.532	0.552	0.501	0.505
c6_lprm.11	0.491	0.511	0.503	0.492	0.514	0.503	0.497	0.535	0.509	0.481
c6_lprm.12	0.505	0.533	0.514	0.503	0.533	0.507	0.427	0.533	0.512	0.512
c6_lprm.13	0.517	0.527	0.527	0.518	0.527	0.528	0.519	0.529	0.530	0.511
c6_lprm.14	0.514	0.522	0.522	0.524	0.523	0.522	0.510	0.521	0.474	0.548
c6_lprm.15	0.524	0.532	0.531	0.514	0.532	0.531	0.525	0.532	0.533	0.509
c6_lprm.16	0.527	0.530	0.530	0.527	0.530	0.530	0.528	0.530	0.530	0.536
c6_lprm.17	0.512	0.524	0.531	0.512	0.525	0.530	0.512	0.526	0.631	0.502
c6_lprm.18	0.523	0.533	0.533	0.522	0.533	0.532	0.524	0.534	0.531	0.482
c6_lprm.19	0.520	0.546	0.562	0.522	0.548	0.560	0.522	0.564	0.558	0.468
c6_lprm.110	0.528	0.461	0.571	0.531	0.455	0.567	0.515	0.438	0.448	0.502
c6_lprm.111	0.501	0.498	0.515	0.502	0.501	0.515	0.489	0.506	0.522	0.457
c6_lprm.112	0.534	0.553	0.537	0.535	0.554	0.537	0.544	0.552	0.538	0.492
c6_lprm.113	0.501	0.492	0.519	0.502	0.496	0.514	0.479	0.496	0.508	0.429
c6_lprm.114	0.500	0.487	0.500	0.499	0.488	0.500	0.502	0.483	0.489	0.467
c6_lprm.115	0.518	0.524	0.524	0.518	0.525	0.525	0.515	0.523	0.528	0.525
c6_lprm.116	0.519	0.525	0.526	0.520	0.525	0.526	0.520	0.523	0.529	0.514
c6_lprm.117	0.581	0.486	0.501	0.482	0.485	0.501	0.490	0.487	0.485	0.519
c6_lprm.118	0.501	0.540	0.556	0.502	0.541	0.556	0.5	0.525	0.4258	0.443

Table 13. DR results for Case 6.2

	M1			M2			M3			M4
C6_aprm.2	0.915	0.923	0.950	0.914	0.920	0.950	0.910	0.917	0.952	0.923
C6_lprm.21	0.544	0.570	0.688	0.542	0.560	0.685	0.552	0.560	0.692	0.735
C6_lprm.22	0.305	0.348	0.498	0.313	0.358	0.500	0.354	0.333	0.504	0.589
C6_lprm.23	0.947	0.957	0.973	0.947	0.957	0.973	0.948	0.959	0.975	0.966
C6_lprm.24	0.866	0.891	0.915	0.863	0.888	0.912	0.858	0.882	0.906	0.935
C6_lprm.25	0.958	0.908	0.979	0.958	0.978	0.978	0.958	0.968	0.979	0.964
C6_lprm.26	0.981	0.986	0.988	0.982	0.987	0.989	0.981	0.987	0.988	0.963
C6_lprm.27	0.921	0.935	0.958	0.922	0.935	0.958	0.918	0.935	0.959	0.937
C6_lprm.28	0.949	0.963	0.968	0.951	0.964	0.970	0.953	0.967	0.968	0.981
C6_lprm.29	0.659	0.701	0.795	0.656	0.680	0.795	0.663	0.713	0.801	0.752
C6_lprm.210	0.522	0.579	0.678	0.526	0.579	0.678	0.519	0.559	0.725	0.672
C6_lprm.211	0.856	0.883	0.928	0.857	0.884	0.927	0.857	0.884	0.931	0.870
C6_lprm.212	0.845	0.877	0.914	0.847	0.876	0.915	0.840	0.870	0.913	0.884
C6_lprm.213	0.873	0.889	0.930	0.874	0.889	0.931	0.898	0.888	0.931	0.876
C6_lprm.214	0.875	0.881	0.927	0.877	0.882	0.928	0.882	0.879	0.924	0.919
C6_lprm.215	0.952	0.960	0.976	0.982	0.960	0.976	0.953	0.961	0.979	0.966
C6_lprm.216	0.953	0.961	0.976	0.952	0.961	0.976	0.952	0.961	0.977	0.966
C6_lprm.217	0.585	0.611	0.727	0.584	0.609	0.727	0.595	0.629	0.729	0.678
C6_lprm.218	0.546	0.517	0.579	0.545	0.526	0.578	0.577	0.475	0.598	0.700

Table 14. Fundamental frequency results for Case 6.2

	M1			M2			M3			M4
c6_aprm.2	0.521	0.522	0.522	0.521	0.522	0.522	0.521	0.522	0.522	0.518
c6_lprm.21	0.506	0.507	0.517	0.506	0.507	0.517	0.510	0.502	0.516	0.519
c6_lprm.22	0.522	0.518	0.516	0.524	0.520	0.516	0.522	0.473	0.517	0.528
c6_lprm.23	0.521	0.522	0.522	0.521	0.522	0.522	0.52	0.522	0.5219	0.520
c6_lprm.24	0.519	0.521	0.511	0.520	0.521	0.521	0.520	0.522	0.521	0.518
c6_lprm.25	0.521	0.522	0.522	0.521	0.522	0.522	0.521	0.522	0.522	0.521
c6_lprm.26	0.522	0.522	0.522	0.522	0.522	0.522	0.522	0.522	0.522	0.521
c6_lprm.27	0.521	0.522	0.521	0.521	0.522	0.521	0.520	0.522	0.521	0.519
c6_lprm.28	0.521	0.522	0.522	0.521	0.522	0.522	0.521	0.522	0.522	0.521
c6_lprm.29	0.508	0.514	0.518	0.509	0.515	0.518	0.510	0.516	0.517	0.517
c6_lprm.210	0.503	0.518	0.513	0.503	0.518	0.514	0.503	0.519	0.518	0.506
c6_lprm.211	0.520	0.520	0.522	0.520	0.521	0.522	0.520	0.521	0.522	0.518
c6_lprm.212	0.520	0.522	0.521	0.520	0.522	0.521	0.520	0.522	0.521	0.516
c6_lprm.213	0.520	0.522	0.522	0.521	0.522	0.522	0.522	0.522	0.522	0.519
c6_lprm.214	0.521	0.521	0.522	0.522	0.522	0.522	0.522	0.522	0.521	0.522
c6_lprm.215	0.521	0.522	0.522	0.521	0.522	0.522	0.521	0.522	0.522	0.520
c6_lprm.216	0.521	0.522	0.522	0.521	0.522	0.522	0.521	0.522	0.522	0.520
c6_lprm.217	0.503	0.510	0.517	0.503	0.511	0.517	0.505	0.517	0.519	0.507
c6_lprm.218	0.508	0.520	0.513	0.507	0.519	0.516	0.508	0.518	0.517	0.511

Singular system analysis

A singular system analysis to analyse neutronic power signals has been presented in Ref. [3]. In order to show the capabilities of this methodology, it has been applied to analyse three signals from the Forsmark 1 & 2 stability benchmark. The first signal is c1_aprm.1, which is a stationary one with low decay ratio, the second signal is c3_test.2, and presents more than one natural frequency, and the third signal is c5_aprm.2, which corresponds to a signal obtained during a small plant transient.

Signal 1: c1_aprm.1

To analyse this signal we used a window length n_w = 36 and we considered ten singular values for the analysis. These singular values are shown in Table 15.

Table 15. First ten singular values for signal c1_aprm.1

Number	Singular value	Number	Singular value
1	21914.16	6	12.93
2	62.71	7	9.16
3	59.60	8	6.65
4	37.72	9	5.28
5	21.74	10	3.96

We observe the large magnitude of the first singular value and two couples of singular values of similar magnitude.

In Figure 5, we compare the auto-correlation function (ACF) calculated from the original signal with the ACF calculated with the partially reconstructed signal using the first ten singular values.

Figure 5. Auto-correlation functions of the original and the partially reconstructed signals

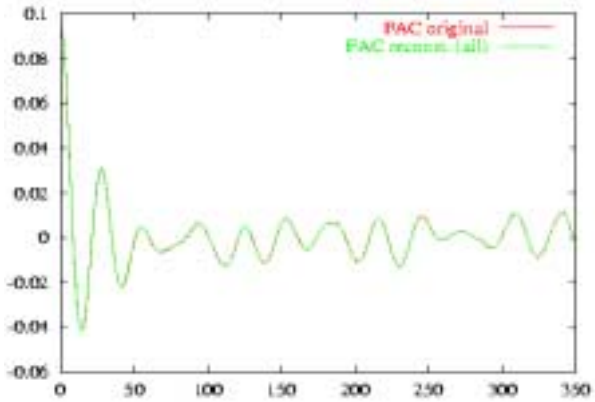

We observe that the main information of this signal is explained by a small number of singular values and their corresponding singular vectors.

In Figure 6, we show the power spectral densities of the original signal and in Figure 7 we show the power spectral density (PSD) of the partially reconstructed signal using the second and third singular values.

Figure 6. Power spectral density (PSD) of the original signal

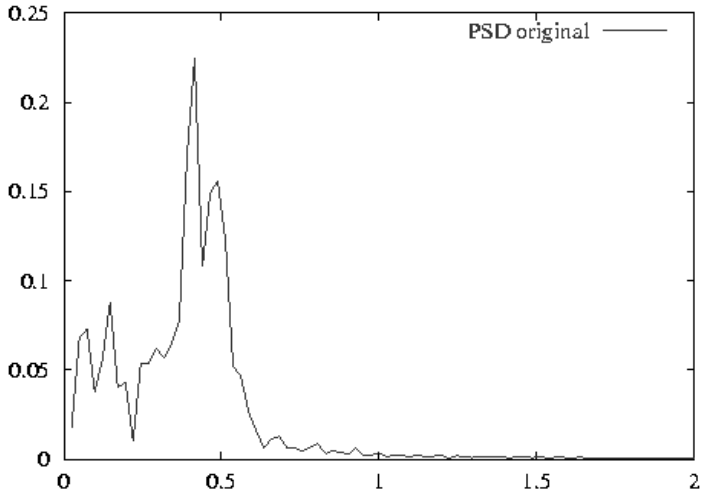

Figure 7. Power spectral density of the partially reconstructed signal (2,3)

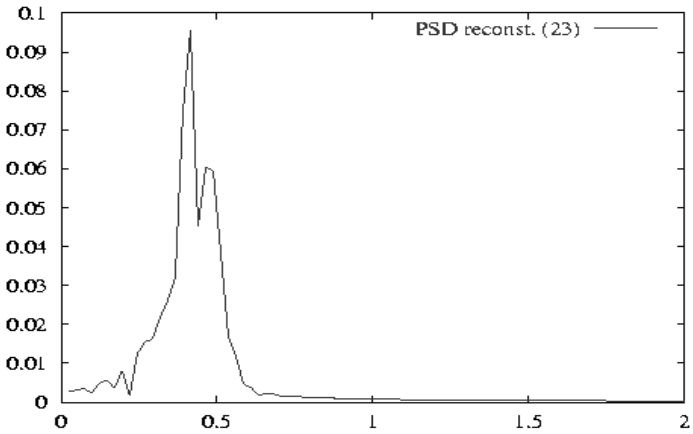

We observe that the power spectral density of the partially reconstructed signal does not show harmonics in the low part of the spectrum, remaining only the contribution of the natural frequency.

The stability analysis can be performed using the ACF [2] and also using the impulse response (IR) obtained from a high order (50) AR model for the signal. Essentially two methods have been proposed, one of which calculates the DR as the ratio of two consecutive maxima. We have called this method the Ratio Method. The other method uses an interpolator polynomial and we have denoted this the Interpolated Method. For more details see Refs. [2,12].

In Table 16 we present the reference results for the DR obtained from the Forsmak 1 & 2 benchmark, and the DR obtained from the ACF using the ratio and interpolated methods.

Table 16. DR values obtained from the ACF and the reference results

ACF		Reference	
Ratio	**Interpolated**	**DR**	**St. dev.**
0.75	0.30	0.49	0.08

We remark that the results obtained from the ACF are very different if we use either the Ratio or the Interpolated Methods. This clearly indicates that this signal presents a bad behaviour for the study of stability characteristics.

In Table 17, we present the DR values obtained from the ACF of the partially reconstructed signal using singular values 2 and 3 and the impulse response of this partially reconstructed signal calculated with an AR(10) model.

Table 17. DR values obtained from the ACF of the partially reconstructed signal (2,3) and the IR [AR(10)] for this signal

ACF		Reference	
Ratio	**Interpolated**	**Ratio**	**Interpolated**
0.47	0.32	0.50	0.42

We observe that the partially reconstructed signal has a better behaviour than the original signal for the determination of its stability characteristics.

Signal 2: c3_test.2

For analysis of the appropriate window length for this signal, 15 singular values were used and a value of n_w = 99 was obtained.

In Figure 8, we show the PSD for the original signal. We observe that this signal presents several harmonics close to the natural frequency.

Figure 8. Power spectral density of the original signal

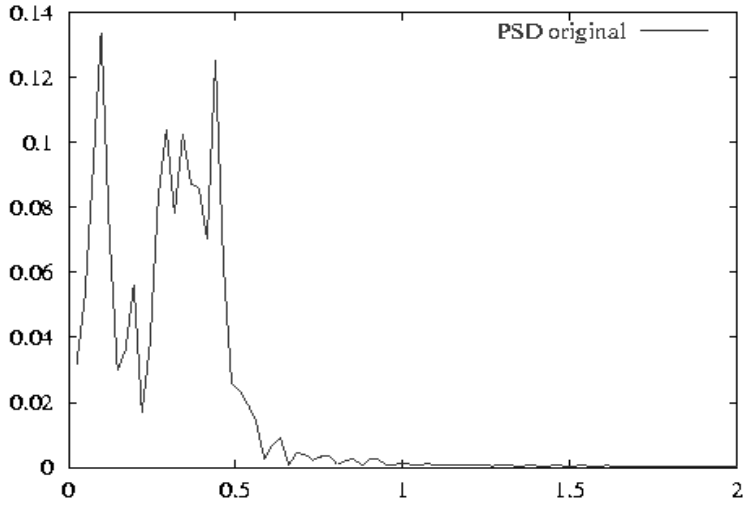

In Figure 9, we show the PSD of the partially reconstructed signal considering the singular values 6,7,8,9,10,11,12,13,14,15 and their corresponding singular vectors.

In this way we have been able to isolate the natural frequency oscillation from the low frequency contributions.

Figure 9. Power spectral density of the partially reconstructed signal (6,7,8,9,10,11,12,13,14,15)

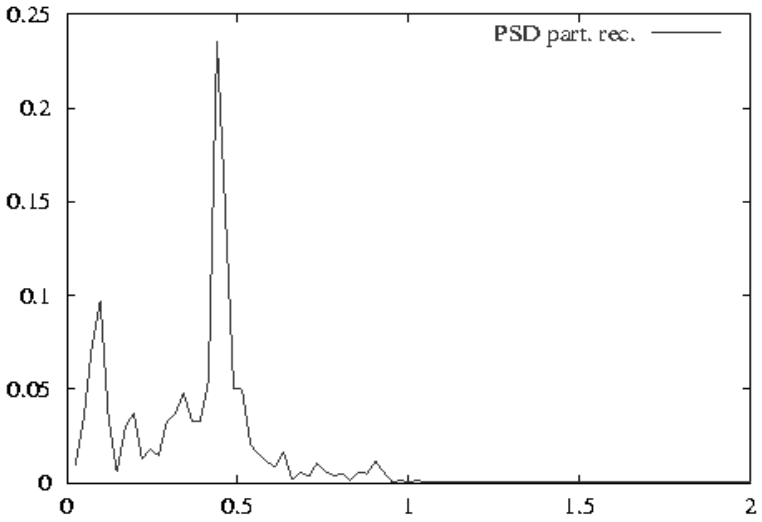

In Table 18, we show the DR values calculated from the ACF for this signal and the reference results.

Table 18. DR values obtained from the ACF and the reference results

ACF		Reference	
Ratio	**Interpolated**	**DR**	**St. Dev.**
–	0.61	0.36	0.15

We observe that this signal has a very bad behaviour for the determination of its stability characteristics, since the ratio method does not provide meaningful results.

In Table 19, we show the DR results for the partially reconstructed signal.

Table 19. DR values obtained from the ACF of the partially reconstructed signal (6,7,8,9,10,11,12,13,14,15)

Ratio	Interpolated
0.64	0.66

We observe that for the reconstructed signal both methods, the Ratio Method and the Interpolated Method provide similar results. Nevertheless these results differ from the reference ones, because the reference results take into account the low frequency oscillations which are damped oscillations.

Signal 3: c5_aprm.2

For this signal we used a window length $n_w = 58$ and 10 singular values were considered for the analysis.

To show that the first singular value is mainly associated with the signal trend, we present in Figure 10 the original signal and the partially reconstructed signal considering only the first singular value and its corresponding singular vector.

Figure 10. Original signal and partially reconstructed signal (1)

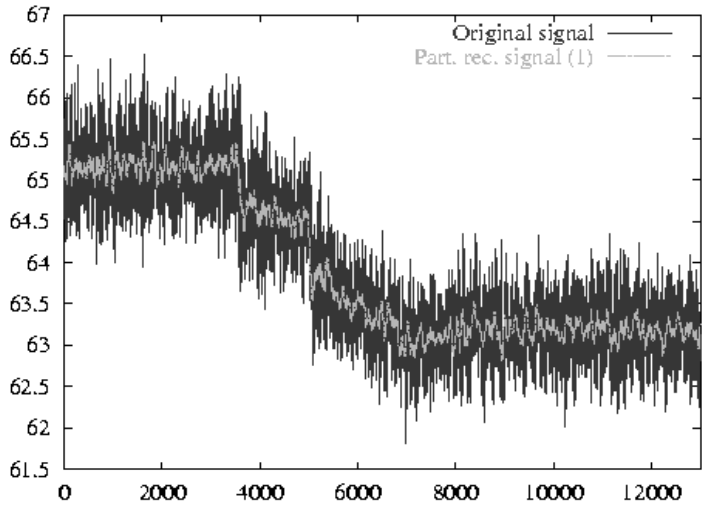

In Figure 11 we show the PSD of the original signal and in Figure 12 we have plotted the PSD for the partially reconstructed signal using singular values 2 and 3.

Figure 11. Power spectral density of the original signal

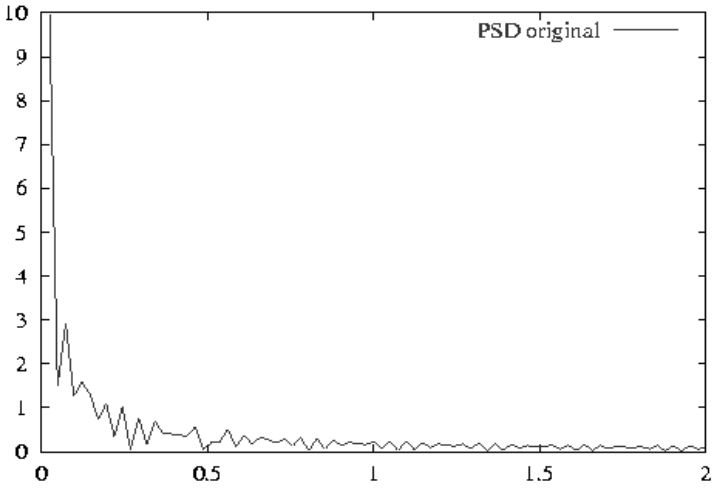

We observe that in the PSD calculated from the original signal we can not distinguish any predominant frequency, but in the PSD calculated from the partially reconstructed signal, the natural frequency peak can be distinguished clearly, indicating the main oscillatory contribution.

In Table 20, we show the DR values calculated from the ACF for this signal and the reference results.

Figure 12. Power spectral density of the partially reconstructed signal (2,3)

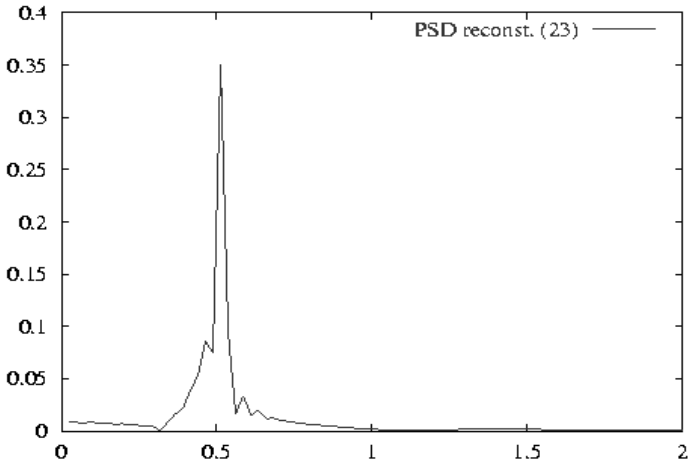

Table 20. DR values obtained from the ACF and the reference results

ACF		Reference	
Ratio	**Interpolated**	**DR**	**St. Dev.**
0.98	0.71	0.68	0.11

As it was the case for the signals studied above, we obtain different results with the ratio and the interpolated method. In Table 21, we show the results obtained from the partially reconstructed signal.

Table 21. DR values obtained from the ACF of the partially reconstructed signal (2,3)

Ratio	Interpolated
0.74	0.71

These results confirm the good behaviour observed in the PSD of the partially reconstructed signal.

REFERENCES

[1] J. Navarro-Esbrí, G. Verdú, D. Ginestar, J.L. Muñoz-Cobo, "Reactor Noise Analysis Based on the Singular Value Decomposition", *Ann. Nucl. Energy*, 25 (12), 907-921 (1998).

[2] T.H.J.J. Van der Hagen, I. Pázsit, O. Thomson, B. Melkerson, "Methods for the Determination of the In-phase and Out-of-phase Stability Characteristics of a Boiling Water Reactor", *Nuclear Technology*, 107, 193-214 (1994).

[3] G. Verdú, D. Ginestar, "Neutronic Signal Conditioning Using a Singular System Analysis", accepted for publication in *Ann. Nucl. Energy*.

[4] J.A. Cadzow, "Spectral Estimation: An Overdetermined Rational Model Equation Approach", Proceedings of the IEEE, 70, 9, 907-939 (1982).

[5] G.H. Golub, C.F. Van Loan, "Matrix Computations", Second Edition, John Hopkins University Press, Baltimore (1990).

[6] D.S. Broomhead, G.P. King, "Extracting Qualitative Dynamics from Experimental Data", *Physica D*, 20, 217-236 (1986).

[7] P.P. Kanjilal and S. Palit, "On Multiple Pattern Extraction Using Singular Value Decomposition", *IEEE Transactions on Signal Processing*, 43, 6, 1 536-1 540 (1995).

[8] G. Verdú, D. Ginestar, M.D. Bovea, P. Jiménez, J. Pea, J.L. Muoz-Cobo, "Complex Lyapunov Exponents from Short and Noisy Sets of Data, Application to Stability Analysis of BWRs", *Ann. Nucl. Energy*, 24 (12), 997-994 (1997).

[9] G. Giona, F. Lentini, V. Cimagalli, "Functional Reconstruction and Local Prediction of Chaotic Time Series", *Physical Review A*, 44, 3 496-3 502 (1991).

[10] R. Brown, "Calculating Lyapunov Exponents for Short and/or Noisy Data Sets", *Physical Review E*, 47, 3 962-3 969 (1993).

[11] G. Verdú, D. Ginestar, V. Vidal, "Dynamics Reconstruction Using Orthonormal Functions", *App. Math. Letters.*, 12, 39-43 (1999).

[12] R. Sanchis, G. Verdú, J.L. Muñoz-Cobo, M.D. Bovea, D. Ginestar, I.M. Tkachenko, "On-line Lyapunov-exponent Estimation of the Decay Ratio in BWR NPP", Proc. of SMORN VII, Vol. 1, Avignon, 19-23 June (1995).

[13] "Forsmark 1 & 2 BWR Stability Benchmark: Time Series Analysis Methods for Oscillations During BWR Operation", NEA/NSC/DOC(99)9.

Annex 3

METHODOLOGIES AND RESULTS PRESENTED BY PSU*

Participants

Anthony J. Baratta
Kostadin N. Ivanov
Robert M. Edwards
Miguel Cecenas-Falcon
Jorge Solis-Rodarte

Introduction

The Organisation for Economic Co-operation and Development (OECD), through the Nuclear Energy Agency (NEA), has organised a database containing extensive power plant process measurements to investigate boiling water reactor stability. Computer codes evaluating stability can be tested and validated using this valuable data. The first collection of plant data was used to specify the Ringhals 1 Stability Benchmark [1,2].

The Forsmark 1 and 2 stability benchmark is a follow-up activity, organised to focus in time series analysis of power signals to determine the stability parameters of the system. The stability parameters considered are decay ratio (DR) and natural frequency.

The Forsmark benchmark is divided into six cases, each case being composed by stability tests performed at Forsmark units 1 and 2 during the period 1989-1997. The data is stored as time series sampled at a frequency of 25 HZ, decimated to 12.5 Hz.

Methodology

The time series analysis is performed using the auto-regressive method (AR) for stationary cases and auto-regressive moving average method (ARMA) for non-stationary series.

For stationary power measurements, the following procedure was applied:

- The series is normalised by its mean value and then the new unitary mean is subtracted to obtain a normalised zero-mean signal.
- The auto-correlation of the series is computed.

* The Pennsylvania State University
Nuclear Engineering Department
USA

- The Yule-Walker equations are solved for the auto-regressive parameters.
- An impulse response of the auto-regressive model is computed.
- If the impulse response is smooth, the decay ratio is computed ignoring the first peak and averaging the decay ratios obtained with subsequent peaks and valleys.
- If the impulse response contains frequencies other than the natural frequency of the system, a low pass filter is applied to remove the extra peaks and valleys contributed by the high frequency noise.

For non-stationary measurements, a similar procedure was used, but omitting the first step and fitting an ARIMA model [3] instead of the AR.

In addition to the Yule-Walker equations needed for the auto-regressive part, the non-linear algebraic equations for the moving average parameters were iteratively solved. A model of the form (p,1,q) was used, where p and q are the order of the AR and MA parts, respectively.

For each case, the order of the auto-regressive and moving average parts was determined by minimising the Schwarz BIC information criteria, and the uncertainty was estimated by varying the model order around the optimal value.

Time series analysis

Case 1

This case consists of 14 APRM readings corresponding to 14 different power and flow operating conditions. Each time series contains 5.4 minutes of power measurements. The data for this case is stationary and the method of auto-regression was applied to determine decay ratios and resonant frequencies. Table 1 shows the results obtained for this case.

Table 1. Decay ratio and frequency results for Case 1

Data name	DR	DR uncertainty	Frequency	Frequency uncertainty
f1_boc_13_3	0.42	0.0345	0.45	0.0099
f1_boc_13-4	0.52	0.0113	0.45	0.0033
f1_boc_14-1	0.30	0.1401	0.46	0.0041
f1_boc_14-3	0.39	0.1245	0.48	0.0045
f1_boc_14-4	0.49	0.0245	0.48	0.0077
f1_moc_14_2	0.44	0.1565	0.47	0.0089
f1_boc_15	0.51	0.1234	0.51	0.0083
f1_moc_16	0.27	0.0905	0.50	0.0192
f2_moc_13	0.55	0.0310	0.40	0.0032
f2_uppst_14	0.45	0.0250	0.43	0.0169
f2_boc_14	0.36	0.0903	0.43	0.0295
f2_moc_14	0.68	0.0284	0.45	0.0132
f2_uppst_15	0.43	0.0773	0.40	0.0097
f2_moc_15	0.56	0.0769	0.48	0.0107

For all 14 series, the AR method was used. Series 4 and 8 have a high frequency signal mounted in the data, of 5.8 and 2.6 Hz respectively. This added contribution to the system noise can be handled if the impulse response is processed by a low-pass filter before the search for the maximums and minimums required by the DR calculations.

Further work in Series 4 and 8 includes an ARIMA model of order (20,1,0). The results for these two series are shown Table 2.

Table 2. Results for Series 4 and 8 using an ARIMA (20,1,0)

Data name	DR	DR uncertainty	Frequency	Frequency uncertainty
f1_boc_14-3	0.52	0.13	0.49	0.04
f1_moc_16	0.41	0.08	0.50	0.04

These new decay ratios are higher than the previous DRs computed with the AR model.

Case 2

This case consists of two non-stationary series of 18.7 minutes. An ARIMA model (p,1,q) was used to be developed to fit the experimental data and obtain decay ratios and frequencies. The AR and MA orders p and q were chosen to minimise the BIC information criteria. The order q was always between 19 and 21, while q was between 0 and 2.

The long series c2_test.l1 contains 13 963 points, and it was divided into four sub-series with three segments of 4 000 points and a last segment with 2 000 points. The different segments of Series 1 yielded similar decay ratios, except for the second segment, which gave a higher decay ratio. The last segment produced a similar decay ratio to the whole series, even when it only contains 160 seconds of measurements. The results for this case are shown in Table 3.

Table 3. Decay ratio and frequency results for Case 2.1

Data name	DR	DR uncertainty	Frequency	Frequency uncertainty
c2_test.l1	0.35	0.12	0.44	0.03
c2_test.s11	0.36	0.13	0.41	0.03
c2_test.s21	0.49	0.06	0.41	0.03
c2_test.s31	0.36	0.19	0.43	0.05
c2_test.s41	0.37	0.11	0.43	0.03

The structure of Series 2 is analogue to that of Series 1. It contains higher decay ratios, and the last segment has a lower decay ratio. This result was expected, given the short length of the last segment. The results obtained for these series are shown in Table 4.

Case 3

Case 3 consists of five power measurements of 5.4 minutes each. The specification states that these five series are contaminated with plant control system effects.

Table 4. Decay ratio and frequency results for Case 2.2

Data name	DR	DR uncertainty	Frequency	Frequency uncertainty
c2_test.l2	0.57	0.12	0.50	0.01
c2_test.s12	0.61	0.08	0.52	0.02
c2_test.s22	0.59	0.08	0.49	0.02
c2_test.s32	0.54	0.12	0.51	0.03
c2_test.s42	0.42	0.11	0.48	0.04

The impulse responses obtained from the AR models for these series do not show frequencies other than the natural frequency of the system. Table 5 shows the results obtained for this case.

Table 5. Decay ratio, frequency and dominant poles for Case 3

Data name	DR	DR uncertainty	Frequency	Frequency uncertainty	Dominant poles
C3_test.1	0.27	0.01	0.39	0.01	0.51 + -2.45i
					-1.01 + 0.00i
					-2.08 + -23.07i
C3_test.2	0.29	0.07	0.39	0.01	-0.48 + -2.45i
					-1.03 + 0.00i
					-1.95 + -5.46i
C3_test.3	0.23	0.09	0.42	0.03	-0.63 + -2.64i
					-1.64 + 0.00i
					-1.81 + -24.59i
C3_test.4	0.34	0.02	0.47	0.01	-0.50 + -2.92i
					-1.01 + 0.00i
					-1.89 + -36.93i
C3_test.5	0.34	0.02	0.47	0.01	-0.50 + -2.92i
					-1.01 + 0.00i
					-1.89 + -36.93i

To find the dominant poles, the discrete poles in the z-domain were computed from the auto-regressive coefficients. The poles closer to the unity circle were chosen and then transformed to the s-plane using the sampling period of 0.08 sec.

Series 4 and 5 seem to have the same stability properties. Further analysis showed that both series are identical.

Case 4

Case 4 contains one APRM and 22 LPRM measurements. A mixture of a global oscillation and a regional oscillation is specified.

The LPRMs at positions 23 and 34 show higher decay ratios, followed by positions 20, 9 and 7. This represents the right-half section of the core.

Table 6. Decay ratio and frequency results for Case 4

Data name	DR	DR uncertainty	Frequency	Frequency uncertainty
c4_lprm.1	0.91	0.01	0.49	0.01
c4_lprm.2	0.91	0.01	0.49	0.01
c4_lprm.3	0.92	0.01	0.49	0.01
c4_lprm.4	0.87	0.08	0.49	0.01
c4_lprm.5	0.85	0.01	0.50	0.01
c4_lprm.6	0.85	0.02	0.50	0.01
c4_lprm.7	0.78	0.02	0.50	0.01
c4_lprm.8	0.69	0.16	0.51	0.01
c4_lprm.9	0.81	0.04	0.51	0.01
c4_lprm.10	0.71	0.12	0.53	0.01
c4_lprm.11	0.77	0.01	0.52	0.01
c4_lprm.12	0.52	0.16	0.53	0.01
c4_lprm.13	0.82	0.01	0.51	0.01
c4_lprm.14	0.81	0.01	0.51	0.01
c4_lprm.15	0.79	0.06	0.51	0.01
c4_lprm.16	0.80	0.02	0.52	0.01
c4_lprm.17	0.86	0.01	0.50	0.01
c4_lprm.18	0.84	0.01	0.49	0.01
c4_lprm.19	0.63	0.11	0.50	0.01
c4_lprm.20	0.70	0.12	0.51	0.01
c4_lprm.21	0.77	0.01	0.51	0.01
c4_lprm.22	0.36	0.15	0.54	0.04
c4_aprm	0.81	0.04	0.51	0.01

Case 5

Case 5 contains two non-stationary APRM measurements taken during a small plant transient. For this case an ARMA model was fitted.

Both power series correspond to APRM readings, the first series containing 5.6 minutes of data, and the second series 18.6 minutes. The results obtained for this case are shown in Table 7.

Table 7. Decay ratio, frequency and dominant poles for Case 5

Data name	DR	DR uncertainty	Frequency	Frequency uncertainty	Dominant poles
C5_aprm.1	0.98	0.03	0.53	0.01	-0.01 + -3.33i
					-0.05 + 0.00i
					-0.30 + -6.68i
C5_aprm.2	0.54	0.05	0.49	0.02	-0.31 + -3.09i
					-0.89 + -10.00i
					-0.90 + -37.42i

The first series exhibits a limit cycle, and the decay ratio is close to the unity. For the second series the AR model gave a decay ratio of 0.54, which agrees with the value shown in the table.

Case 6

Case 6 contains APRM and LPRM signals for two different operating conditions. The obtained results for the decay ratio and the fundamental frequency for Case 6.1 are presented in Table 8.

Table 8. Decay ratio and frequency results for Case 6.1

Data name	DR	DR uncertainty	Frequency	Frequency uncertainty
c6_lprm.11	0.08	0.06	0.43	0.03
c6_lprm.21	0.08	0.04	0.50	0.06
c6_lprm.31	0.24	0.13	0.50	0.02
c6_lprm.41	0.23	0.01	0.51	0.01
c6_lprm.51	0.27	0.14	0.50	0.03
c6_lprm.61	0.56	0.11	0.52	0.01
c6_lprm.71	0.25	0.14	0.49	0.03
c6_lprm.81	0.50	0.04	0.53	0.02
c6_lprm.91	*0.10	0.03	0.46	0.08
c6_lprm.101	*0.15	0.03	0.50	0.06
c6_lprm.111	*0.10	0.07	0.46	0.04
c6_lprm.121	**			
c6_lprm.131	*0.10	0.07	0.46	0.06
c6_lprm.141	*0.27	0.09	0.53	0.06
c6_lprm.151	0.24	0.13	0.50	0.04
c6_lprm.161	0.26	0.14	0.50	0.02
c6_lprm.171	0.09	0.11	0.43	0.03
c6_lprm.181	**			
c6_aprm.1	*0.29	0.10	0.49	0.02

* Contains extra high frequency noise; a low pass filter had to be used to obtain the decay ratios.

** Very low decay rations, difficult to obtain from a non-oscillatory impulse response.

The results obtained for the decay ratio and the fundamental frequency for Case 6.1 are presented in Table 9.

For Test 2, series pairs 5-6, 7-8, 13-14 and 15-16 show higher decay ratios, and every pair is located in a common string. It is interesting to observe that the locations of those four strings are symmetrical (strings 11, 6, 31 and 24), and that all those strings with high decay ratios are located in the left-half side of the core.

The series for the test number 2 (63.3% power and 4 298 kg/s core flow) have in general wider amplitudes than those of test number 1 (64.4% power and 4 416 kg/s core flow), and the decay ratios for the test number 2 are also higher. This can suggest a relationship between the amplitude of the fluctuations around the mean value and the stability of the system. It is known that as an instability develops, the oscillation will reach a noticeable amplitude and frequency, easy to be visually observed from a time plot.

Table 9. Decay ratio and frequency results for Case 6.2

Data name	DR	DR uncertainty	Frequency	Frequency uncertainty
c6_lprm.12	0.20	0.15	0.51	0.03
c6_lprm.22	0.23	0.08	0.51	0.04
c6_lprm.32	0.88	0.10	0.52	0.01
c6_lprm.42	0.70	0.04	0.52	0.01
c6_lprm.52	0.90	0.07	0.52	0.01
c6_lprm.62	0.96	0.03	0.52	0.01
c6_lprm.72	0.83	0.15	0.52	0.01
c6_lprm.82	0.89	0.02	0.52	0.01
c6_lprm.92	0.37	0.17	0.52	0.03
c6_lprm.102	0.30	0.16	0.50	0.03
c6_lprm.112	0.61	0.18	0.53	0.02
c6_lprm.122	0.59	0.13	0.52	0.01
c6_lprm.132	0.72	0.18	0.53	0.01
c6_lprm.142	0.77	0.09	0.52	0.01
c6_lprm.152	0.88	0.09	0.52	0.01
c6_lprm.162	0.89	0.09	0.52	0.01
c6_lprm.172	0.28	0.14	0.50	0.04
c6_lprm.182	0.33	0.07	0.51	0.06
c6_aprm.2	0.84	0.07	0.52	0.01

Reduced-order model analysis

Using a reduced-order model and optimal estimation techniques, the decay ratio for the system can be estimated. It can be shown that the gain of the thermal-hydraulic feedback reactivity is basically the void reactivity coefficient, and the stability properties of the system strongly depend on this value. A non-linear estimator is used to estimate the feedback gain based on point kinetics for the forward loop and linear transfer functions for the feedback loop.

The transfer functions are obtained from a frequency-domain code, such as LAPUR. This method considers the operating conditions of the plant and can produce a decay ratio as a function of time. The method can be applied to both stationary and non-stationary power measurements.

The benchmark is intended to study the different time series analysis methods, and plant data other than power measurements is not supplied. The specification provides the power and flow for Cases 1 and 6 only. To prepare LAPUR runs, both power and flow conditions must be known, as well as extra information regarding core geometry and power distributions.

To evaluate the method, a gross LAPUR input deck was prepared with one thermal-hydraulic channel and assumed a bottom-peaked axial power distribution.

The results show that the method has a tendency to underestimate the natural frequency of the system at small decay ratios. As the decay ratios increases, the estimates for the frequency improve.

Case 1

This case consists of 14 APRM readings corresponding to 14 different power and flow operating conditions. Each time series contains 5.4 minutes of power measurements. Table 10 shows the results obtained for this case.

Table 10. Decay ratio and frequency results for Case 1 with the reduced-order model

Data name	DR	Frequency
f1_boc_13_3	0.58	0.35
f1_boc_13-4	0.50	0.33
f1_boc_14-1	0.25	0.27
f1_boc_14-3	0.26	0.28
f1_boc_14-4	0.70	0.37
f1_moc_14_2	0.51	0.32
f1_boc_15	0.37	0.29
f1_moc_16	0.22	0.27
f2_moc_13	0.34	0.29
f2_uppst_14	0.52	0.33
f2_boc_14	0.23	0.27
f2_moc_14	0.43	0.30
f2_uppst_15	0.26	0.27
f2_moc_15	0.27	0.28

Case 4

Even when the power and flow conditions are not specified for this case, the method was applied as an exercise. This case is of particular interest because of the local oscillations present in the core.

The LPRMs at positions 23 and 34 show higher decay ratios, followed by positions 20, 9, and 7. This represents the right-half section of the core. The obtained results for this case are shown in Table 11.

Case 6

Case 6 contains APRM and LPRM signals for two different operating conditions. The results obtained for Case 6.1 are shown in Table 12.

The results obtained for Case 6.1 are shown in Table 13.

Table 11. Decay ratio and frequency results for Case 4 with the reduced-order model

Data name	DR	Frequency
c4_lprm.1	0.90	0.48
c4_lprm.2	0.90	0.48
c4_lprm.3	0.91	0.49
c4_lprm.4	0.91	0.49
c4_lprm.5	0.91	0.49
c4_lprm.6	0.89	0.47
c4_lprm.7	0.86	0.45
c4_lprm.8	0.74	0.40
c4_lprm.9	0.85	0.45
c4_lprm.10	0.50	0.36
c4_lprm.11	0.88	0.47
c4_lprm.12	0.27	0.29
c4_lprm.13	0.87	0.46
c4_lprm.14	0.88	0.47
c4_lprm.15	0.87	0.46
c4_lprm.16	0.88	0.47
c4_lprm.17	0.90	0.48
c4_lprm.18	0.88	0.46
c4_lprm.19	0.85	0.45
c4_lprm.20	0.84	0.44
c4_lprm.21	0.88	0.47
c4_lprm.22	0.86	0.45
c4_aprm	0.90	0.48

Table 12. Decay ratio and frequency results for Case 6.1 with the reduced-order model

Data name	DR	Frequency
c6_lprm.11	0.41	0.31
c6_lprm.21	0.20	0.26
c6_lprm.31	0.26	0.27
c6_lprm.41	0.15	0.25
c6_lprm.51	0.27	0.28
c6_lprm.61	0.17	0.25
c6_lprm.71	0.24	0.27
c6_lprm.81	0.14	0.25
c6_lprm.91	0.28	0.28
c6_lprm.101	0.17	0.25
c6_lprm.111	0.28	0.28
c6_lprm.121	0.15	0.25
c6_lprm.131	0.29	0.28
c6_lprm.141	0.16	0.25
c6_lprm.151	0.27	0.28
c6_lprm.161	0.25	0.27
c6_lprm.171	0.33	0.29
c6_lprm.181	0.15	0.25
c6_aprm.1	0.22	0.27

Table 13. Decay ratio and frequency results for Case 6.1 with the reduced-order model

Data name	DR	Frequency
c6_lprm.12	0.68	0.38
c6_lprm.22	0.71	0.39
c6_lprm.32	0.77	0.42
c6_lprm.42	0.75	0.41
c6_lprm.52	0.79	0.43
c6_lprm.62	0.92	0.53
c6_lprm.72	0.79	0.43
c6_lprm.82	0.21	0.26
c6_lprm.92	0.67	0.38
c6_lprm.102	0.68	0.38
c6_lprm.112	0.45	0.31
c6_lprm.122	0.20	0.26
c6_lprm.132	0.76	0.42
c6_lprm.142	0.87	0.48
c6_lprm.152	0.87	0.48
c6_lprm.162	0.86	0.48
c6_lprm.172	0.69	0.39
c6_lprm.182	0.19	0.25
c6_aprm.2	0.72	0.40

REFERENCES

[1] T. Lefvert, “BWR Stability Benchmark, Final Specifications”, OECD/NEA/NSC/DOC(94)13.

[2] T. Lefvert, “Ringhals 1 Stability Benchmark, Final Report”, OECD/NEA/NSC/DOC(96)22, November 1996.

[3] G.E.P. Box, G.M. Jenkins, G.C. Reinsel, “Time Series Analysis: Forecasting and Control”, Prentice-Hall, 1994.

Annex 4

METHODOLOGIES AND RESULTS PRESENTED BY TSUKUBA*

Methodology

Decay ratio DR is calculated based on the normalised correlation function $R(t)$:

$$DR = R(T\_p)$$

where T_p = period of oscillation.

A statistical method for averaging sequences of peak amplitudes in $R(t)$ is not adopted because of the existence of long-time coherence and entrainment by the noise sources. Frequency is calculated based on the AR PSD with the use of the least square (LSQ) fitting algorithm. In this case, the ARPAD that gives the minimum AIC is selected. Among the various algorithms (Yule-Walker, Burg and others) for the AR model fitting, the LSQ algorithm was chosen because of its ability to separate peaks of resonant frequencies in many cases.

Results

Case 1

Table 1. DR and frequency results for Case 1

Data name	DR	DR uncertainty	Frequency	Frequency uncertainty
c1_aprm.1	0.33	± 0.1	0.45	± 0.04
c1_aprm.2	0.42	± .10	0.45	± 0.04
c1_aprm.3	0.30	± 0.07	0.45	± 0.04
c1_aprm.4	0.23	± 0.10	0.47	± 0.04
c1_aprm.5	0.20	± 0.10	0.48	± 0.04
c1_aprm.6	0.42	± 0.15	0.47	± 0.04
c1_aprm.7	0.15	± 0.05	0.51	± 0.03
c1_aprm.8	0.37	± 0.12	0.50	± 0.04
c1_aprm.9	0.43	± 0.15	0.49	± 0.03

* H. Konno
Institute of Information Sciences and Electronics
University of Tsukuba, Tsukuba, Ibaraki 305-8573
Tel: +81-298-53-5016, Fax: +81-298-53-6471
E-mail: hkonno@sakura.cc.tsukuba.ac.jp

Table 1. DR and frequency results for Case 1 (*cont.*)

Data name	DR	DR uncertainty	Frequency	Frequency uncertainty
c1_aprm.10	0.30	± 0.10	0.44	± 0.03
c1_aprm.11	0.18	± 0.10	0.47	± 0.03
c1_aprm.12	0.56	± 0.12	0.45	± 0.03
c1_aprm.13	0.37	± 0.15	0.40	± 0.04
c1_aprm.14	0.38	± 0.10	0.48	± 0.03

Case 2

Table 2. DR and frequency results for Case 2

Data name	DR	DR uncertainty	Frequency	Frequency uncertainty
c2_test.l1	0.16	± 0.10	0.43	± 0.02
c2_test.l2	0.34	± 0.10	0.52	± 0.02
c2_test.s11	0.10	± 0.10	0.49	± 0.04
c2_test.s12	0.32	± 0.12	0.53	± 0.02
c2_test.s21	0.21	± 0.07	0.43	± 0.04
c2_test.s22	0.33	± 0.10	0.51	± 0.02
c2_test.s31	0.19	± 0.07	0.41	± 0.10
c2_test.s32	0.22	± 0.07	0.52	± 0.02
c2_test.s41	0.18	± 0.07	0.38	± 0.12
c2_test.s42	0.33	± 0.10	0.48	± 0.02

Case 3

Table 3. DR and frequency results for Case 3

Data name	DR	DR uncertainty	Frequency	Frequency uncertainty
c3_test.1	0.17	± 0.10	0.38	± 0.04
c3_test.2	0.21	± 0.10	0.33	± 0.12
c3_test.3	0.10	± 0.10	0.45	± 0.04
c3_test.4	0.24	± 0.12	0.47	± 0.04
c3_test.5	0.24	± 0.12	0.47	± 0.04

Case 4

Table 4. DR and frequency results for Case 4

Data name	DR	DR uncertainty	Frequency	Frequency uncertainty
c4_aprm	0.85	± 0.05	0.47-0.52	± 0.02
c4_lprm.1	0.89	± 0.05	0.47-0.52	± 0.02
c4_lprm.2	0.90	± 0.05	0.47-0.52	± 0.02
c4_lprm.3	0.90	± 0.05	0.47-0.52	± 0.02
c4_lprm.4	0.85	± 0.05	0.47-0.52	± 0.02
c4_lprm.5	0.82	± 0.05	0.47-0.52	± 0.02
c4_lprm.6	0.81	± 0.05	0.47-0.52	± 0.02
c4_lprm.7	0.77	± 0.05	0.47-0.52	± 0.02
c4_lprm.8	0.62	± 0.05	0.47-0.52	± 0.02
c4_lprm.9	0.78	± 0.05	0.47+0.52	± 0.02
c4_lprm.10	0.67	± 0.15	0.52	± 0.04
c4_lprm.11	0.71	± 0.15	0.47-0.52	± 0.02
c4_lprm.12	0.45	± 0.05	0.52	± 0.03
c4_lprm.13	0.77	± 0.05	0.47-0.52	± 0.02
c4_lprm.14	0.75	± 0.05	0.47-0.52	± 0.02
c4_lprm.15	0.76	± 0.05	0.47-0.52	± 0.04
c4_lprm.16	0.80	± 0.05	0.47-0.52	± 0.02
c4_lprm.17	0.83	± 0.05	0.47-0.52	± 0.02
c4_lprm.18	0.82	± 0.05	0.47-0.52	± 0.02
c4_lprm.19	0.45	± 0.15	0.47-0.52	± 0.02
c4_lprm.20	0.67	± 0.2	0.47-0.52	± 0.02
c4_lprm.21	0.67	± 0.2	0.47-0.52	± 0.04
c4_lprm.22	0.38	± 0.1	0.47-0.52	± 0.04

Case 5

Table 5. DR and frequency results for Case 5

Data name	DR	DR uncertainty	Frequency	Frequency uncertainty
c5_test.1	0.98	± 0.05	0.52	± 0.02
c5_test.2	0.47	± 0.1	0.50	± 0.02

Table 6. First four dominant poles for Case 5

Data name	Frequency (Hz)	Real part	Imaginary part
c5_test.1	0.52	-0.937	0.120
	1.08	-0.819	0.447
	1.49	-0.676	0.712
	1.27	-0.138	0.046
c5_test.2	0.50	0.975	0.000
	0.41	-0.819	0.525
	0.27	0.676	0.712
	0.13	-0.130	0.977

Case 5

Table 7. DR and frequency results for Case 6

Data name	DR	DR uncertainty	Frequency	Frequency uncertainty
c6_aprm.1	0.16	± 0.05	0.52	± 0.04
c6_aprm.2	0.70	± 0.1	0.51	± 0.02
c6_lprm.11	0.09	± 0.05	0.50	± 0.04
c6_lprm.12	0.21	± 0.12	0.50	± 0.03
c6_lprm.21	0.10	± 0.07	0.50	± 0.04
c6_lprm.22	0.20	± 0.12	0.51	± 0.04
c6_lprm.31	0.12	± 0.07	0.51	± 0.04
c6_lprm.32	0.80	± 0.1	0.51	± 0.02
c6_lprm.41	0.20	± 0.05	0.50	± 0.04
c6_lprm.42	0.63	± 0.1	0.51	± 0.02
c6_lprm.51	0.13	± 0.1	0.51	± 0.03
c6_lprm.52	0.80	± 0.05	0.51	± 0.02
c6_lprm.61	0.42	± 0.1	0.51	± 0.03
c6_lprm.62	0.92	± 0.05	0.51	± 0.02
c6_lprm.71	0.15	± 0.05	0.51	± 0.03
c6_lprm.72	0.71	± 0.05	0.51	± 0.02
c6_lprm.81	0.57	± 0.1	0.51	± 0.02
c6_lprm.82	0.87	± 0.1	0.51	± 0.02
c6_lprm.91	0.03	± 0.05	0.53	± 0.06
c6_lprm.92	0.30	± 0.1	0.51	± 0.02
c6_lprm.101	0.13	± 0.05	0.52	± 0.04
c6_lprm.102	0.32	± 0.1	0.50	± 0.03
c6_lprm.111	0.11	± 0.05	0.51	± 0.03
c6_lprm.112	0.50	± 0.05	0.51	± 0.02
c6_lprm.121	0.23	± 0.1	0.52	± 0.03
c6_lprm.122	0.53	± 0.05	0.51	± 0.02

Table 7. DR and frequency results for Case 6 (*cont.*)

Data name	DR	DR uncertainty	Frequency	Frequency uncertainty
c6_lprm.131	0.04	± 0.05	0.50	± 0.04
c6_lprm.132	0.53	± 0.1	0.51	± 0.02
c6_lprm.141	0.28	± 0.05	0.49	± 0.04
c6_lprm.142	0.68	± 0.1	0.51	± 0.02
c6_lprm.151	0.12	± 0.05	0.51	± 0.03
c6_lprm.152	0.78	± 0.1	0.51	± 0.02
c6_lprm.161	0.13	± 0.05	0.51	± 0.03
c6_lprm162	0.82	± 0.05	0.51	± 0.02
c6_lprm171	0.08	± 0.05	0.44-0.53	± 0.12
c6_lprm172	0.20	± 0.1	0.51	± 0.03
c6_lprm181	0.21	± 0.1	0.48	± 0.06
c6_lprm182	0.42	± 0.1	0.50	± 0.04

Annex 5

METHODOLOGIES AND RESULTS PRESENTED BY PSI*

Introduction

Time series analysis is an essential part of BWR stability analysis. From the measured or calculated time series the stability properties such as the decay ratio (as a linear stability criterion) can be extracted. Hence, the uncertainties of the time series analysis should be known. These uncertainties should be the basis for the assessment of the accuracy of the calculated results of system codes. To this end, this time series analysis benchmark was defined as a follow-up benchmark to the first NEA stability benchmark 1996 (Ringhals 1). In this summary the PSI results from 1999 are discussed. In PSI, we use parametric and non-parametric time series analysis approaches but the current (year 2000) methodology is developed in some detail (see Askari and Hennig, [1]). The results from 1999, documented here, will be verified using new methods and the results will be published later.

Methodology

Non-parametric methods

Roughly speaking, the non-parametric approaches are based on the multi-parametric fit of the auto-correlation function of the filtered power spectral density of the discrete time signals (Behringer, Hennig [2]). First, the signal is filtered at the power spectrum peak in order to avoid background problems. The (modified) auto-correlation (ACF) function is estimated by an inverse fast Fourier transform [2] (all codes written by K. Behringer). The parameters to be determined by the (in general 3- or 5-parametric) fit are the amplitude and the oscillation frequency of the ideal ACF, the decay time constant, the background amplitude and, optionally, a decay constant of the background in the frequency domain (this method has recently been modified [2]).

Parametric methods

In the framework of the parametric time series analysis constructed a linear dynamical system characterised by a difference equation (or a system of difference equations) on the basis of a measured or calculated discontinuous parameter time series [3,4]. The unknown coefficients of the difference equation(s) are to be determined by a fit procedure based on a maximum likelihood technique. In practice, the coefficients are obtained by minimising the sum of the squared residuals (called system identification problem). Depending of the number of coefficients on the left and right-hand side of the model equation (see e.g. [3]) used for the identification procedure we generate an auto-regressive (AR)

* D. Hennig
Paul Scherrer Institute
Switzerland

or an auto-regressive moving average (ARMA) model. In addition to the estimation of the model parameter, the determination of the model order is essential. In 1999 we used a so-called plateau method for the ARMA best model order estimation and an Akaike information criterion for the AR model order optimisation (since then, both methods have been revised and extended, e.g. for ARMA model order optimisation we use the Akaike and the Ressanen [1] criterion and the plateau method was improved by Askari, see [1]). The decay ratio (DR) of the oscillation with the so-called natural frequency (NF) of the reactor is determined from the poles of the transfer function of the estimated linear dynamical system [4]. In our experience, the parametric methods provide more reliable results than the non-parametric ones (particularly for small and large DRs). The parametric time series analysis at PSI is based on the MATLAB toolboxes "system identification" and "signal analysis" [5,6].

Results

Parametric methods

Case 1

Table 1. NEA benchmark: Time series analysis. Task 1: c1_aprm.i, i = 1…14.

Case no.	Data name	DR ARMA model (plateau method)	DR AR model (optimised by AIC)	DR uncertainty (ARMA) (±)	NF (Hz) ARMA/AR	Frequency uncertainty (ARMA) (±)
1	f1_boc_13_3	0.50	0.42	0.07	0.46/0.46	0.01
2	f1_boc_13_4	0.51	0.51	0.09	0.46/0.46	0.01
3	f1_boc_14_1	0.5	0.63	0.10	0.48/0.49	0.02
4	f1_boc_14_3	0.53	0.42	0.09	0.49/0.46	0.03
5	f1_boc_14_4	0.51	0.51	0.03	0.49/0.49	0.01
6	f1_moc_14_2	0.55	0.51	0.05	0.49/0.49	0.02
7	f1_boc_15	0.59	0.68	0.08	0.52/0.53	0.02
8	f1_moc_16	0.45	0.46	0.03	0.52/0.53	0.02
9	f2_moc_13	0.50	0.53	0.05	0.40/0.40	0.01
10	f2_uppst_14	0.45	0.49	0.05	0.44/0.44	0.01
11	f2_boc_14	0.50	0.56	0.03	0.46/0.46	0.02
12	f2_moc_14	0.78	0.78	0.03	0.46/0.46	0.01
13	f2_uppst_15	0.45	0.46	0.05	0.40/0.40	0.01
14	f2_moc_15	0.65	0.71	0.05	0.48/0.49	0.02

The given ARMA model uncertainties base on the standard deviation of the (old) plateau method.

Case 2

Table 2. NEA benchmark: Time series analysis. Task 2.

Case no.	Data name	DR ARMA model (plateau method)	DR AR model (optimised by AIC)	DR uncertainty (ARMA) (±)	NF (Hz) ARMA/AR	Frequency uncertainty (ARMA) (±)
1	c2_test.L1	0.35	0.55	0.07	0.45/0.46	0.03
2	c2_test.S11	0.20	0.20	0.10	0.44/0.42	0.03
3	c2_test.S21	0.45	0.41	0.08	0.46/0.43	0.03
4	c2_test.S31	0.40	0.47	0.05	0.46/0.48	0.03
5	c2_test.S41	0.40	0.39	0.05	0.46/0.41	0.03
6	c2_test.L2	0.63	0.60	0.05	0.53/0.51	0.03
7	c2_test.S12	0.60	0.64	0.05	0.54/0.53	0.02
8	c2_test.S22	0.60	0.55	0.05	0.52/0.51	0.03
9	c2_test.S32	0.53	0.45	0.05	0.53/0.51	0.03
10	c2_test.S42	0.58	0.42	0.08	0.51/0.50	0.03

Case 3

Table 3. NEA benchmark: Time series analysis. Task 3.

Case no.	Data name	DR ARMA model (plateau method)	DR uncertainty (±)	NF/ Hz	Frequency uncertainty (±) Hz	Real and imaginary parts of the dominant poles (at the z-plane)	DR/NF for the same time series after filtering (5th order butterworth highpass, cut frequency 0.25 Hz)
1	c3_test1	0.4	0.09	0.42	0.02	0.95 ± i*0.20 0.93 ± i*0.07	0.60±0.05 0.36±0.03 Hz
2	c3_test2	0.31	0.1	0.43	0.03	0.94 ± i*0.22 0.89 ± i*0.06	0.61±0.04 0.33±0.04 Hz
3	c3_test3	0.4	0.1	0.46	0.03	0.94 ± i*0.22 0.94 ± i*0.09	0.70±0.09 0.31±0.04 Hz 0.55±0.05* 0.47±0.03 Hz
4 (5)	c3_test4	0.42	0.15	0.48	0.03	0.94 ± i*0.23 0.92 ± i*0.06	0.74±0.03 0.31±0.03 (0.65;0.45 Hz)*†

* Second peak at the ASD (calculated from the poles of the transfer function).

† By using a 5th order highpass filter with a cut frequency at 0.35 Hz → DR = 0.80±0.05, NF = 0.48±0.03 Hz.

Case 4

Table 4. NEA benchmark: Time series analysis. Task 4: c4_aprm; c4_lprm_i, i = 1…22.

Case no.	Data name	DR ARMA model (plateau method)	DR AR model (optimised by AIC)	DR uncertainty (ARMA) (±)	NF (Hz) ARMA/AR	Frequency uncertainty (ARMA) (±)
1	c4_aprm	0.85	0.85	0.04	0.51/0.48	0.01
2	c4_lprm.23:1	0.90	0.90	0.04	0.49/0.49	0.01
3	c4_lprm.23:2	0.90	0.90	0.04	0.49/0.49	0.01
4	c4_lprm.23:3	0.90	0.95	0.04	0.49/0.48	0.01
5	c4_lprm.23:4	0.88	0.88	0.04	0.49/0.49	0.01
6	c4_lprm.34:1	0.86	0.85	0.04	0.50/0.50	0.02
7	c4_lprm.34:2	0.85	0.85	0.04	0.50/0.50	0.02
8	c4_lprm.34:3	0.80	0.76	0.05	0.50/0.50	0.02
9	c4_lprm.34:4	0.76	0.71	0.09 (!)	0.50/0.51	0.02
10	c4_lprm.7:1	0.80	0.81	0.04	0.51/0.50	0.01
11	c4_lprm.7:4	0.75	0.73	0.04	0.53/0.53	0.02
12	c4_lprm.11:1	0.77	0.76	0.05	0.52/0.52	0.01
13	c4_lprm.11:4	0.58	0.56	> 0.10 (!)	0.53/0.53	0.03
14	c4_lprm.20:1	0.81	0.83	0.04	0.51/0.51	0.01
15	c4_lprm.20:2	0.81	0.8	0.03	0.51/0.51	0.01
16	c4_lprm.20:3	0.80	0.80	0.04	0.51/0.51	0.01
17	c4_lprm.20:4	0.80	0.81	0.04	0.52/0.52	0.02
18	c4_lprm.9:1	0.85	0.86	0.04	0.49/0.49	0.01
19	c4_lprm.9:2	0.85	0.85	0.02	0.49/0.49	0.01
20	c4_lprm.9:3	0.80	0.79	0.04	0.50/0.50	0.02
21	c4_lprm.9:4	0.75	0.74	0.05	0.50/0.50	0.01
22	c4_lprm.31:1	0.77	0.76	0.04	0.51/0.51	0.01
23	c4_lprm.31:4	0.39	0.36	> 0.10 (!)	0.53/0.55	0.03

Case 5

Table 5. NEA benchmark: Time series analysis. Task 5.

Case no.	Data name	DR ARMA model (plateau method)	DR uncertainty (±)	NF/ Hz	Frequency uncertainty (±) Hz	Real and imaginary parts of the dominant poles (at the z-plane)
1*	c5_aprm.1 (t = 1-144s)	Limit cycle/ unstable DR = 1.00	0.01	0.53	0.01	0.97 ± i*0.26 0.86 ± i*0.51
	c5_aprm.1 (t = 145-336 s)	0.94	0.02	0.54	0.01	0.96 ± i*0.27 0.81 ± i*0.49
2*	c5_aprm.2 (t = 1-250 s)	0.67**	0.05	0.49**	0.02	0.95 ± i*0.24 0.94 ± i*0.07
	c5_aprm.2 (t = 640-1 170 s)	0.47***	0.05	0.5	0.02	0.94 ± i*0.24 0.93 ± i*0.06

* Time series non-stationary, hence divided into two parts.
** AR model (model order AIC optimised): DR = 0.75, NF = 0.51 Hz.
*** AR model (model order AIC optimised): DR = 0.58, NF = 0.51 Hz.

Case 6.1

Table 6. NEA Benchmark: Time series analysis. Task 6: OP 1: c6_aprm.1; c6_lprm.j1; j = 1:9.

Case no.	Data name	DR ARMA model (plateau method)	DR AR model	DR uncertainty (ARMA) (±)	NF (Hz) ARMA/AR	Frequency uncertainty (ARMA) (±)
1	c6_lprm23:4	0.22	–*	0.08	0.49	0.02
2	c6_lprm26:4	0.20	–	0.06	0.51	0.01
3	c6_lprm11:4	0.80	–	0.08	0.53	0.01
4	c6_lprm6:4	0.50	–	0.05	0.52	0.01
5	c6_lprm34:4	0.20	–	0.06	0.52	0.02
6	c6_lprm20:4	0.20	–	0.05	0.53	0.02
7	c6_lprm31:4	0.35	–	0.04	0.50	0.02
8	c6_lprm24:4	0.43	–	0.06	0.52	0.01
9	c6_lprm29:4	0.20	–	0.05	0.50	0.02
10	c6_aprm2	0.35	–	0.05	0.49	0.02
11	c6_lprm23:1	0.15	–	–	0.46	–
12	c6_lprm26:1	0.42	–	0.04	0.52	0.01
13	c6_lprm11:1	0.58	–	0.05	0.52	0.01
14	c6_lprm6:1	0.50		0.05	0.51	0.02
15	c6_lprm34:1	0.32	–	0.08	0.52	0.02
16	c6_lprm20:1	0.23	–	0.05	0.53	0.02
17	c6_lprm31:1	0.20	–	0.08	0.51	0.02
18	c6_lprm24:1	0.44	–	0.05	0.52	0.01
19	c6_lprm29:1	0.19	–	0.05	0.47	0.02

* "–" means: not checked.

Case 6.2

Table 7. NEA Benchmark: Time series analysis. Task 6: OP 2[**]: c6_aprm.2; c6_lprm.j2; j = 1:9.

Case no.	Data name	DR ARMA model (plateau method)	DR AR model (optimised by AIC)	DR uncertainty (ARMA) (±)	NF (Hz) ARMA/AR	Frequency uncertainty (ARMA) (±)
1	c6_lprm23:4	0.25	0.25	0.04	0.51/0.53	0.02
2	c6_lprm26:4	0.95	0.98	0.03	0.52/0.52	0.01
3	c6_lprm11:4	0.98	–[*]	0.01	0.52	
4	c6_lprm6:4	0.95	0.93	0.02	0.52/0.52	0.01
5	c6_lprm34:4	0.51	0.67	0.02	0.50/0.51	0.02
6	c6_lprm20:4	0.83	0.9	0.05	0.52/0.52	0.02
7	c6_lprm31:4	0.82	0.93	0.05	0.52/0.52	0.02
8	c6_lprm24:4	0.95	–	0.04	0.52	
9	c6_lprm29:4	0.51	–	0.03	0.51	0.02
10	c6_aprm2	0.90	–	0.03	0.52	0.01
11	c6_lprm23:1	0.54	–	–	0.51/–	–
12	c6_lprm26:1	0.95	0.98	0.04	0.52/0.52	0.01
13	c6_lprm11:1	0.98	0.94	0.03	0.52/0.52	0.01
14	c6_lprm6:1	0.97			0.52	
15	c6_lprm34:1	0.65	0.5	0.05	0.51/0.51	0.02
16	c6_lprm20:1	0.98	0.95	0.10 (!)	0.52/0.52	0.02
17	c6_lprm31:1	0.95	0.94	0.10 (!)	0.52/0.52	0.02
18	c6_lprm24:1	0.95	-	0.04	0.52	0.02
19	c6_lprm29:1	0.58	0.41	0.10 (!)	0.52/0.51	0.02

[*] "–" means: not checked.

[**] See: G. Analytis, D. Hennig, J. Karlsson, "The Physical Mechanism of Core-wide and Local Instabilities at the Forsmark-1 BWR", PSI-Report No. 98-13.

Non-parametric methods (see [2])

Case	ACF results		ARMA results	
	DR	**NF/Hz**	**DR**	**NF/Hz**
c1_aprm3	0.582	0.483	0.500	0.480
c1_aprm4	0.555	0.485	0.530	0.490
c1_aprm12	0.723	0.462	0.780	0.460
c2_test.L1	0.224	0.458	0.350	0.450
c2_test.L2	0.583	0.525	0.630	0.530
c2_test.s42	0.451	0.504	0.580	0.510
c3_test.1	0.377	0.415	0.400	0.420
c3_test.2	0.312	0.400	0.310	0.430
c3_test.3	0.347	0.425	0.400	0.460
c3_test.4	0.619	0.472	0.420	0.480
c4_lprm.8	0.717	0.507	0.760	0.500
c4_lprm12	0.704	0.536	0.580	0.530
c4_lprm22	0.569	0.532	0.390	0.530
c6_lprm22	0.567	0.522	0.250	0.510
c6_lprm210	0.547	0.512	0.510	0.500
c6_lprm211	0.976	0.523	0.980	0.520
c6_lprm212	0.884	0.521	0.830	0.520
c6_lprm213	0.993	0.524	0.950	0.520
c6_lprm214	0.983	0.523	0.820	0.520
c6_lprm215	0.997	0.523	0.950	0.520

Conclusions (preliminary)

- The DR ratio (and NF) estimation on the basis of system identification approaches (parametric methods) is a very efficient and reliable method. For system identification and signal analysis powerful MATLAB [5] toolboxes are available.

- The plateau method should be improved (more quantitative plateau estimation; this has been changed in the new version).

- The model order optimisation on the basis of optimisation criteria (Akaike and others) should be used for AR and ARMA methods (included in the new version).

- The strong space dependence of the DR for Case 6.2 is until now not explainable from the physical point of view (see [7]).

REFERENCES

[1] B. Askari, D. Hennig, “High Performance Time Series Analysis Code”, PSI internal report, Nov. 2000 (in progress).

[2] K. Behringer, D. Hennig, “On the Decay Ratio Determination in BWR Stability Analysis by the Auto-correlation Technique” (paper in preparation).

[3] T. Söderström, P. Stoica, “System Identification”, Prentice-Hall, 1989.

[4] D. Hennig, “Time Series Analysis for BWR Stability Studies”, PSI internal report, TM-41-97-1, 1997.

[5] The Math-Work, Inc., “MATLAB: High Performance Numerical Computation and Visualization Software, System Identification Toolbox”, Natick, Massachusetts.

[6] The Math-Work, Inc., “MATLAB: High Performance Numerical Computation and Visualization Software, Signal Analysis Toolbox”, Natick, Massachusetts.

[7] G. Analytis, D. Hennig, J. Karlsson, “The Physical Mechanism of Core-wide and > Local Instabilities at the Forsmark-1 BWR”, NURETH-9, San Francisco, 1999.

Annex 6

METHODOLOGIES AND RESULTS PRESENTED BY JAERI*

Methodology

The methodology adopted for the evaluation of decay ratio (DR) and oscillation frequency is:

- The direct current (DC) component from the time series was removed. (The best fit linear trend was removed.) For Case 5, the time series was divided into small parts (~2 000 points), and from each time series the best fit linear trend was removed.

- The time series data was fitted using an auto-regressive (AR) model. The order of the model was determined by the Akaike Information Criteria (AIC). For the fitting, the Yule-Walker method was adopted.

- The impulse response of the identified AR model was calculated.

- The impulse response was fitted by the function:

$$y(t) = \lambda_1 e^{-\lambda_2 t}\cos(\lambda_3 t + \lambda_4)$$

  where $y(t)$ is an impulse response at time t; λ_1-λ_4 are fitting parameters. The Gauss-Newton method of the non-linear optimisation technique was used. The fitting region of impulse response was ~10 sec. from the beginning, but the first 1 second of time series was discarded. In Case 6 some fittings failed, and in these cases the next 10 seconds were used for the second fitting.

- DR and the oscillation frequency f are evaluated by:

$$DR = e^{-(2\pi\lambda_2/\lambda_3)}, \quad f = \frac{2\pi}{\lambda_3}$$

In the Appendix, source codes of the calculation program are given.

* Tomoaki Suzudo
Control and AI Laboratory
Japan Atomic Energy Research Institute
Tokai-mura, Ibaraki-ken, 319-1195 Japan
suzudo@clsu3aO.tokai.jaeri.go.jp

Results

Case 1

Table 1. Results of the DR and the frequency for Case 1

Name of the time series	DR	Frequency (Hz)
c1_aprm.1	0.422	0.464
cl_aprm.2	0.523	0.458
c1_aprm.3	0.511	0.497
cl _aprm.4	0.549	0.480
cl_aprm.5	0.534	0.497
cl_aprm.6	0.559	0.477
cl_aprm.7	0.657	0.524
cl_aprm.8	0.495	0.537
c1_aprm.9	0.487	0.403
c1_aprm.10	0.482	0.455
c1_aprm.11	0.440	0.484
c1_aprm.12	0.757	0.467
c1_aprm.13	0.383	0.416
c1_aprm.14	0.658	0.492

Case 2

Table 2. Results of the DR and the frequency for Case 2

Name of the time series	DR	Frequency (Hz)
c2_test.Ll	0.339	0.457
c2_test.S11	0.113	0.361
c2_test.S21	0.476	0.451
c2_test.S31	0.323	0.482
c2_test.S41	0.263	0.442
c2_test.L2	0.622	0.537
c2_test.S12	0.625	0.529
c2_test.S22	0.656	0.524
c2_test.S32	0.539	0.512
c2_test.S42	0.50	0.502

Case 3

Table 3. Results of the DR and the frequency for Case 3

Name of the time series	DR	Frequency (Hz)
c3_test.1	0.287	0.417
c3_test.2	0.345	0.422
c3_test.3	0.177	0.434
c3_test.4	0.744	0.489
c3_test.4	0.744	0.489

Case 4

Table 4. Results of the DR and the frequency for Case 4

Name of the time series	DR	Frequency (Hz)
c4_aprm	0.768	0.508
c4_lprm.1	0.834	0.494
c4_lprm.2	0.829	0.495
c4_lprm.3	0.845	0.494
c4_lprm.4	0.859	0.489
c4_lprm.5	0.774	0.498
c4_lprm.6	0.768	0.498
c4_lprm.7	0.765	0.502
c4_lprm.8	0.729	0.504
c4_lprm.9	0.703	0.504
c4_lprm.10	0.749	0.527
c4_lprm.11	0.714	0.522
c4_lprm.12	0.677	0.531
c4_lprm.13	0.737	0.504
c4_lprm.14	0.728	0.505
c4_lprm.15	0.790	0.513
c4_lprm.16	0.796	0.520
c4_lprm.17	0.854	0.494
c4_lprm.18	0.845	0.495
c4_lprm.19	0.785	0.497
c4_lprm.20	0.756	0.500
c4_lprm.21	0.770	0.511
c4_lprm.22	0.422	0.512

Case 5

Table 5. Results of the DR and the frequency for Case 5

Name of the time series	DR	Frequency (Hz)
c5_aprm.1	1.020	0.526
c5_aprm.2	0.823	0.520

Case 6

Table 6. Results of the DR and the frequency for Case 6.1

Name of the time series	DR	Frequency (Hz)
c6_aprm.1	0.503	0.532
c6_lprm.11	0.382	0.526
c6_lprm.21	0.552	0.464
c6_lprm.31	0.296	0.489
c6_1prm.41	(0.321)	(0.512)
c6_lprm.51	0.589	0.525
c6_1prm.61	(0.781)	(0.528)
c6_lprm.71	0.477	0.522
c6_lprm.81		
c6_lprm.91	0.266	0.669
c6_1prm.101		
c6_1prm.111	0.277	0.558
c6_1prm.121	(0.545)	(0.520)
c6_1prm.131	0.239	0.586
c6_lprm.161		
c6_lprm.151	0.296	0.494
c6_1prm.161	0.318	0.492
c6_1prm.171	0.733	0.394
c6_lprm.181		

The values in parentheses are evaluated by fitting the impulse response during 10-20 [s] from the beginning, as the fitting of 1-10 [s] failed because of some low frequency noise. The empty space means that both fittings failed.

Table 7. Results of the DR and the frequency for Case 6.2

Name of the time series	DR	Frequency (Hz)
c6_aprm.2	(0.965)	(0.523)
c6_lprm.12	0.575	0.499
c6_1prm.22	0.332	0.471
c6_lprm.32	0.986	0.524
c6_lprm.42	(0.959)	(0.523)
c6_lprm.52	0.981	0.524
c6_1prm.62	1.006	0.520
c6_lprm.72	0.986	0.524
c6_lprm.82	(0.91)	(0.523)
c6_1prm.92	0.923	0.528
c6_lprm.102	(0.709)	(0.516)
c6_lprm.112	0.966	0.523
c6_lprm.122	(0.952)	(0.521)
c6_lprm.132	0.935	0.524
c6_lprm.142	(0.965)	(0.523)
c6_lprm.152	0.988	0.524
c6_lprm.162	0.983	0.524
c6_lprm.172	0.603	0.503
c6_1prm.182	(0.507)	(0.498)

The values in parentheses are evaluated by fitting the impulse response during 10-20 [s] from the beginning, as the fitting of 1-10 [s] failed because of some low frequency noise.

An alternative stability indicator based on non-linear dynamical theory

Characteristic quantities of non-linear dynamics

The dynamics reconstruction method proposed by Takens [1], enabled any random and non-linear phenomena to be investigated from their time-series data. Let u_i be a scalar time-series data of interest sampled from signal $u(t)$ with the frequency of f_s,[Hz], and let x_i be d-dimensional time series data obtained from u_i by the embedding method as:

$$x_i = \left\{ u_i, u_{i+1}, \ldots, u_{i+(d-1)} \right\} \tag{1}$$

where d is called an embedding dimension. The trajectory drawn by x_i, in the d-dimensional state space can be the reconstruction of the dynamics if the embedding dimension d and the sampling frequency, f_s, are selected properly. Let an f be a characteristic frequency of the dynamics, then the two-dimensional trajectory drawn by $\{u(t),u(t + 1/4f)\}$ is the best reconstruction; consequently the reconstruction by Eq. (1) at least covers the frequency of:

$$\frac{f_s}{4(d-1)} \le f \le \frac{f_s}{4} \tag{2}$$

Normally f_s is large enough compared to f, therefore one must only make sure that d is not too small to reconstruct the dynamics properly.

The reconstructed dynamics have the characteristic quantities of the original dynamics; for instance the information dimension, Lyapunov exponents and the entropy are principal quantities characterising the dynamics. It is not practical, however, to estimate the Lyapunov exponent in the presence of stochastic noise. Estimating the entropy is not practical either because it is calculated from the estimated Lyapunov exponents.

The information dimension, based on the probability measure, is one way of defining the fractal dimension; it is the same as the number of unstable oscillation modes (or excited modes), unless these modes are correlated with one another. For instance, the information dimension is zero when the system is asymptotically stable; the quantity becomes one when an oscillation mode is excited and causes a limit-cycle; the quantity becomes n when n oscillation modes are excited and any pair of these are not correlated, a regime which is called quasi-periodic motion. If some modes from the n excited mode are correlated, the information dimension for that dynamics may be less than n, and may sometimes be non-integer, which means the system has chaotic motion. The information dimension is therefore an important quantity of the non-linear dynamics. See Ref. [2] for more details of the embedding method and the information dimension.

The slope of the correlation integral (SOCI) is a generalisation of the information dimension, and is defined as in Ref. [3]:

$$\nu(r) = \frac{d\left(\log C(r)\right)}{d\log(r)} \tag{3}$$

where $C(r)$ is a correlation integral, and is defined as:

$$C(r) = \frac{1}{N}\left(number\ of\ \ pairs\ \ (i,j)\ whose\ distance\ \left|x_i - x_j\right|\ is\ less\ than\ r\right) \tag{4}$$

where N is the number of x_i and x_j combinations and r is the measuring resolution or the amplitude of the fluctuation to be examined. Eq. (4) is recognised as measuring the spatial correlation of reconstructed dynamics. See Ref. [4] for the basic concept of the correlation integral. SOCI provides "the information dimension" for a certain value of the resolution, which as a whole forms a continuous spectrum, and we can investigate the dynamics accordingly as the resolution changes. If the calculated SOCI does not vary within a certain range of r, the reconstructed dynamics has a self-similarity and its value indicates the information dimension.

Stability indicator

When the time series data is caused by dumping oscillation with stochastic noise, its trajectory given by the dynamics-reconstruction moves around the equilibrium.

On the other hand, sustained or limit-cyc1e oscillation causes the trajectory to be a closed orbit and the trajectory can then be characterised by the diameter of the orbit, say r_0. The SOCI given by such time series data has a peak at its right edge because the correlation integral soars at $r = r_0$. In other words, SOCI shows the spatial correlation of the trajectory. One can easily deduce the

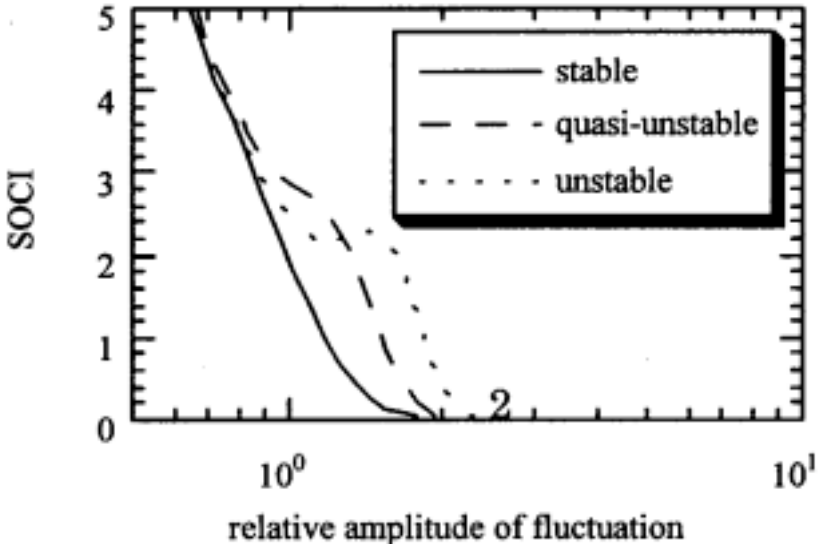

position of the peak r_0 corresponding to the peak-to-peak amplitude of the oscillation. In this way SOCI can discriminate dumping oscillations from persistent oscillations in a noisy environment and consequently can present the signals in another way.

In actual cases, we see three kinds of SOCI shapes, all of which are depicted in the above figure. The solid line is simply a decreasing curve and the corresponding oscillation is presumed to be stable. The dashed and dotted lines have a small bump and a peak, respectively. The bump is recognised by checking that the second-order derivative of the curve has positive value. The peak is recognised by checking that the first-order derivative of the curve has positive value. From the numerical study it is found that the peak appears only when the oscillation becomes limit-cycle, i.e. unstable (see Ref. [3]). The existence of the small bump is accordingly understood as a sign of quasi-unstable state.

In summary it is possible to classify the time-series data into the above three states, stable, quasi-unstable and unstable.

Results

Because this method is meaningful at the border between stability and instability, Case 6.2 was selected as a test case. Because the characteristic frequency *f* is ~0.5 Hz and the sampling frequency *f* is 12 Hz, the embedding dimension *d* was set to be 20 as it satisfies Eq. (2).

The obtained results, shown in Table 8 with the corresponding decay ratios, indicate that the SOCI can be an alternative stability indicator and can complement the decay ratio, especially when we determine the accurate limit to the stable behaviour of reactor core. The data processing of SOCI is simpler than that of DR, and neither fitting nor model estimation are used, therefore the results from different persons do not vary as much as DR, which is another advantage of SOCI.

Table 8. Results for Case 6.2

Data name	DR	SOCI indicator
c6_lprm.62	1.006	Unstable
c6_lprm.152	0.988	Quasi-unstable
c6_lprm.32	0.986	Quasi-unstable
c6_lprm.72	0.986	Quasi-unstable
c6_lprm.162	0.983	Quasi-unstable
c6_lprm.52	0.981	Quasi-unstable
c6_lprm.82	0.981	Quasi-unstable
c6_lprm.112	0.966	Stable
c6_aprm.2	0.965	Quasi-unstable
c6_lprm.142	0.965	Quasi-unstable
c6_lprm.42	0.959	Quasi-unstable
c6_lprm.122	0.952	Stable
c6_lprm.132	0.935	Stable
c6_lprm.92	0.923	Stable
c6_lprm.102	0.709	Stable
c6_lprm.172	0.603	Stable
c6_lprm.12	0.575	Stable
c6_lprm.182	0.507	Stable
c6_lprm.22	0.332	Stable

REFERENCES

[1] F. Takens, *Lecture Note in Mathematics*, 898, 336 (198l).

[2] J-P. Eckmann and D. Ruelle, *Rev. Mod. Phys*., 57 [3], 617 (1985).

[3] T. Suzudo, *Nucl. Sci. Eng*., 113,145 (1993).

[4] P. Grassberger and I. Procaccia, *Physica*, 9D, 189 (1983).

Appendix

SOURCE CODES OF CALCULATION PROGRAM

MATLAB version 5 was used to calculate the DR. Source codes of three newly developed functions for this purpose, “decay_ratio”, “impul”, “impulerr” are given in the following pages. The main function is “decay_ratio” and the remaining two functions are called by “decay_ratio”. The Optimization TOOLBOX and Identification TOOLBOX are necessary. The usage of the function is simple. Type “[DR,FREQ,NA]=decay_ratio(Y,T);” at the MATLAB command interpreter, where DR, FREQ, NA are the obtained decay ratio, the fundamental frequency and the AR order determined by Akaike Information Criteria (AIC). Y is the time series vector examined such as Y(l)=63.2, Y(2)=64.5, ... and T is a sampling period of Y.

```
function [yi,na] = impul(y,T,maxn)
%       function[yi, na] = IMPUL(yj,maxn)
%
%       Calculate impulse response of the time-series data
%
%       y:              Time-series data
%       T:              Sampling Period
%       maxn:   Maximum AR-order for searching AIC order
%       y¡:             impulse
%       na:             AR-order
%
%       Note    Yule-Waker Method is used.
%       AIC is used to, determine the AR-
%               ldentification TOOLBOX is necessary.
%
%            OCT-27-1998 T. Suzudo

%
%       Determine the AR-order
%
nn=l:maxn;
nn=nn';
V=arxstruc(y,y,nn);
na=selstruc(V,'AIC');
if maxn == na
                        warning('Maximum AR-order is not enough');
end

%       AR Identification

th=ar(y,na,'yW’,-1, T);
%
%       Impulse response
%
e=y*0;
```

```
e(1)=1;
yi=idsim(e,th)



function [dr,freq,na] = dacay_ratio(y,T)
%          [dr,freq,na] =DECAY_RATIO(y,T)
%
%          Calculate decay ratio of the oscillatory time-series data
%          from the impulse response.
%          To execute this function Optimization TOOLBOX and Identification
%          TOOLBOX are necessary.
%
%          dr         : Decay Ratio
%          freq: Frequency of oscillation
%          yi        : impulse response
%          na : AR-order
%
%          y          Time-series data
%          T          Sampling Period
%
%          First Coded                                OCT-23-1998
%          Last Modified                              OCT-28-1988
%
%                    T. Suzudo
%                    Japan Atomic Energy Research Institute
%                    Control and Al Lab.
%                    suzudo@clsu3a0.tokai.jaeri.go.jp

% Default resolution of time-series
%
eps = 10^-10;

y_size = size(y);
y_length = y_size(1);                              %Length of data set
n_max = 100;                                         % Maximum AR-order

% Delete Trend (delete linear value)
%
y=dtrend(y,1);

% Calculate impulse response
%
[yi,na]=impul(y,T,n_max);
if (na==n_max) warning('AR fitting is difficult.'); end
yi_length = min([y_length 4096]);

%          Make x-axis data for fitting the impulse response
%
x(1:yi_length,1) = (T:T:T*yi_length)';

%Initial values of the fitting parameters
%
lam = [0.02,0.2,3.,0];

%          Gauss-Newton method is selected
%
```

```
method = 0;
OPTIONS = 0;
OPTIONS(5)=1;

%          Mixed polynominal interpolation is used
%
bof = 13; % start point of fitting
eof = 130; % end point of fitting
OPTIONS(7) = 0;
OPTIONS(2) = 1e-6;
[lam,OPTIONS] = leastsq('impulerr,lam,OPTIONS,[],[x(bof:eof)
yi(bof:eof)]);

dr = exp(-Iam(2)*2*pi/lam(3));
freq = lam(3)l(2*pi);


function J = impulerr(lam,Data)
%         J = IMPULERR(lam, Data)
%
%         IMPULERR returns the error
%         between the Data and the values computed by
%
%         y = lam(1) * exp(-Iam(2)*x) * cos(lam(3)*x + lam(4))
%
%         With four parameters of given by 'lam'.
%
%                  First Coded        OCT-28-1998
%                  Last Modified      OCT-28-1998
%
%                            T. Suzudo
%                            suzudo@clsu3a0.tokai.jaeri.go.jp
x = Data(:1);  y = Data(:,2);
y_fit = zeros(length(x),1);
for jj = 1:length(x)
                             y_fit(jj,1) = lam(1) * exp(-Iam(2)*x(jj,1)) *
cos(lam(3)*x(jj,1) + lam(4));
end
J = y_fit - y;
plot(x(1: 125),y(1: 125),x(2:2:124),y_fit(2:2:124),'o')
drawnow
```

Annex 7

METHODOLOGIES AND RESULTS PRESENTED BY SIEMENS*

Introduction

Two methods were used to calculate decay ratio and natural frequency for the given time series sets. These are auto-regression analysis (AR) and recursive auto-correlation (RAC).

The error for the AR case was obtained by varying the model order in the range of 30-50 and calculating the statistical average and standard deviation from the results that pass certain acceptability criteria. This was found to be more robust than a single optimised solution, as the latter is predicted in the range of model order used, and the error variation is slow. Additional calculations not reported here (will be reported if the organisers request it), use sequential subsets of the noise data and estimate the error as the variation of the calculated DR and FRQ. The latter is a better definition of the error, but is limited by the fact that the number of data subsets must be small to keep each subset long enough for a meaningful calculation. This could be done more accurately for the long time series representing steady operation (no transients). The magnitude of the error was found close to the model order variation method.

There is no equivalent error calculation in the RAC method. The error was estimated by running data subsets and found equivalent to the AR error. The difference between the decay ratio from the two methods was reported as an additional measure of uncertainty. Frequency calculated from the RAC method is similar to that obtained from AR, and thus not reported separately.

Results

Case 1

Table 1. Case 1 – Results using AR and RAC

	Auto-regression				RAC	
Data name	**DR**	**DR uncert.**	**Freq.**	**Freq. uncert.**	**DR**	**DR difference**
f1_boc_13_3	0.460	0.041	0.459	0.006	0.42	0.04
f1_boc_13_4	0.613	0.015	0.470	0.002	0.65	-0.04
f1_boc_14_1	0.537	0.031	0.483	0.004	0.52	0.02

* Yousef M. Farawila and Douglas W. Pruitt
Siemens Power Corporation – Nuclear Division
Richland, Washington, USA
E-mail: yousef_farawila@nfuel.com
Tel: +1 (509) 375-8720

Soma Mojumder, Roger Velten, Franz Wehle
Siemens Power Generation Group (KWU)
Erlangen, Germany

Table 1. Case 1 – Results using AR and RAC (*cont.*)

	Auto-regression				RAC	
Data name	**DR**	**DR uncert.**	**Freq.**	**Freq. uncert.**	**DR**	**DR difference**
f1_boc_14_3	0.528	0.024	0.490	0.005	0.51	0.02
f1_boc_14_4	0.517	0.022	0.501	0.004	0.47	0.05
f1_moc_14_2	0.526	0.044	0.477	0.004	0.55	-0.02
f1_boc_15	0.669	0.024	0.530	0.004	0.66	0.01
f1_moc_16	0.483	0.033	0.526	0.005	0.44	0.04
f2_moc_13	0.530	0.021	0.422	0.006	0.47	0.06
f2_uppst_14	0.585	0.033	0.454	0.008	0.47	0.06
f2_boc_14	0.551	0.044	0.472	0.007	0.39	0.12
f2_moc_14	0.792	0.013	0.465	0.002	0.78	0.01
f2_uppst_15	0.532	0.022	0.403	0.002	0.59	-0.06
f2_moc_15	0.698	0.024	0.493	0.003	0.66	0.04

Case 2

Table 2. Case 2 – Results using AR and RAC

	Auto-regression				RAC	
Data name	**DR**	**DR uncert.**	**Freq.**	**Freq. uncert.**	**DR**	**DR difference**
c2_test.L1	0.360	0.018	0.444	0.003	0.27	0.09
c2_test.S11	0.168	0.024	0.424	0.008	0.15	0.02
c2_test.S21	0.479	0.028	0.449	0.005	0.40	0.08
c2_test.S31	0.359	0.024	0.453	0.005	0.27	0.09
c2_test.S41	0.416	0.033	0.433	0.010	0.39	0.03
c2_test.L2	0.597	0.022	0.526	0.006	0.57	0.03
c2_test.S12	0.646	0.024	0.535	0.004	0.64	0.01
c2_test.S22	0.633	0.020	0.524	0.007	0.62	0.01
c2_test.S32	0.522	0.027	0.522	0.008	0.52	0.00
c2_test.S42	0.538	0.048	0.504	0.008	0.51	0.03

Notice that there is a slow power transient in the first set, while the second set is remarkably steady. Applying AR to the c2_test.L2 at 2 000 data point intervals (160 seconds), we get seven data points with an average decay ratio of 0.611 and a standard deviation of 0.053 which is very similar to the result obtained from using the entire time series. The slightly higher error comes from using shorter time series. Using a data window of 4 000 points sliding by 2 000 points, we can make six data sets for which the average decay ratio is 0.600 ± 0.05 which is similar to the previous result.

It can be concluded that 2 000-4 000 data points are adequate for practical decay ratio estimation.

Case 3

Table 3. Case 3 – Results using AR and RAC

	Auto-regression				RAC	
Data name	**DR**	**DR uncert.**	**Freq.**	**Freq. uncert.**	**DR**	**DR difference**
c3_test.1	0.409	0.011	0.408	0.010	0.36	0.05
c3_test.2	0.330	0.020	0.411	0.009	0.37	-0.04
c3_test.3	0.395	0.020	0.455	0.006	0.33	0.07
c3_test.4	0.517	0.032	0.480	0.004	0.55	-0.03

Notice that the time series c3_test.5 was found identical to c3_test.4 and will not be calculated or reported separately. The power spectral density shows peaks (presumably due to the control system) at nearly 0.1 and 0.3 Hz in addition to the natural frequency. The default internal filtering in the AR algorithm was used. For the RAC algorithm, the filter cut-off was increased from 0.1 to 0.3 Hz.

Case 4

Table 4(a). Case 4 – Time series using AR and RAC

	Auto-regression				RAC	
Data name	**DR**	**DR uncert.**	**Freq.**	**Freq. uncert.**	**DR**	**DR difference**
c4_aprm	0.763	0.032	0.491	0.005	0.71	0.05
c4_lprm.1	0.876	0.020	0.486	0.004	0.83	0.05
c4_lprm.2	0.898	0.017	0.486	0.003	0.86	0.04
c4_lprm.3	0.901	0.018	0.485	0.003	0.88	0.02
c4_lprm.4	0.894	0.005	0.488	0.002	0.90	-0.01
c4_lprm.5	0.811	0.024	0.493	0.005	0.75	0.06
c4_lprm.6	0.803	0.016	0.495	0.005	0.75	0.05
c4_lprm.7	0.787	0.018	0.499	0.004	0.74	0.05
c4_lprm.8	0.760	0.011	0.507	0.001	0.70	0.06
c4_lprm.9	0.758	0.017	0.499	0.005	0.69	0.07
c4_lprm.10	0.751	0.007	0.526	0.002	0.71	0.04
c4_lprm.11	0.678	0.046	0.514	0.008	0.67	0.01
c4_lprm.12	0.677	0.022	0.536	0.003	0.71	-0.03
c4_lprm.13	0.787	0.019	0.498	0.005	0.70	0.09
c4_lprm.14	0.767	0.019	0.501	0.005	0.70	0.07
c4_lprm.15	0.740	0.039	0.506	0.003	0.69	0.05
c4_lprm.16	0.690	0.050	0.504	0.009	0.68	0.01
c4_lprm.17	0.838	0.009	0.490	0.003	0.81	0.03
c4_lprm.18	0.829	0.009	0.490	0.003	0.81	0.02
c4_lprm.19	0.812	0.020	0.495	0.002	0.80	0.01
c4_lprm.20	0.767	0.008	0.502	0.001	0.70	0.07
c4_lprm.21	0.738	0.030	0.507	0.003	0.67	0.07
c4_lprm.22	0.517	0.036	0.526	0.004	0.49	0.03

The decay ratio and frequency for each time series is listed in Table 4(a) using the two methods. The APRM signal analysis is primarily indicative of the global mode, where a decay ratio of 0.76 is obtained. The other signals have mixed information of global, regional (out of phase), as well as local characteristics. Further analysis was performed to discern further information.

In Table 4(b), four time series were created by subtracting (after the proper normalisation) two diagonal LPRM signals at the same axial level. The results are indicative of the regional mode stability. Other possibilities for creating time series with information content biased towards the regional mode are possible.

Table 4(b). Case 4 – Regional mode using AR and RAC

Auto-regression							RAC	
Axial level	**Radial locations**	**Phase shift**	**Decay ratio**	**SDV ±**	**Freq. (Hz)**	**SDV ±**	**Decay ratio**	**Decay ratio difference**
1	11-23	135	0.933	0.005	0.483	0.001	0.93	0.00
4	11-23	52	0.877	0.015	0.486	0.001	0.92	-0.04
1	07-34	7	0.686	0.022	0.507	0.004	0.65	0.04
4	07-34	4	0.649	0.022	0.518	0.001	0.66	-0.01
1	11-34	23	0.808	0.013	0.489	0.003	0.78	0.03
4	11-34	4	0.624	0.029	0.504	0.002	0.65	-0.03
1	09-31	62	0.849	0.003	0.489	0.001	0.85	0.00
4	09-31	59	0.602	0.045	0.503	0.003	0.61	-0.01

It can be remarked from Table 4(b) that a high decay ratio of 0.93 was obtained for the one case where two nearly out-of-phase signals are used. For the other cases, the global mode still dominates the difference signal, a hypothesis supported by the small phase shift, and the decay ratio is closer to the APRM result. It is also noted that for the difference signals where noticeable (but not quite out-of-phase) phase shift is calculated, result in decay ratios that are perhaps somewhere between the global and regional values. It can be also noticed that the upper level LPRM, where the core is highly voided and the reactivity sensitive to global pressure perturbation, could not filter out the global noise component by the difference method. The bottom level LPRMs are more promising.

A phase shift map at axial level 1 is tabulated in Table 4(c) relative to the LPRM at the radial location 07.

Table 4(c). Case 4 – Radial phase shifts relative to LPRM at position 07

Radial location	Phase shift
23	60
34	7
11	-33
20	-6
09	29
31	-24

It appears from Table 4(c) that the half core (containing radial locations 09 and 23) and the other half (containing radial locations 11 and 31) have noise component that is out of phase superimposed on the generally dominant in-phase component. The neutral line where regional oscillations vanish is

perhaps the line close to the radial locations 07,20,34. The picture would have been clearer if other LPRM signals were made available. It is not surprising to find the difference signals 09-31 and 11-23 with the largest phase difference give higher decay ratios different from that of the global mode, and we suggest that this higher decay ratio is the best estimate of the regional decay ratio given the limited data.

In the regional mode attempt, we used LPRMs at the same axial level to avoid the axial phase shift effects. It was interesting to study the axial phase shifts and examine whether an axial flux mode is excited due to travelling density waves. Table 4(d) summarises these results, where it was confirmed that the upper core response lags the lower core. The magnitude of the axial phase shift was found smaller near the core periphery compared with the high power and flow locations.

Table 4(d). Case 4 – Axial phase shifts

Radial location	Axial levels	Phase shift
23	1-2	10
23	1-3	27
23	1-4	40
34	1-2	16
34	1-3	42
34	1-4	63
20	1-2	15
20	1-3	34
20	1-4	45
09	1-2	14
09	1-3	16
09	1-4	63
07	1-4	68
11	1-4	78
31	1-4	75

Case 5

There are two time series that include mild transients. In the first case, the intervals (0.0,140.0 sec) and (200.0-336.0 sec) represent steady state. For the second time series, the interval (260.0,650.0 sec) does not represent steady operation, and the results are therefore divided accordingly. Analysis which includes transient portions was performed as well, and the results of the mixing are well-behaved in the sense that the mixing produced decay ratios which lie somewhere between the two steady state limits and closer to the one represented by a longer interval. In that manner, a running monitor in real time can tolerate mild transients fairly well. The results are shown in Table 5 for the two series at different time intervals.

Case 6

The analysis performed for this case is similar to that of Case 4. For the first set, it was found necessary to use a low-pass filter with the RAC method for the same reasons of external signal (control system) removal. The AR method default settings were used. Given the relatively small decay ratios and the control system interference, regional mode studies were dropped for the first set.

Table 5. Case 5 – Time series using AR and RAC

Auto-regression						RAC	
Data name	**Interval (sec)**	**Decay ratio**	**SDV ±**	**Freq. (Hz)**	**SDV ±**	**Decay ratio**	**Decay ratio difference**
c5_aprm.1	0-140	0.998	0.005	0.524	0.013	0.99	0.01
	200-336	0.699	0.050	0.556	0.010	0.69	0.01
c5_aprm.2	0-260	0.620	0.049	0.500	0.005	0.66	-0.04
	260-650	0.659	0.039	0.516	0.002	0.67	-0.01
	650-1 040	0.515	0.026	0.504	0.004	0.55	-0.03

Table 6(a). Case 6 set 1 time series using AR and RAC

Auto-regression					RAC (0.35 Hz filter)	
Data name	**DR**	**DR uncert.**	**Freq.**	**Freq. uncert.**	**DR**	**DR difference**
c6_aprm.1	0.474	0.033	0.523	0.005	0.52	-0.05
c6_lprm.11	0.358	0.048	0.498	0.009	0.45	-0.09
c6_lprm.21	0.170	0.021	0.472	0.012	0.24	-0.07
c6_lprm.31	0.473	0.053	0.524	0.004	0.64	-0.17
c6_lprm.41	0.405	0.043	0.522	0.007	0.37	0.03
c6_lprm.51	0.603	0.038	0.525	0.005	0.70	-0.10
c6_lprm.61	0.758	0.045	0.528	0.002	0.79	-0.03
c6_lprm.71	0.529	0.037	0.517	0.005	0.56	-0.03
c6_lprm.81	0.565	0.061	0.527	0.005	0.49	0.08
c6_lprm.91	0.349	0.037	0.526	0.012	0.33	0.02
c6_lprm.101	0.204	0.024	0.534	0.011	0.16	0.04
c6_lprm.111	0.361	0.027	0.504	0.004	0.40	-0.04
c6_lprm.121	0.333	0.025	0.535	0.009	0.32	0.01
c6_lprm.131	0.341	0.047	0.509	0.012	0.38	-0.04
c6_lprm.141	0.379	0.064	0.509	0.007	0.43	-0.05
c6_lprm.151	0.478	0.058	0.525	0.003	0.66	-0.08
c6_lprm.161	0.482	0.060	0.525	0.002	0.66	-0.08
c6_lprm.171	0.310	0.020	0.496	0.012	0.34	0.03
c6_lprm.181	0.267	0.018	0.508	0.008	0.16	0.11

Table 6(b). Case 6 set 2 time series using AR and RAC

Auto-regression					RAC (0.35 Hz filter)	
Data name	**DR**	**DR uncert.**	**Freq.**	**Freq. uncert.**	**DR**	**DR difference**
c6_aprm.2	0.915	0.008	0.520	0.001	0.96	-0.04
c6_lprm.12	0.546	0.034	0.509	0.004	0.70	-0.05
c6_lprm.22	0.293	0.048	0.517	0.010	0.40	-0.11
c6_lprm.32	0.950	0.009	0.521	0.000	0.99	-0.05

Table 6(b). Case 6 set 2 time series using AR and RAC (*cont.*)

Auto-regression					RAC (0.35 Hz filter)	
Data name	**DR**	**DR uncert.**	**Freq.**	**Freq. uncert.**	**DR**	**DR difference**
c6_lprm.42	0.858	0.019	0.520	0.001	0.92	-0.06
c6_lprm.52	0.961	0.008	0.521	0.000	0.99	-0.03
c6_lprm.62	0.983	0.003	0.522	0.000	1.00	-0.02
c6_lprm.72	0.923	0.011	0.520	0.000	0.98	-0.06
c6_lprm.82	0.951	0.009	0.521	0.000	0.97	-0.02
c6_lprm.92	0.674	0.037	0.511	0.002	0.83	-0.16
c6_lprm.102	0.513	0.033	0.501	0.009	0.58	-0.07
c6_lprm.112	0.858	0.031	0.521	0.001	0.95	-0.09
c6_lprm.122	0.837	0.031	0.519	0.001	0.94	-0.10
c6_lprm.132	0.878	0.016	0.521	0.000	0.95	-0.07
c6_lprm.142	0.877	0.015	0.521	0.001	0.95	-0.07
c6_lprm.152	0.954	0.008	0.521	0.000	0.99	-0.04
c6_lprm.162	0.955	0.008	0.521	0.000	0.99	-0.03
c6_lprm.172	0.591	0.035	0.506	0.004	0.73	-0.14
c6_lprm.182	0.503	0.027	0.507	0.007	0.47	0.03

The regional mode studies using the diagonal LPRM subtraction method resulted in decay ratios close to unity (similar to the high decay ratios from individual signal analysis). The phase relations did not indicate dominance of the regional mode as the radial phase shifts were found small. The variation of decay ratios can only indicate local variations instead of a uniform core response. It was observed that the low decay ratio signals were obtained from LPRMs located on the periphery and the associated frequency is slightly (but noticeably) smaller. A preliminary hypothesis would be that the peripheral region could be decoupled from the rest of the core if the conditions (void fraction and flow) become significantly different from the core average conditions. The alternative hypothesis of individual channel local instabilities can not be supported at this time until more (preferably all) LPRM signals are provided for a detailed study.

Annex 8

METHODOLOGIES AND RESULTS PRESENTED BY TOSHIBA*

Methodology

There are two main methods for core stability estimation from nuclear instrumental signals, one being time domain analysis and the other frequency domain analysis. The former is based on impulse response and the latter is based on power spectrum density. The former method was used for the decay ratio estimation, and the latter was applied to check the accuracy of the former method. Therefore, the results presented in this report were calculated using time domain analysis. Non-linear methods, the correlation dimension and Lyapunov exponents were also applied; however the results are preliminary.

For the impulse response calculation, the maximum entropy method was applied [1]. In the maximum entropy method, the prediction error filter a_k is estimated as an auto-regression process for the time series data x_t as follows:

$$x_t + \sum_{k=1}^{m} a_k x_{t-k} = e_t$$

where e_t is the estimated error. The prediction error filter is calculated by Burg's algorithm based on the maximum information entropy. The filter order m is estimated using Akaike's information criterion (AIC). The impulse response of the time series data x_t is calculated with the prediction error filter a_k as follows:

$$h_j = 1.0 - \sum_{k=1}^{m} a_k h_{j-k}$$

where h_j is the impulse response. The decay ratio γ is calculated using the impulse response as follows:

$$\gamma = E\left[\left(\left(P_{n+1} - P_n\right)/\left(P_n - P_{n-1}\right)\right)^2\right]$$

where $E[]$ is the expected value and P_{n+1}, P_n, P_{n-1} are successive peak values of the impulse response, as shown in Figure 1. The resonant frequency f is also calculated as follows:

* Yutaka Takeuchi and Shigeru Kanemoto
Nuclear Engineering Laboratory
Power & Industrial Systems Technology R&D Centre
TOSHIBA Corporation
4-1 Ukishima-cho Kawasaki-ku
Kawasaki 210-0862, Japan

H. Miyamoto
Computer on Silicon Development Centre
TOSHIBA Corporation
580-1 Horikawa-cho Saiwai-ku
Kawasaki 210-8520, Japan

$$f = E\left[1/\left(T_{n+1} - T_{n-1}\right)\right]$$

where T_{n+1} means the time when the peak P_{n+1} appears. The peak of the impulse response is selected from the asymptotic response and number of averaging is 10.

The spectrum density function $S(f)$ is calculated using the prediction error filter a_k as follows:

$$S(f) = \frac{\sigma_e^2 \Delta t}{\left|1 + \sum_{k=1}^{m} a_k \exp\left(-j2\pi f k \Delta t\right)\right|^2}$$

where σ_e^2 is the variance of the filter error and Δt is the sampling time. The resonant frequency is estimated by the location of the spectrum peak and the decay ratio is estimated by the buckling of the spectrum peak [1].

We originally developed the computational programs used for the time series analysis. We also used the IMSL statistical library package, the TIMSAC time series analysis package developed by the Institute of Statistical Mathematics of Japan and the signal processing toolbox of MATLAB version 5.

We define the accuracy of estimated decay ratio and resonant frequency in the following way. The decay ratio is not constant among the whole test data interval. Especially in the transient state such as in the Case 5, the decay ratio changes according to the change of the state. Therefore, we estimated the decay ratios with the partial interval data (60 seconds, 750 points) by shifting the time origin (6 seconds, 75 points) among the whole test data interval. Examples of the estimated results are shown in Figure 2(a) and Figure 2(b). Figure 2(b) shows the decay ratio change during the transient. The decay ratio decreases along with the time. Figure 2(a) shows the estimated decay ratio during normal operation. It can be seen that the decay ratio fluctuates even in conditions without any transient. Therefore, we define the accuracy of the estimated decay ratio as the standard deviation of the decay ratios calculated with the above-mentioned partial interval data. Namely, define the decay ratio calculated with the n-th partial interval data as $DR(n)$, the average decay ratio, $\overline{DR}$ and the standard deviation of $DR(n)$, DDR are calculated as follows:

$$\overline{DR} = \frac{1}{N} \sum_{n=1}^{N} DR(n)$$

$$DDR = \sqrt{\frac{1}{N} \sum_{n=1}^{N} \left(DR(n) - \overline{DR}\right)^2}$$

where N is the number of estimated decay ratios with the partial interval data. The definition for the resonant frequency is same.

All the parameters listed hereafter are calculated by the impulse response.

Results

Case 1

The summary of results is as follows: DR is the average decay ratio, DDR is the standard deviation of decay ratios, FR is the average resonant frequency and DFR is the standard deviation of resonant frequencies, respectively. The results are plotted in Figure 3.

Case no.	DR	DDR	FR (Hz)	DFR (Hz)
1	5.12E-01	6.78E-02	4.48E-01	2.07E-02
2	5.77E-01	1.21E-01	4.56E-01	2.24E-02
3	4.99E-01	1.19E-01	4.82E-01	2.62E-02
4	5.58E-01	7.07E-02	5.18E-01	3.74E-02
5	5.32E-01	8.92E-02	4.96E-01	2.60E-02
6	5.87E-01	6.68E-02	4.77E-01	1.13E-02
7	6.30E-01	1.07E-01	5.17E-01	1.57E-02
8	4.45E-01	5.02E-02	5.18E-01	2.49E-02
9	5.61E-01	8.39E-02	4.01E-01	2.09E-02
10	5.37E-01	9.25E-02	4.33E-01	2.22E-02
11	4.69E-01	1.66E-01	4.43E-01	4.49E-02
12	7.40E-01	8.48E-02	4.59E-01	9.57E-03
13	6.10E-01	7.48E-02	4.01E-01	1.89E-02
14	6.62E-01	7.88E-02	4.96E-01	1.47E-02

We also applied non-linear parameters, such as the correlation dimension [3] and the Lyapunov exponents [4]. However, because of the relatively noisy data and short data length, the convergence of the calculated parameters is uncertain. In Figure 4, the correlation integral versus norm (distance between two correlated data) and the correlation dimension versus the embedding dimension are shown. From these figures, the convergence is not certain, but we selected the embedding dimension as 10 for the present. Comparison between decay ratios and correlation dimensions is shown in Figure 5. There appears to be a slight trend between them, as they are inversely proportional to each other, but this is not clear. They are divided into two groups, high order dimension (7~8) group (Group 1) and low order dimension (3~4) group (Group 2). By the comparison of PSDs of two groups which is shown in Figure 6, the PSD of the high dimension group (Test no. 3-8) has large contribution from high frequency noise or contaminated by the large background noise. The question is whether all provided data are APRM data or the data of Group 2 are not APRM but LPRM data. For the Lyapunov exponents, the reliable results have not been realised. The study for the non-linear parameters is still underway.

Case 2

The summary of results is as follows and is plotted in Figure 7.

Case no.	DR	DDR	FR (Hz)	DFR (Hz)
long-1	3.86E-01	1.27E-01	4.41E-01	4.06E-02
short-11	4.16E-01	7.85E-02	4.78E-01	4.27E-02
short-21	5.25E-01	1.04E-01	5.10E-01	1.30E-02
short-31	4.16E-01	7.85E-02	4.78E-01	4.27E-02
short-41	4.06E-01	7.45E-02	4.30E-01	1.67E-02
long-2	5.76E-01	1.04E-01	5.16E-01	1.53E-02
short-12	5.23E-01	1.04E-01	5.10E-01	1.37E-02
short-22	6.01E-01	9.16E-02	5.17E-01	1.32E-02
short-32	5.23E-01	1.04E-01	5.10E-01	1.37E-02
short-42	5.37E-01	6.75E-02	5.15E-01	1.57E-02

Case 3

The summary of results is as follows and is plotted in Figure 8.

Case no.	DR	DDR	FR (Hz)	DFR (Hz)
1	4.35E-01	1.84E-01	3.92E-01	3.41E-02
2	4.95E-01	9.79E-02	3.97E-01	3.91E-02
3	3.73E-01	1.02E-01	4.50E-01	2.46E-02
4	5.20E-01	9.40E-02	4.73E-01	2.59E-02
5	5.20E-01	9.40E-02	4.73E-01	2.59E-02

As the data of this case contain many peaks in PSD except for the core stability related peak, we should use high order auto-regression number. However, we assumed that the most dominant peak is related to the core stability, then we used a relatively small regression number for the core stability estimation. With a higher order, the decay ratio tends to increase. However, as we were not convinced of the reliability of the higher order, we listed the results of a relatively low order AR model.

In order to evaluate a set of the dominant poles of the transfer function, we used the function “residuez” of the MATALB signal processing toolbox. It decomposes the transfer function in the Z-plain into the expansion of the partial fractions. The importance of each pole can be evaluated by the residue of each partial fraction. The poles of the transfer function can also be evaluated by the PSD. Specifically, the imaginary part of the pole in the S-plain is related to the peak of the PSD, and the real part of the pole is related to the buckling of the PSD peak. We thus verified the dominant poles evaluated by MATLAB with those by the PSD analysed with FFT, as shown in Figure 9. Also, we checked the validity by comparing the composed PSD, which includes only the set of evaluated dominant poles, with the original PSD, which includes the all poles, as shown in Figure 10. The results are summarised in below. The results from Case 5 are the same as those for Case 4. We compare the decay ratio and resonant frequency with the impulse response method, which are listed in the previous page and those estimated by the pole location in Figure 11. The resonant frequency results agrees well with each other, however the decay ratio estimated by the pole location is much higher than that by impulse response. As a next step, the methodology of decay ratio estimation for such disturbed data should be studied in detail.

Case 1	Pole			
	Z-plain		S-plain	
	Real	Imaginary	Real	Imaginary
1	0.9816	±0.0422	-0.2205	±0.5368
2	0.9731	±0.1487	-0.1960	±1.8952
3	0.9655	±0.1925	-0.1951	±2.4604
4	0.9697	±0.0828	-0.3398	±1.0645
5	0.9605	±0.2299	-0.1561	±2.9366
6	0.9422	±0.2824	-0.2062	±3.6400

Case 2	Pole			
	Z-plain		S-plain	
	Real	Imaginary	Real	Imaginary
1	0.9851	±0.0466	-0.1735	±0.5901
2	0.9807	±0.1436	-0.1107	±1.8174
3	0.9655	±0.2180	-0.1279	±2.7756
4	0.9696	±0.1809	-0.1727	±2.3053
5	0.9774	±0.0956	-0.2261	±1.2192
6	0.9724	±0.0303	-0.3441	±0.3893

Case 3	Pole			
	Z-plain		S-plain	
	Real	Imaginary	Real	Imaginary
1	0.9603	±0.2327	-0.1496	±2.9715
2	0.9887	±0.0568	-0.1218	±0.7175
3	0.9827	±0.1332	-0.1046	±1.6840
4	0.9698	±0.2010	-0.1200	±2.5539
5	0.9771	±0.1604	-0.1239	±2.0343
6	0.9858	±0.0916	-0.1245	±1.1578

Case 4	Pole			
	Z-plain		S-plain	
	Real	Imaginary	Real	Imaginary
1	0.9643	±0.2324	-0.1018	±2.9565
2	0.9884	±0.0405	-0.1356	±0.5119
3	0.9842	±0.1359	-0.0811	±1.7154
4	0.9774	±0.1606	-0.1195	±2.0362
5	0.9864	±0.0176	-0.1690	±0.2234
6	0.9877	±0.0696	-0.1234	±0.8794

Case 4

For the purpose of investigating the oscillation mode of this case, we only used the same level signals axially, which are located at the level-4 (GE's notation is level-A). This was selected because the level-4 signal is most sensitive to stability among the four axial levels. Using seven level-4 signals, we estimated the centreline of the regional oscillation mode. We introduced the new signal, designated as the regionally averaged power range monitor (RPRM), which is calculated as follows:

$$RPRM_m(t) = \sum_{n=1}^{N} W_{mn} LPRM_n(t)$$

where $LPRM_n(t)$ is the n-th LPRM signal and W_{mn} is the weight factor of m-th mode related to the signal location. Normally, the weight factor is calculated by the neutron harmonic analysis, but for this case the analysis can not be performed because of the absence of the nuclear constants. Therefore, we used the Bessel function, which represents the neutron flux distribution of a uniform bare reactor. We show the amplitude response of RPRM in Figure 12, with the change in azimuthal direction (angle) of the zero line in the weight factor distribution. In the figure, mode0 means the fundamental mode and mode'm' means the m-th azimuthal mode. We can see that the fundamental mode amplitude is largest and the first azimuthal mode is the second. The responses of other modes are not visible because of there are too few signals. The zero-line angle, which realises the largest amplitude for the first azimuthal mode, is about 95°. Therefore, we can estimate that the centreline of the regional oscillation mode of this case divides the core region into the right half region and the left half region. Thus, we adapted the signal that realises the largest amplitude of the first azimuthal mode as the regional stability monitoring signal and designated it as RPRM-1. The summary of results is listed below and plotted in Figure 13.

	DR	DDR	FR (Hz)	DFR (Hz)
APRM	4.50E-01	8.67E-02	5.22E-01	2.41E-02
RPRM-1	8.51E-01	2.00E-02	4.89E-01	3.60E-03
LPRM-23A	9.03E-01	1.54E-02	4.90E-01	3.35E-03
LPRM-34A	7.33E-01	7.93E-02	5.07E-01	7.64E-03
LPRM-07A	7.56E-01	4.63E-02	5.29E-01	8.07E-03
LPRM-11A	6.54E-01	4.97E-02	5.34E-01	8.47E-03
LPRM-20A	7.71E-01	3.52E-02	5.16E-01	1.13E-02
LPRM-09A	7.69E-01	5.27E-02	5.02E-01	8.06E-03
LPRM-31A	4.47E-01	8.71E-02	5.23E-01	2.36E-02

We compare the PSD of APRM and RPRM-1 in Figure 14. The peak of PSD is much sharper for RPRM-1, which means that the core condition of this case was potentially regionally unstable. However, there is no clear peak at the double natural frequency (about 1 Hz) in the PSD of APRM, which is a remarkable characteristic of regional oscillation, so we can conclude that there was still some margin for a regionally unstable boundary in this case. In Figure 15, we compare the amplitude change between mode0 (fundamental) and mode1 (first azimuthal) every five seconds. There is a slight trend that the amplitude of mode0 decreases and that of mode1 increases according to the time advance. This trend is also shown in the change of decay ratio. In Figure 16, the phase delay of each LPRM signal from the signal LPRM-23A, whose amplitude is largest, is shown. The trend of phase delay is not clear, however between 150 to 250 seconds; the phase delay increases for the LPRM which is located at the opposite half core region (LPRM-07/11/31) from LPRM-23. The amplitude of mode0 decreases in this time interval. We show the coherence between LPRM-23 and other LPRM signals in Figure 17. The characteristic shown in this figure is that there are two peaks in coherence, namely at about 0.49 Hz and 0.52 Hz. From Figure 13, the former frequency represents the resonant frequency of RPRM-1 and the LPRM which is located at the right half core region and the latter one represents the resonant frequency of APRM and the LPRM located at the left half core region. In Figure 18, we compare the change of decay ratio and resonant frequency between APRM and RPRM. In this figure, the resonant frequency of RPRM takes almost the same value the whole time. On the contrary, the resonant frequency of APRM changes, and between 110 to 240 seconds (as stability

parameters are calculated with data length of 60 seconds, the time interval may shift to forward about 50 seconds in reality), it is entrained to that of RPRM. The decay ratio of APRM also decreases in that time interval. The regional stability mode (first azimuthal mode) is most dominant in that interval.

Case 5

The data of this case contains trend components that are caused by some plant transient. First, we estimated the trend components using a polynomial trend model. The estimated trend is shown in Figure 19. We then extracted the estimated trend components from the original time series data. Next, we calculated the PSD with FFT as shown in Figure 20. Many peaks are shown in both cases. The stability related peak is remarkable in the Case 1, though in Case 2 it is not so remarkable and is contaminated by other peaks. Decay ratio estimation is therefore more difficult in Case 2.

To see the estimated decay ratio dependency on the sharpness of estimated PSD peak, we calculated decay ratio while varying the AR order; M. Results are summarised below and plotted in Figure 21.

	DR	**DDR**	**FR (Hz)**	**DFR (Hz)**
Case 1				
M=25	9.18E-01	6.99E-02	5.29E-01	6.71E-03
M=99	9.55E-01	1.11E-02	5.25E-01	2.62E-02
M=200	9.61E-01	6.50E-03	5.27E-01	2.39E-02
Case 2				
M=30	5.89E-01	1.39E-01	5.16E-01	2.67E-02
M=99	8.81E-01	7.76E-02	5.13E-01	2.16E-02
M=200	9.33E-01	4.48E-02	5.09E-01	2.93E-02

The dependency of the estimated decay ratio on the AR order is remarkable in Case 2, but is relatively small in Case 1, which is the imaginable result from the shapes of PSD as shown in Figure 20.

In order to estimate poles, we estimated with partial data because of the possibility of changing the dominant poles as shown in Figure 22. For Case 1, we used total data, front half data and end half data. For Case 2, we used total data, front one-third data, middle one-third data and end one-third data. The results are listed below.

Case 1 (total)	**Pole**			
	Z-plain		**S-plain**	
	Real	**Imaginary**	**Real**	**Imaginary**
1	0.9636	±0.2628	-0.0154	±3.3286
2	0.9585	±0.2708	-0.0497	±3.4420
3	0.9699	±0.2368	-0.0204	±2.9931
4	0.9433	±0.3045	-0.1102	±3.9027
5	0.8588	±0.5074	-0.0313	±6.6701
6	0.9716	±0.1990	-0.1028	±2.5250

Case 1 (front)	Pole			
	Z-plain		S-plain	
	Real	Imaginary	Real	Imaginary
1	0.9640	±0.2629	-0.0100	±3.3276
2	0.9571	±0.2711	-0.0654	±3.4502
3	0.9648	±0.0053	-0.0649	±0.0664
4	0.9702	±0.2352	-0.0213	±2.9734
5	0.9413	±0.2977	-0.1604	±3.8289
6	0.8598	±0.5077	-0.0285	±6.6729

Case 1 (end)	Pole			
	Z-plain		S-plain	
	Real	Imaginary	Real	Imaginary
1	0.9590	±0.2709	-0.0433	±3.4416
2	0.9510	±0.2777	-0.1168	±3.5510
3	0.9690	±0.2399	-0.0223	±3.0336
4	0.9694	±0.2091	-0.1047	±2.6563
5	0.9388	±0.3077	-0.1515	±3.9586
6	0.9292	±0.3393	-0.1357	±4.3763

Case 2 (total)	Pole			
	Z-plain		S-plain	
	Real	Imaginary	Real	Imaginary
1	0.9628	±0.2563	-0.0458	±3.2522
2	0.9840	±0.0584	-0.1803	±0.7404
3	0.9621	±0.2239	-0.1532	±2.8585
4	0.9677	±0.1966	-0.1571	±2.5048
5	0.9796	±0.1344	-0.1410	±1.7045
6	0.9829	±0.0961	-0.1560	±1.2188

Case 2 (front)	Pole			
	Z-plain		S-plain	
	Real	Imaginary	Real	Imaginary
1	0.9636	±0.2557	-0.0388	±3.2424
2	0.9876	±0.0523	-0.1390	±0.6616
3	0.9640	±0.2240	-0.1300	±2.8539
4	0.9671	±0.1928	-0.1751	±2.4597
5	0.9743	±0.1658	-0.1465	±2.1067
6	0.9855	±0.0087	-0.1332	±1.1089

Case 2 (middle)	Pole			
	Z-plain		S-plain	
	Real	Imaginary	Real	Imaginary
1	0.9602	±0.2599	-0.0655	±3.3038
2	0.9810	±0.0673	-0.2102	±0.8564
3	0.9772	±0.1368	-0.1669	±1.7392
4	0.9644	±0.1978	-0.1951	±2.5290
5	0.9787	±0.0394	-0.2594	±0.5030
6	0.9537	±0.2261	-0.2507	±2.9095

Case 2 (end)	Pole			
	Z-plain		S-plain	
	Real	Imaginary	Real	Imaginary
1	0.9632	±0.2548	-0.0460	±3.2332
2	0.9916	±0.0588	-0.0837	±0.7408
3	0.9718	±0.2003	-0.0976	±2.5414
4	0.9923	±0.0217	-0.0935	±0.2738
5	0.9621	±0.2265	-0.1452	±2.8906
6	0.9867	±0.1017	-0.1008	±1.2833

We show the change of dominant poles in Figure 23. In both of cases, the more dominant pole which is closest to the ordinate (real = 0), represents core stability. Change of real part of the dominant pole represents the change of decay ratio. It is consistent with the result of decay ratio estimation [Figure 2(b)].

Case 6

The results of Test 1 are summarised below and plotted in Figure 24.

Test 1	DR	DDR	FR (Hz)	DRF (Hz)
APRM	4.59E-01	4.39E-02	5.10E-01	1.39E-02
LPRM-06A	5.17E-01	7.18E-02	5.17E-01	2.72E-02
LPRM-06D	4.21E-01	8.02E-02	5.14E-01	1.36E-02
LPRM-11A	6.64E-01	1.06E-01	5.16E-01	2.07E-02
LPRM-11D	4.49E-01	7.20E-02	5.19E-01	1.71E-02
LPRM-20A	2.92E-01	1.35E-01	5.17E-01	3.77E-02
LPRM-20D	3.44E-01	1.24E-01	5.29E-01	2.21E-02
LPRM-23A	2.61E-01	9.34E-02	4.75E-01	4.48E-02
LPRM-23D	2.67E-01	8.29E-02	4.81E-01	3.68E-02
LPRM-24A	3.95E-01	1.13E-01	5.24E-01	2.90E-02
LPRM-24D	4.02E-01	1.03E-01	5.22E-01	2.37E-02
LPRM-26A	4.13E-01	9.64E-02	5.06E-01	2.66E-02
LPRM-26D	3.73E-01	1.17E-01	5.25E-01	2.40E-02
LPRM-29A	4.11E-01	5.27E-02	4.72E-01	4.80E-02
LPRM-29D	3.06E-01	9.82E-02	5.02E-01	3.52E-02
LPRM-31A	4.08E-01	1.03E-01	5.53E-01	3.07E-02
LPRM-31D	3.30E-01	1.30E-01	5.24E-01	4.56E-02
LPRM-34A	2.90E-01	9.59E-02	5.56E-01	2.69E-02
LPRM-34D	3.39E-01	5.31E-02	5.24E-01	2.44E-02

The results of Test 2 are summarised in the table on the following page and plotted in Figure 25.

In Test 2, the amplitude of LPRM-11A was largest, so we inferred that it is the signal closest to the disturbance source. We first calculated the phase delay of each LPRM signal from LPRM-11A. Results are shown in Figure 26. In Test 2, signals of LPRM located at the left half core region where LPRM-11 is also located have no phase delay, therefore they fluctuate in-phase with LPRM-11. However, LPRM-24 is an exception whose phase is also delayed in Test 1. The phase delay of the right half core region fluctuates between about 20° to 120°, so it is not so large as out-of-phase.

Test 2	DR	DDR	FR (Hz)	DFR (Hz)
APRM	8.86E-01	2.23E-02	5.19E-01	2.94E-03
LPRM-06A	9.19E-01	1.94E-02	5.21E-01	2.94E-03
LPRM-06D	8.90E-01	2.23E-02	5.20E-01	2.48E-03
LPRM-11A	9.60E-01	1.24E-02	5.21E-01	2.33E-03
LPRM-11D	9.34E-01	1.39E-02	5.21E-01	2.44E-03
LPRM-20A	7.47E-01	4.71E-02	5.16E-01	1.09E-02
LPRM-20D	7.68E-01	6.05E-02	5.19E-01	3.87E-03
LPRM-23A	3.57E-01	7.31E-02	5.13E-01	1.64E-02
LPRM-23D	4.70E-01	7.33E-02	5.06E-01	1.44E-02
LPRM-24A	9.28E-01	2.17E-02	5.21E-01	2.90E-03
LPRM-24D	9.22E-01	2.16E-02	5.21E-01	2.94E-03
LPRM-26A	8.07E-01	2.63E-02	5.18E-01	4.16E-03
LPRM-26D	9.28E-01	1.97E-02	5.21E-01	3.01E-03
LPRM-29A	5.18E-01	8.42E-02	4.54E-01	3.81E-02
LPRM-29D	5.00E-01	7.52E-02	4.94E-01	1.05E-02
LPRM-31A	8.32E-01	3.10E-02	5.21E-01	3.32E-03
LPRM-31D	8.36E-01	3.07E-02	5.20E-01	4.12E-03
LPRM-34A	5.35E-01	5.48E-02	4.85E-01	2.62E-02
LPRM-34D	5.60E-01	6.08E-02	5.02E-01	1.39E-02

We analysed the noise source contribution among LPRM signals with the multivariate AR model. Results are shown in Figure 27. From these figures, we can see that the most contributed noise source is of LPRM-11 for all LPRM signals. As there were limited LPRM signals and no flow related data, we can not investigate the phenomena of this case further.

REFERENCES

[1] Y. Takeuchi, *et al*., *Nucl. Technol*., 106 [3] (1994), 300.

[2] S. Kanemoto, *et al*., *Progress in Nuclear Energy*, 21 (1988), 745.

[3] P. Grassberger, *et al., Phys. Rev. Lett.*, 50 (1983), 346-349.

[4] M. Sano, *et al., Phys. Rev*. 29A (1984), 975-977.

Figure 1. Definition of decay ratio and resonant frequency by impulse response

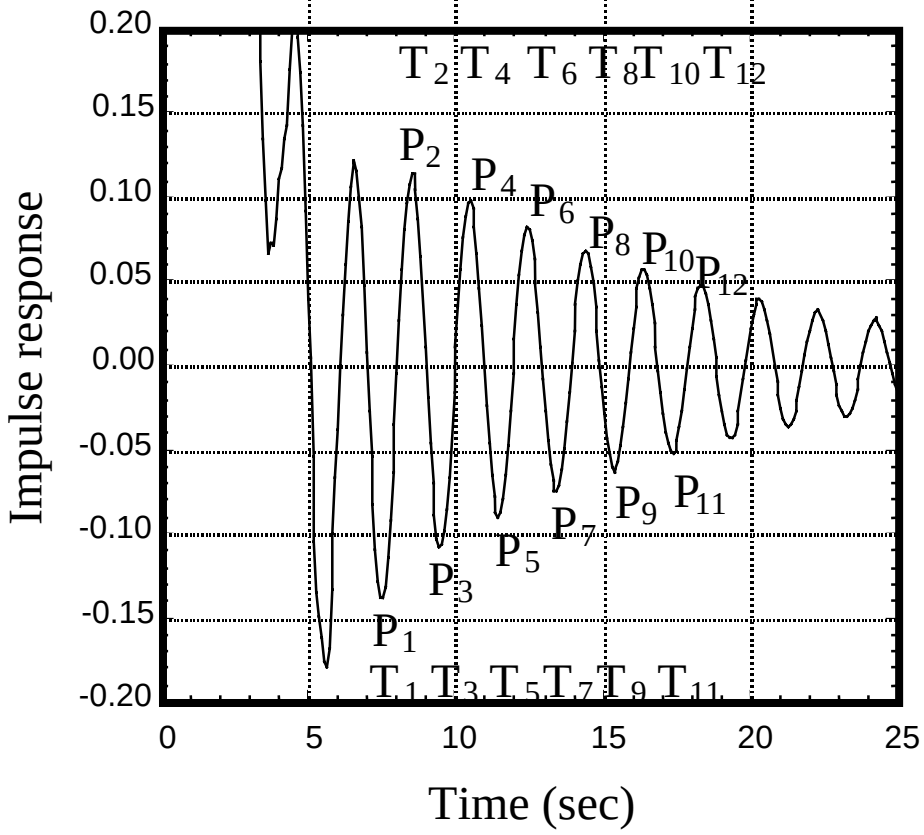

Decay ratio $\gamma = E\left[\left\{(P_{n+1} - P_n)/(P_n - P_{n-1})\right\}^2\right]$

Frequency $f = E\left[1/(T_{n+1} - T_{n-1})\right]$

Figure 2(a). Estimated decay ratio in normal operation

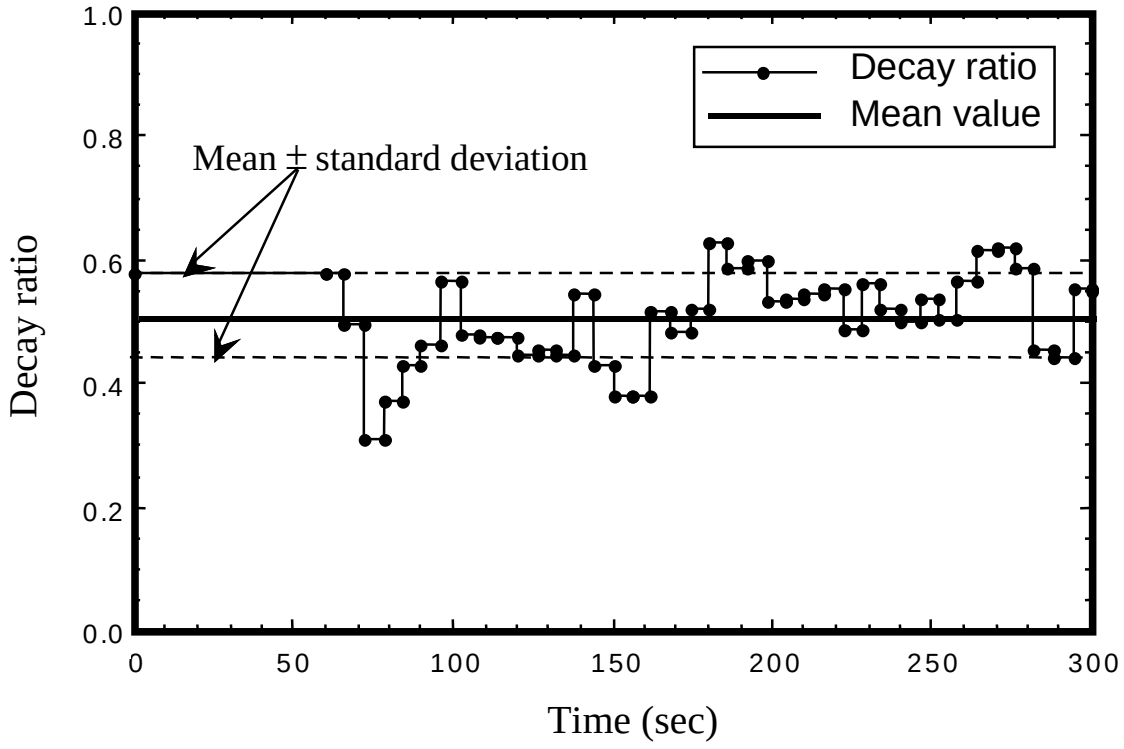

Figure 2(b). Estimated decay ratio in transient operation

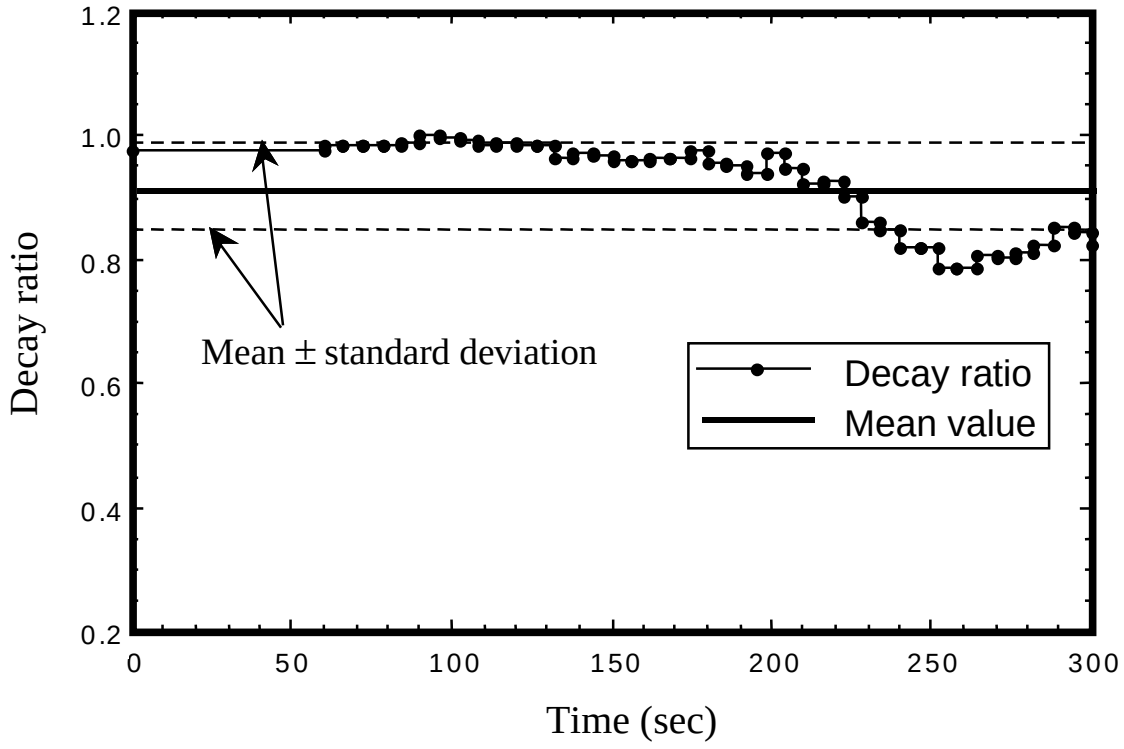

Figure 3. Results of Case 1

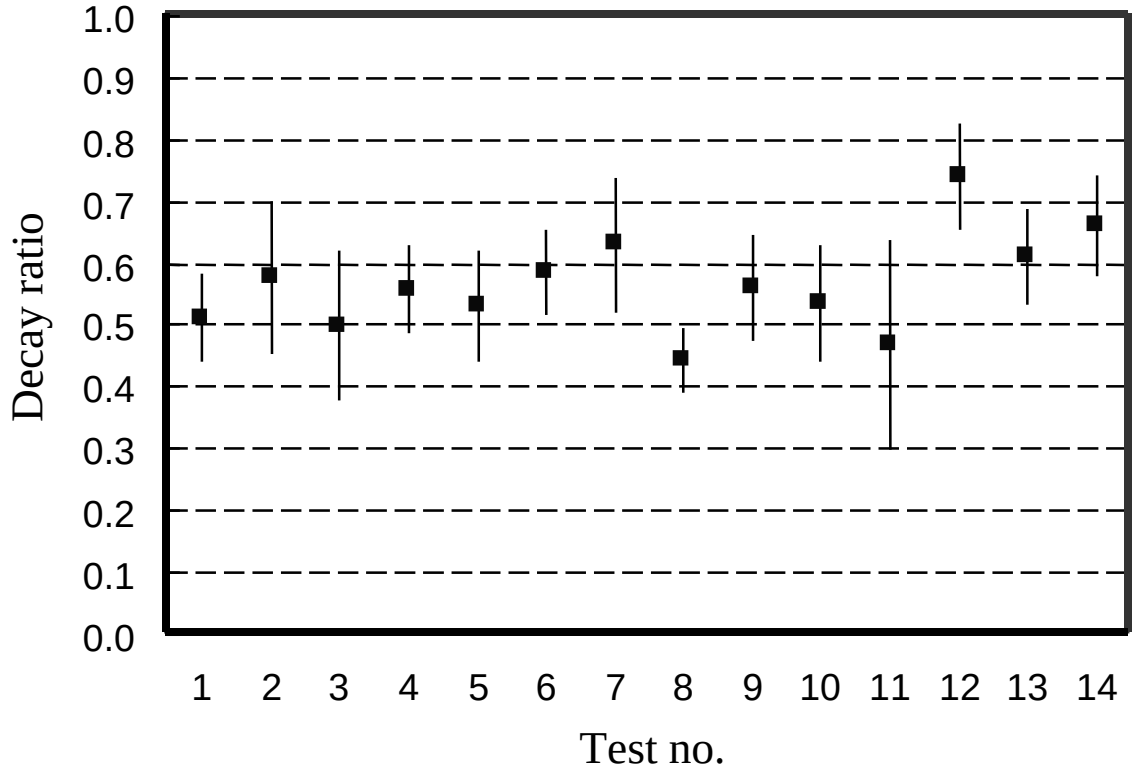

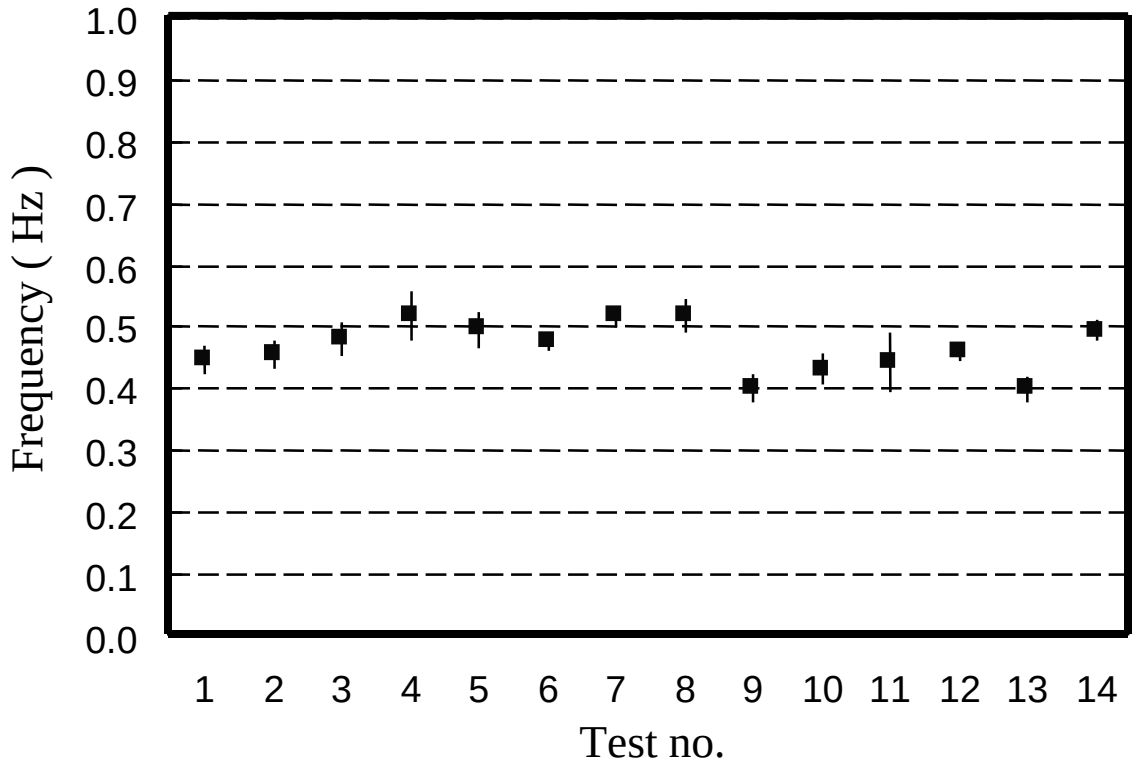

Figure 4(a). Correlation integral vs. norm

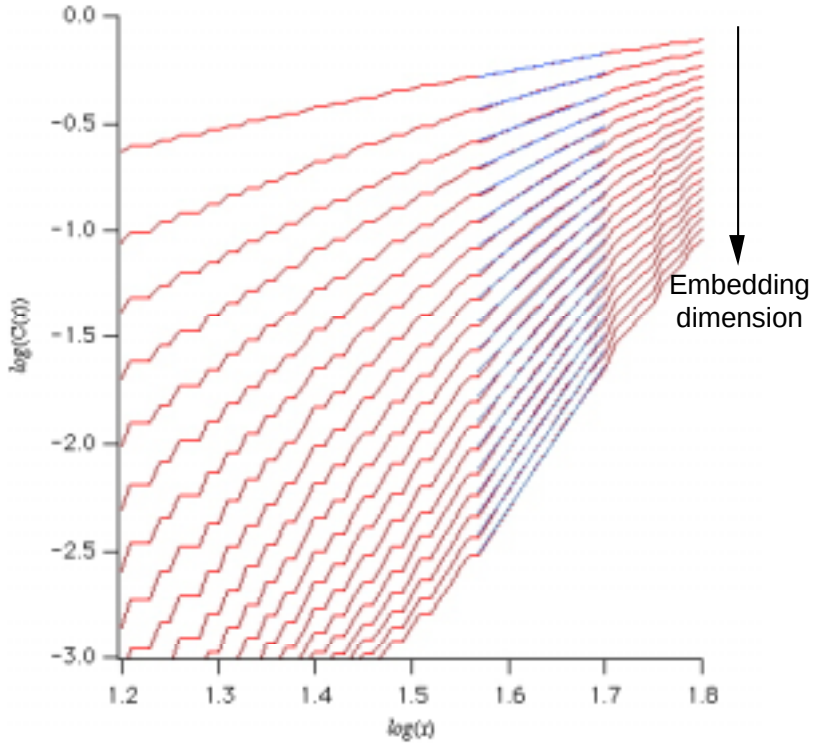

Figure 4(b). Correlation dimension vs. embedding dimension

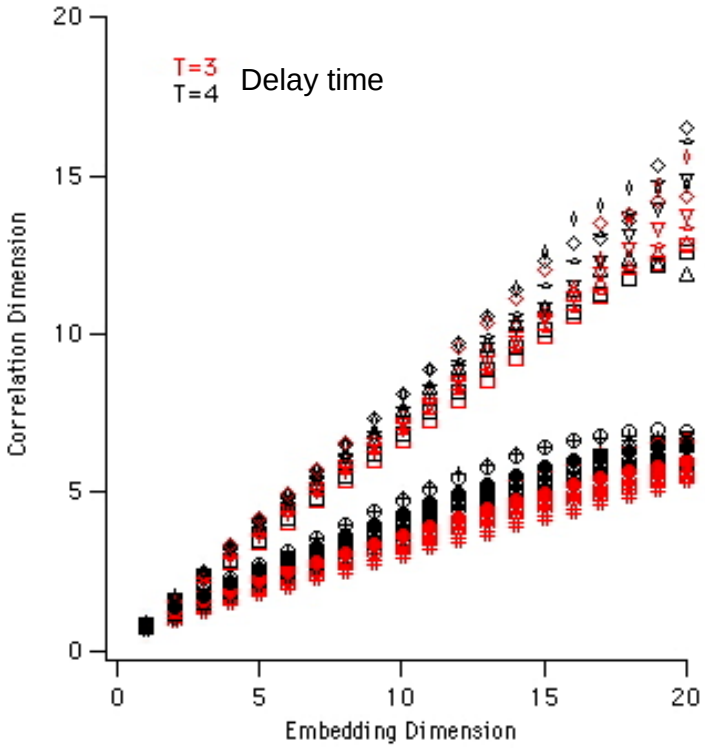

Figure 5. Correlation dimension vs. decay ratio

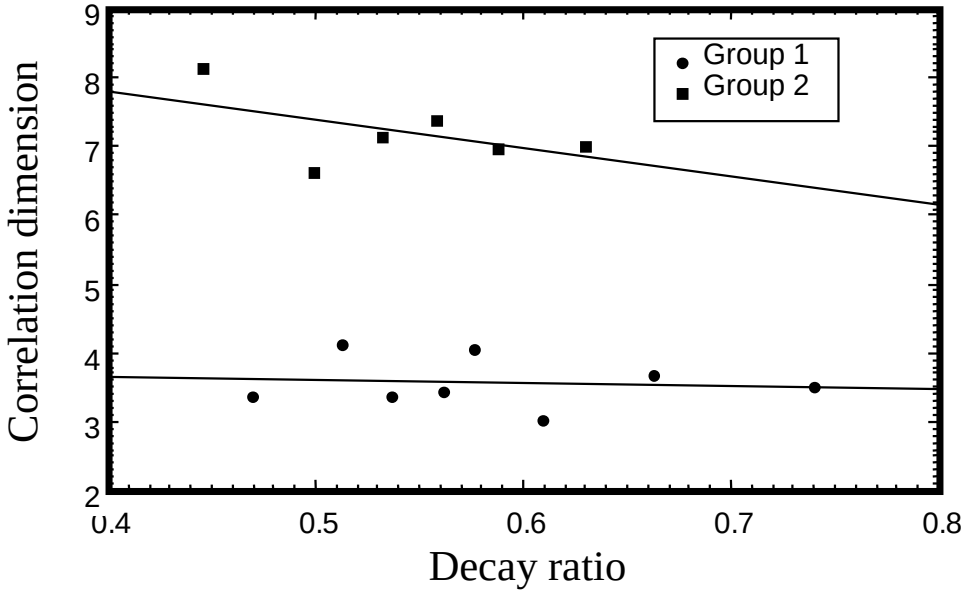

Figure 6. Comparison of PSDs between two groups

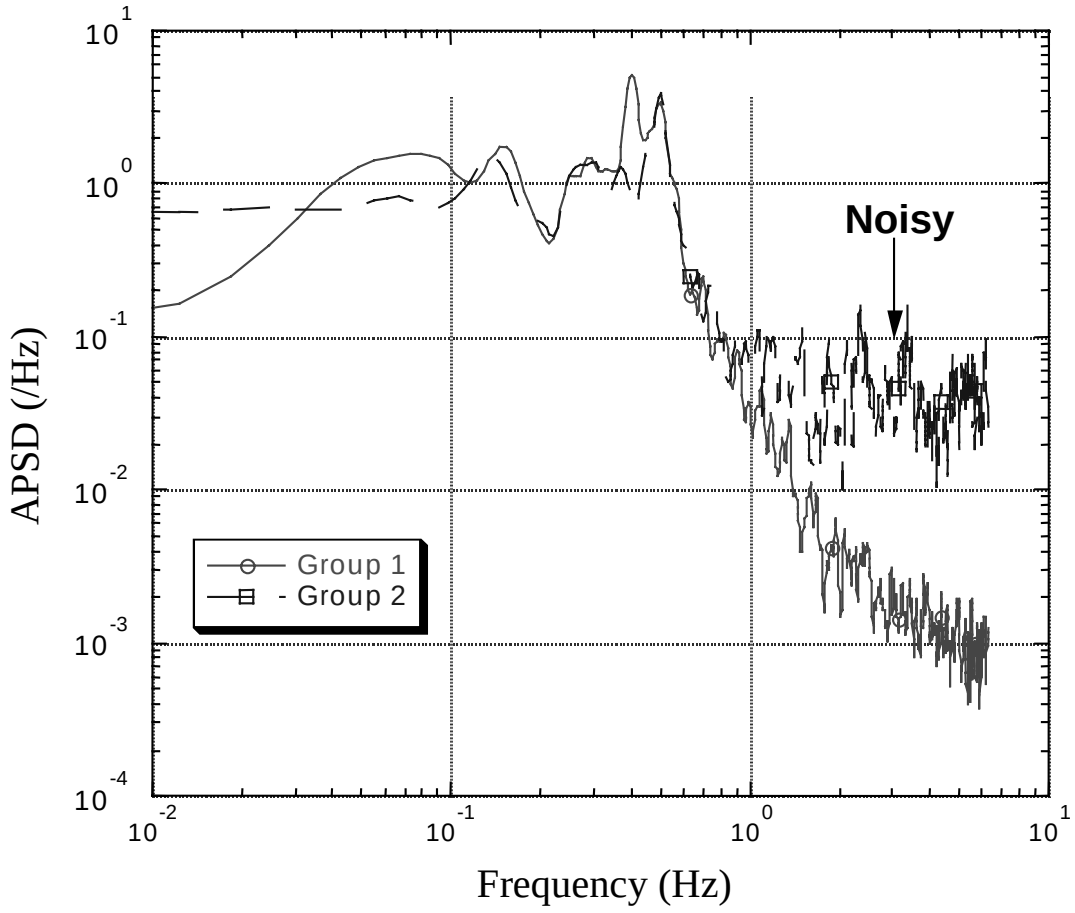

Figure 7. Results of Case 2

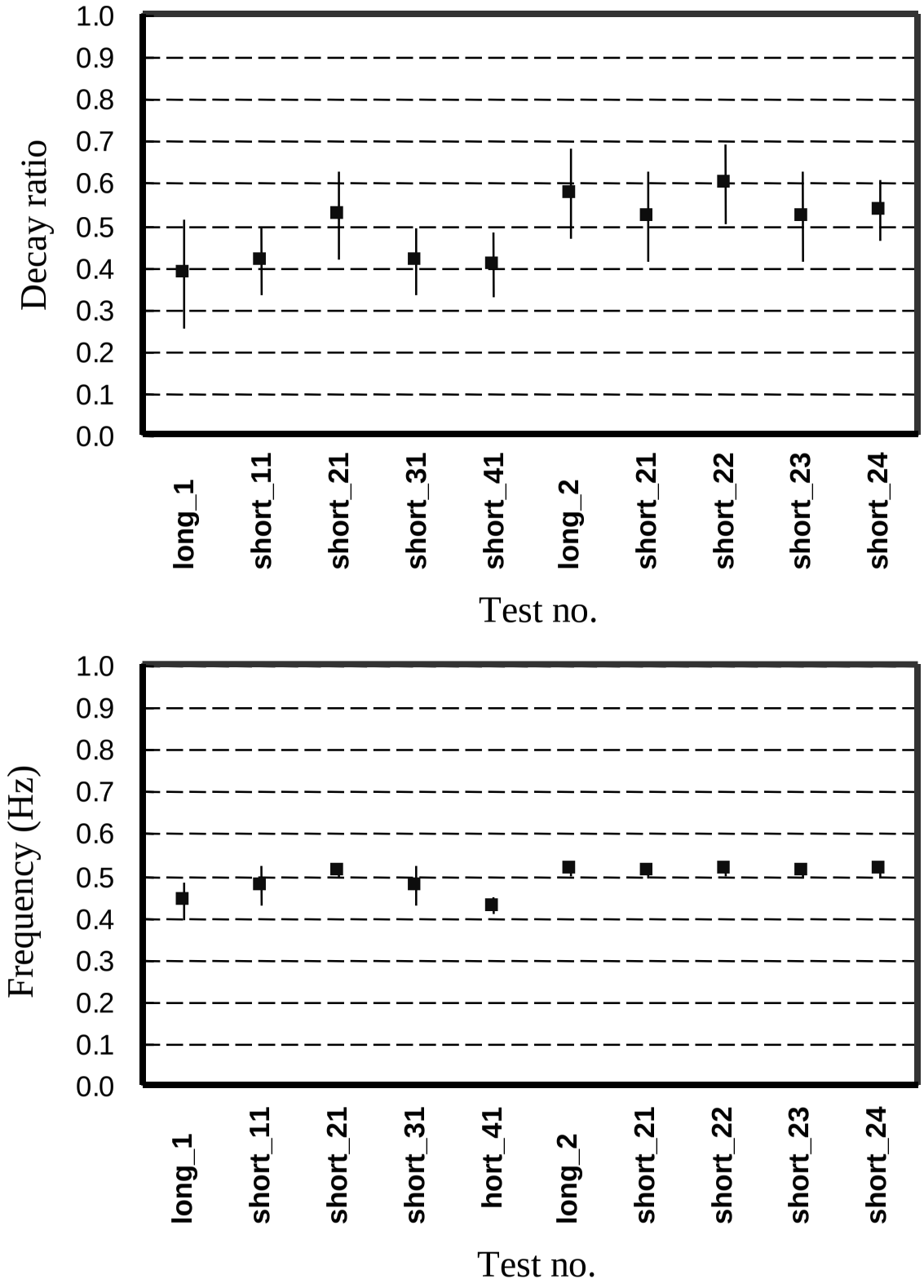

Figure 8. Results of Case 3

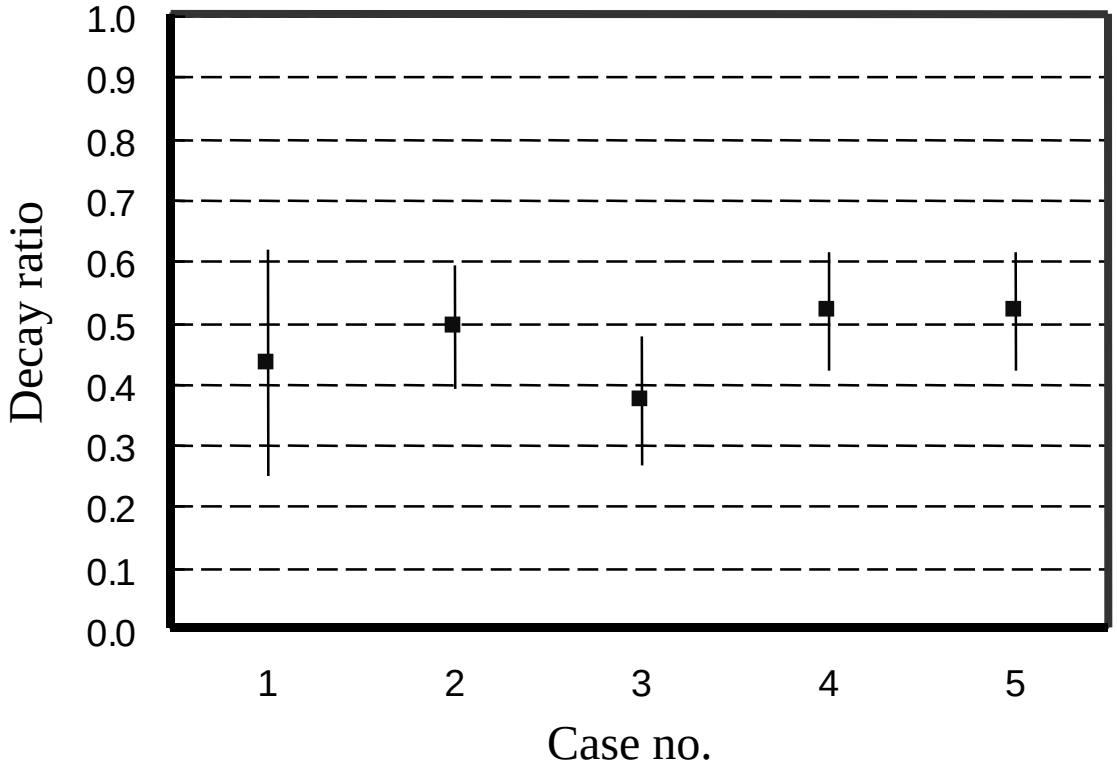

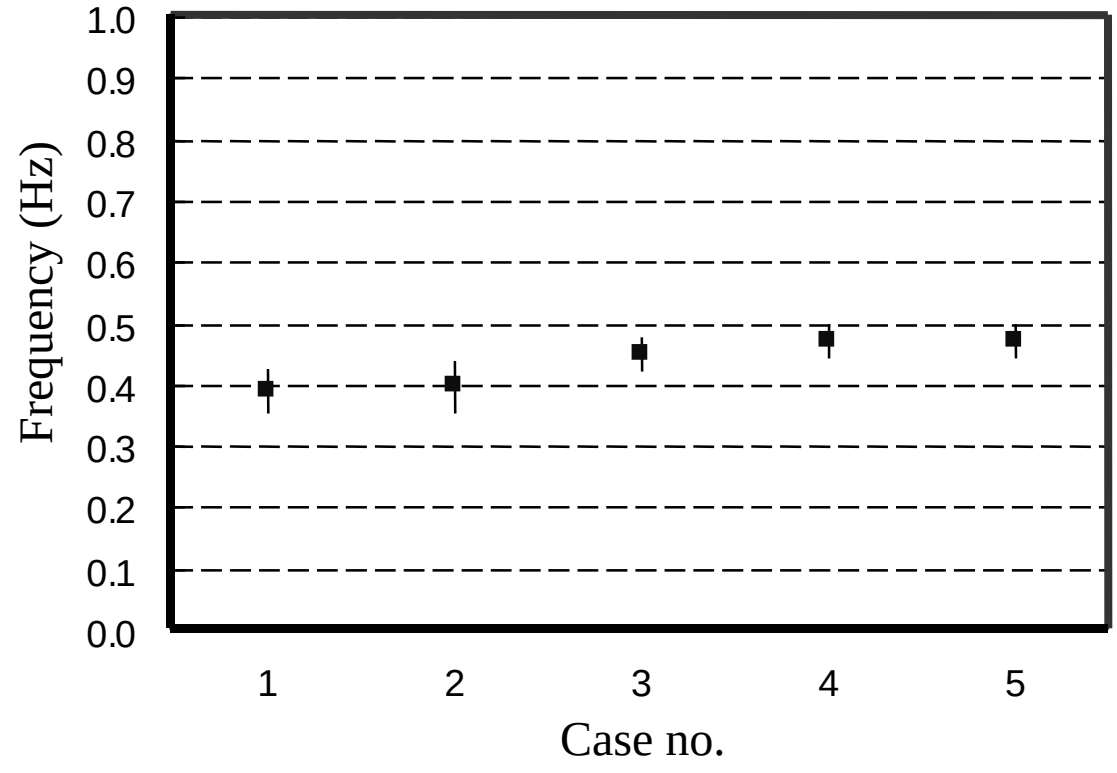

Figure 9. FFT analysed PSD for Case 3

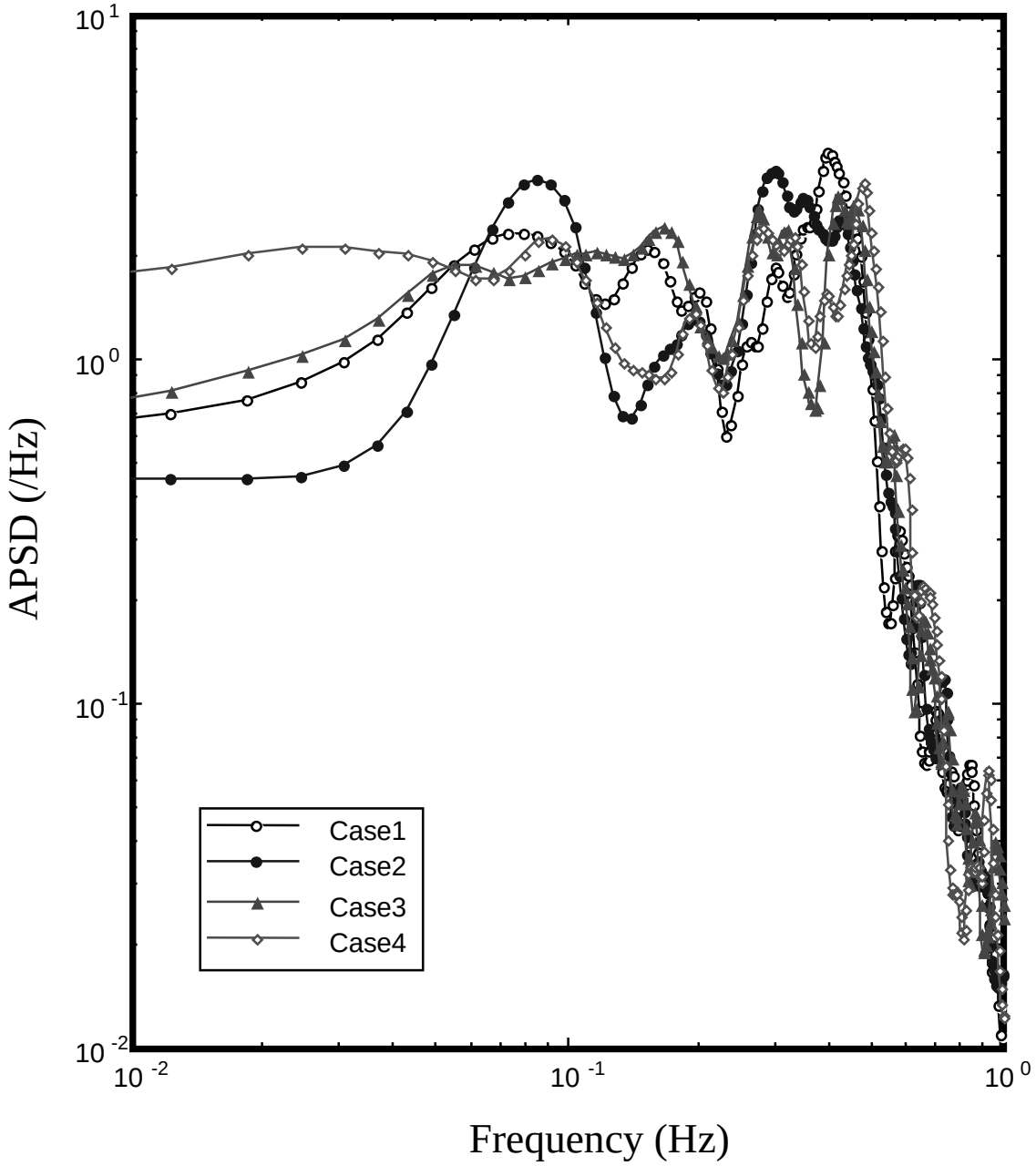

Figure 10. Comparison of original PSD and composed PSD with a set of dominant poles

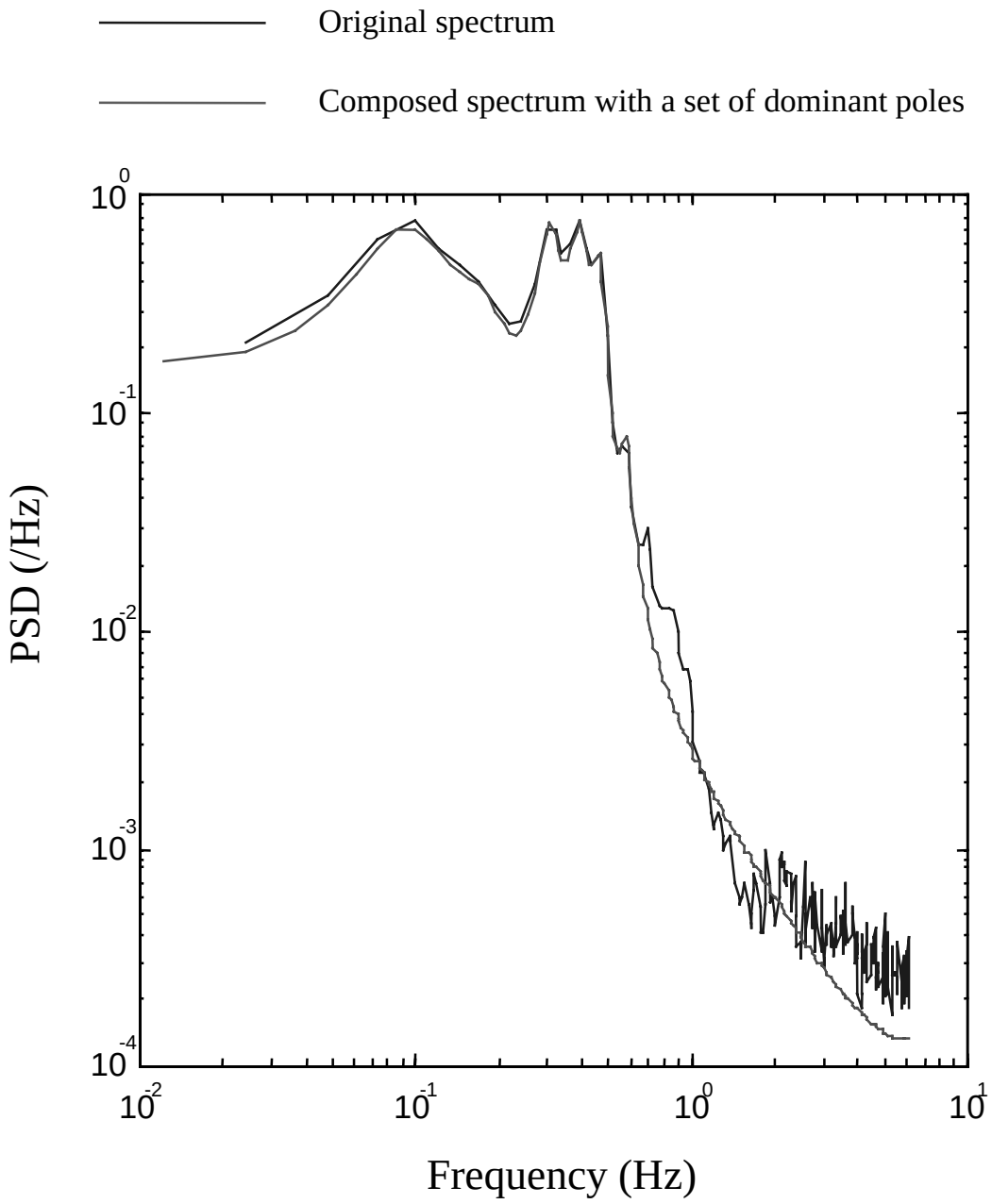

Figure 11. Comparison of decay ratio and frequency between two methods: impulse response and dominant pole

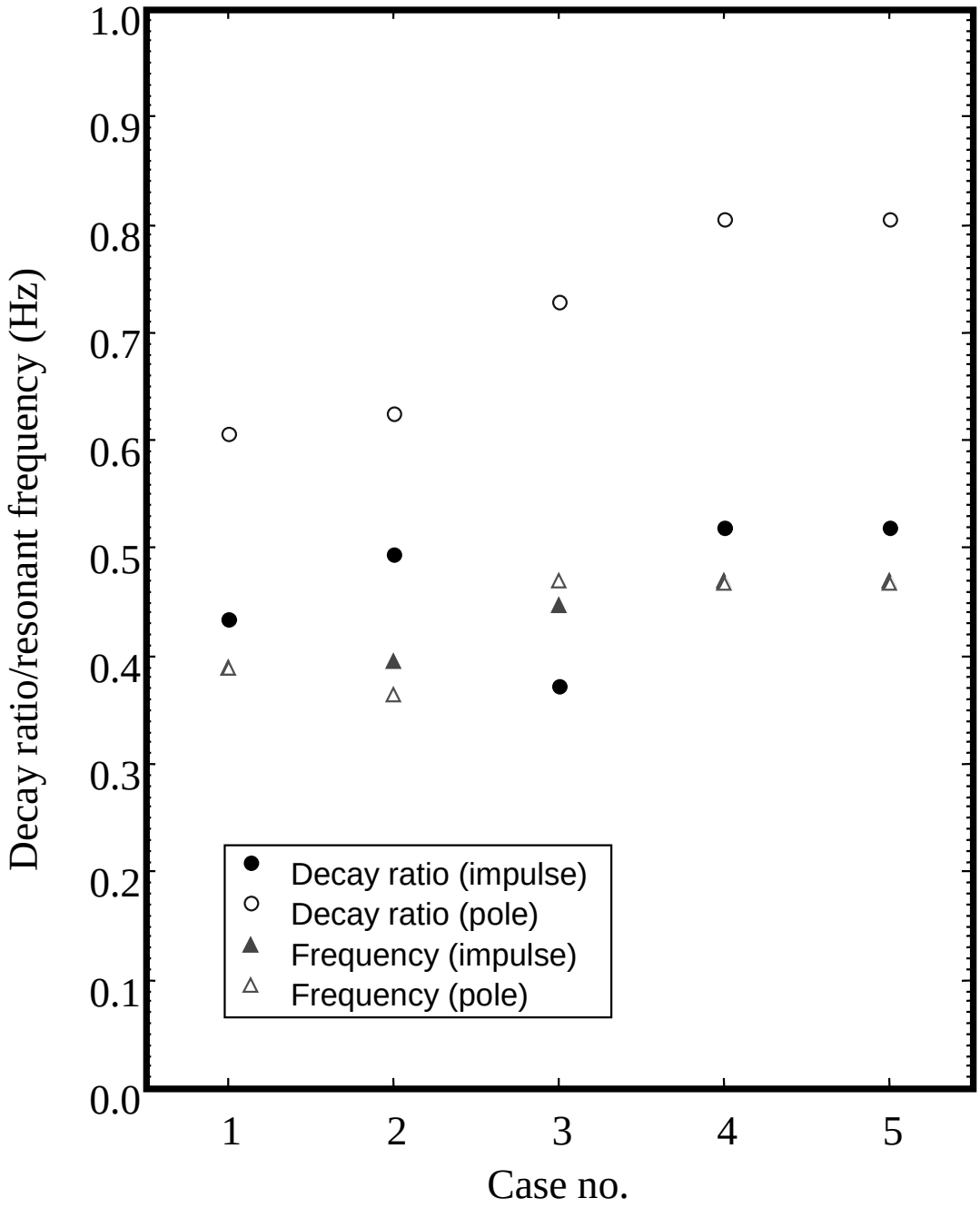

Figure 12. Mode amplitude response to the angle of averaging weights

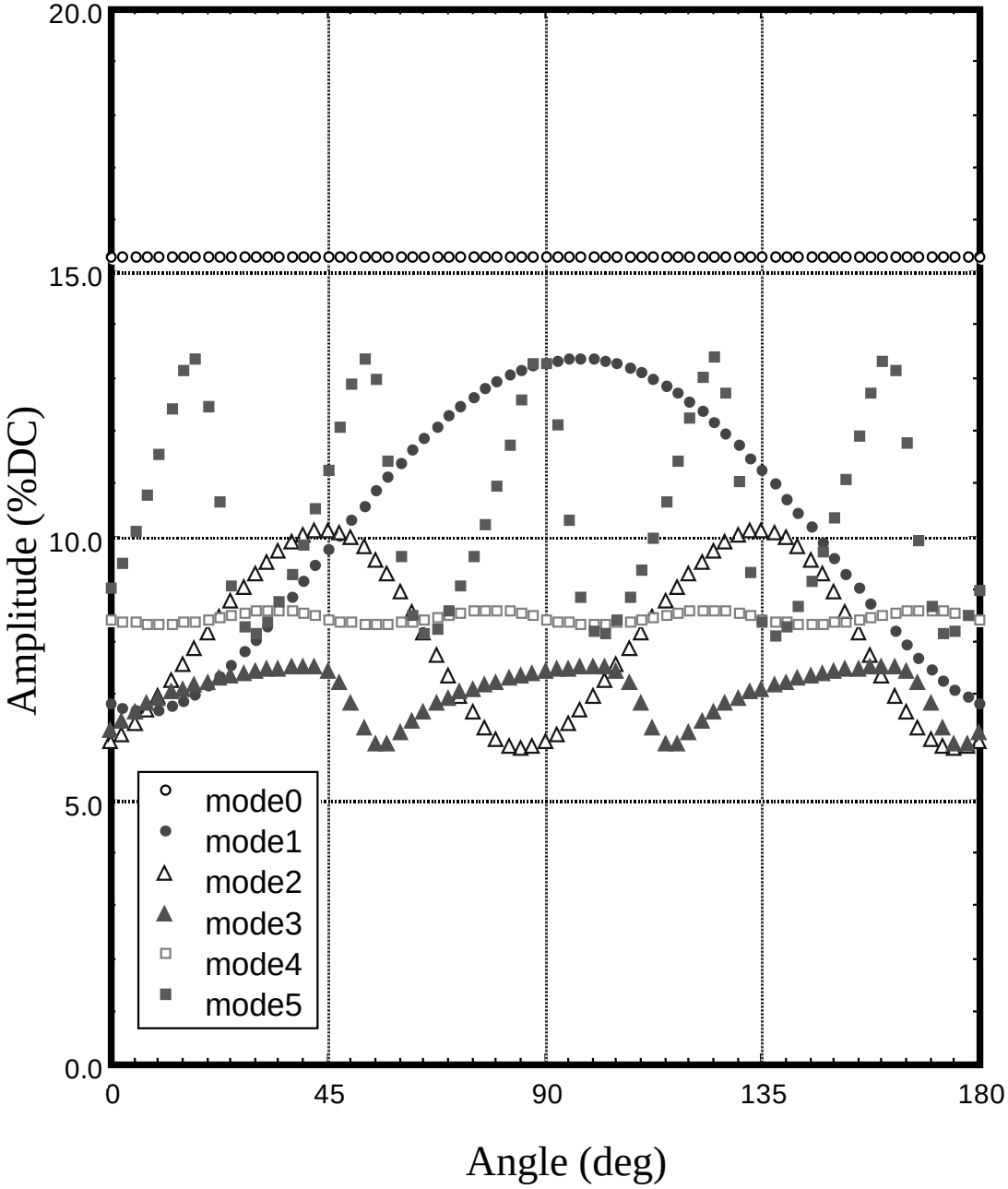

Figure 13. Results of Case 4

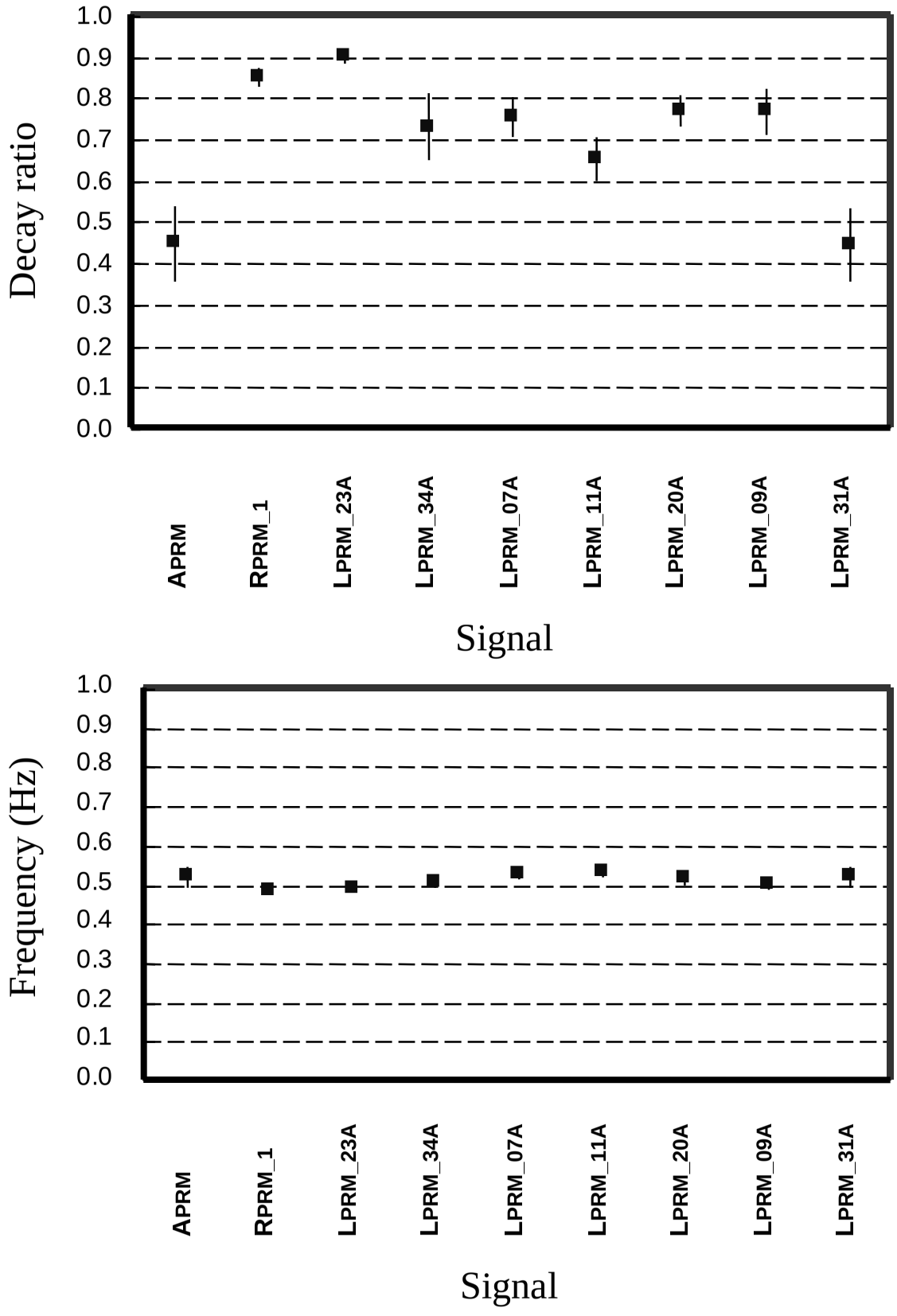

Figure 14. APSD of APRM and RPRM-1 in Case 4

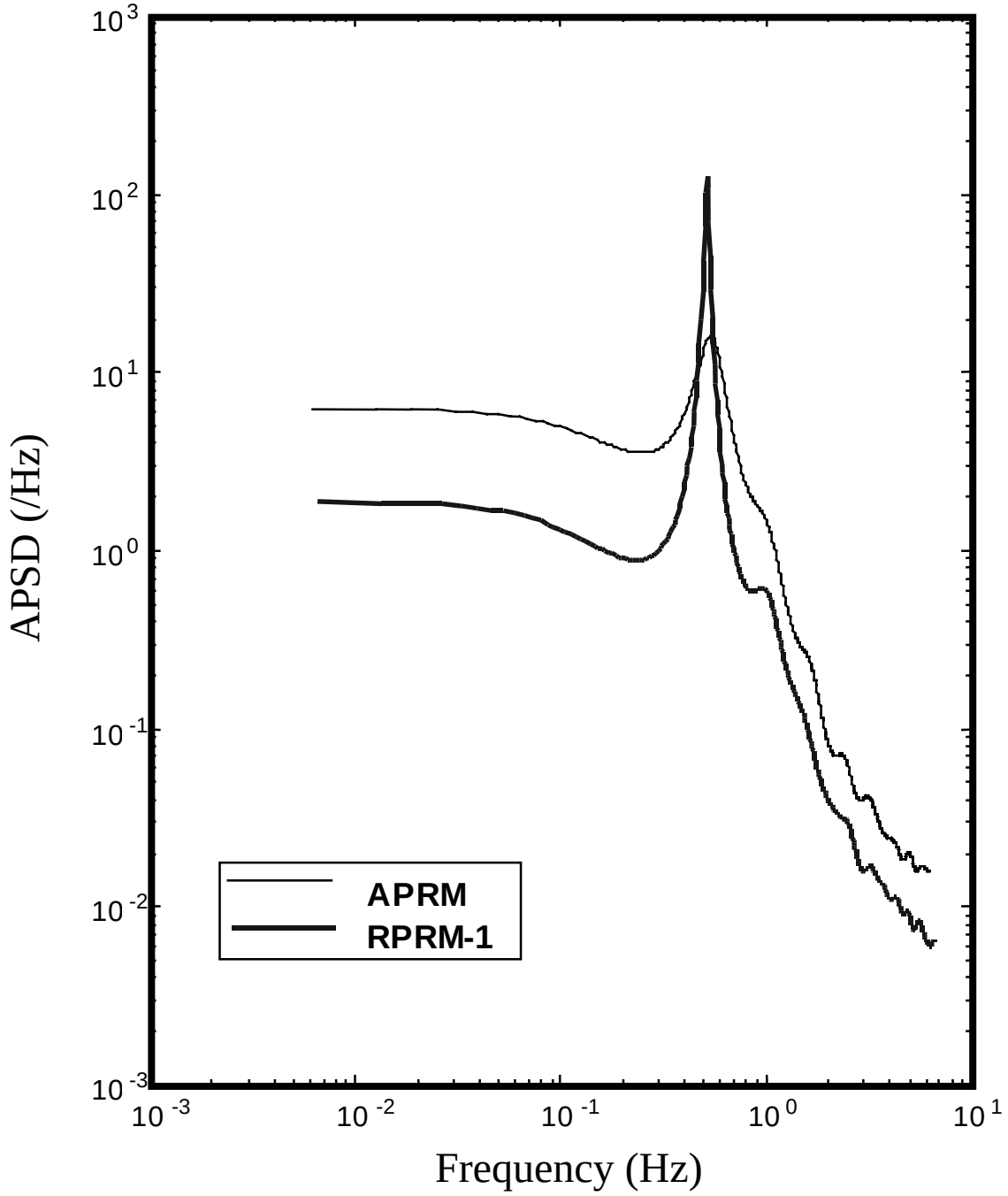

Figure 15. Comparison of amplitude between mode0 and mode1

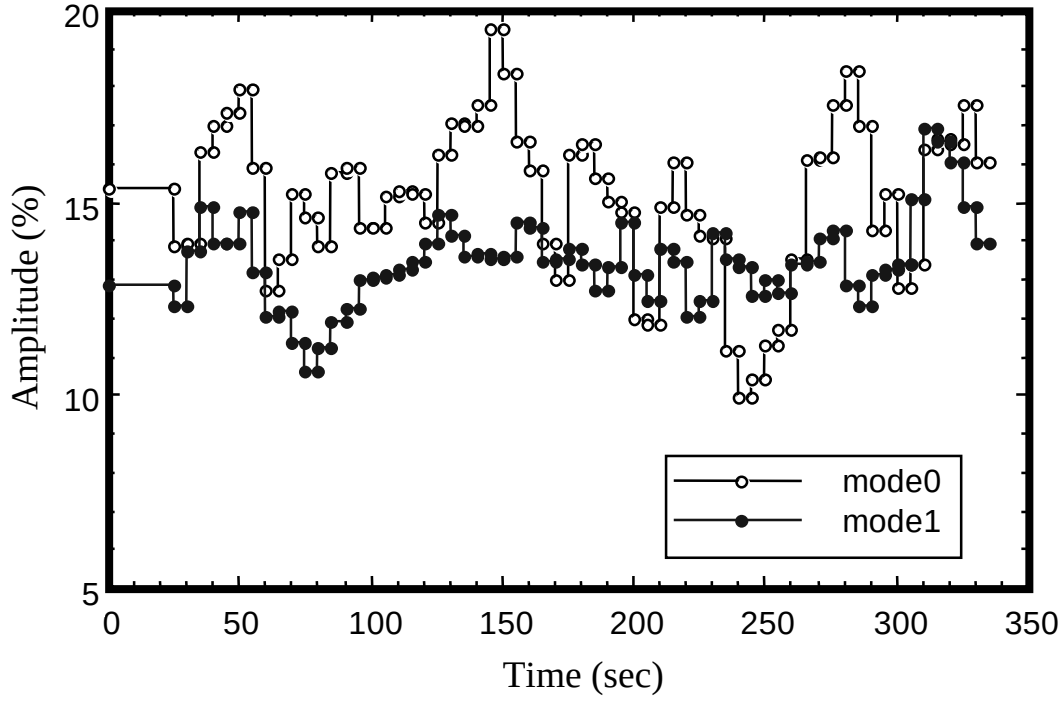

Figure 16. Phase delay of LPRM signals from LPRM-23A

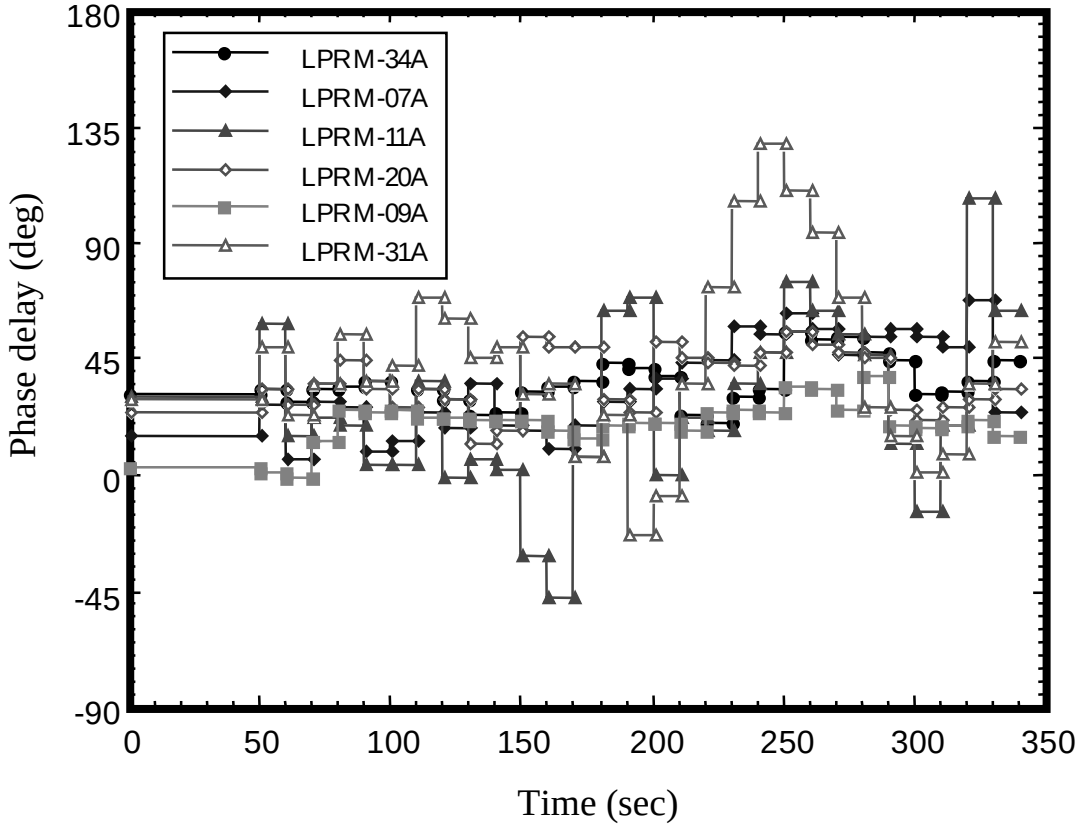

Figure 17. Coherence of each LPRM between LPRM-23

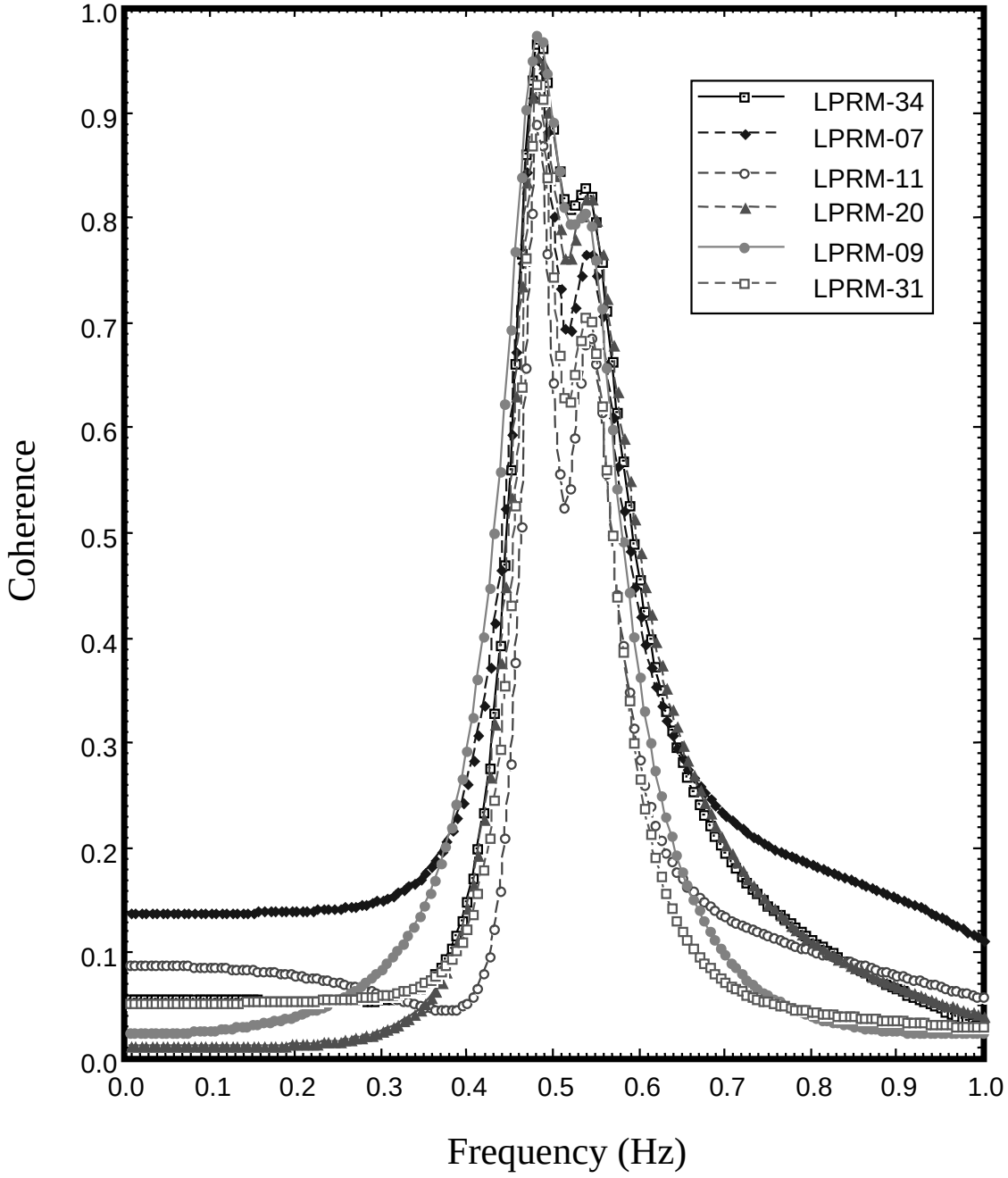

Figure 18. Comparison of decay ratio and resonant frequency change

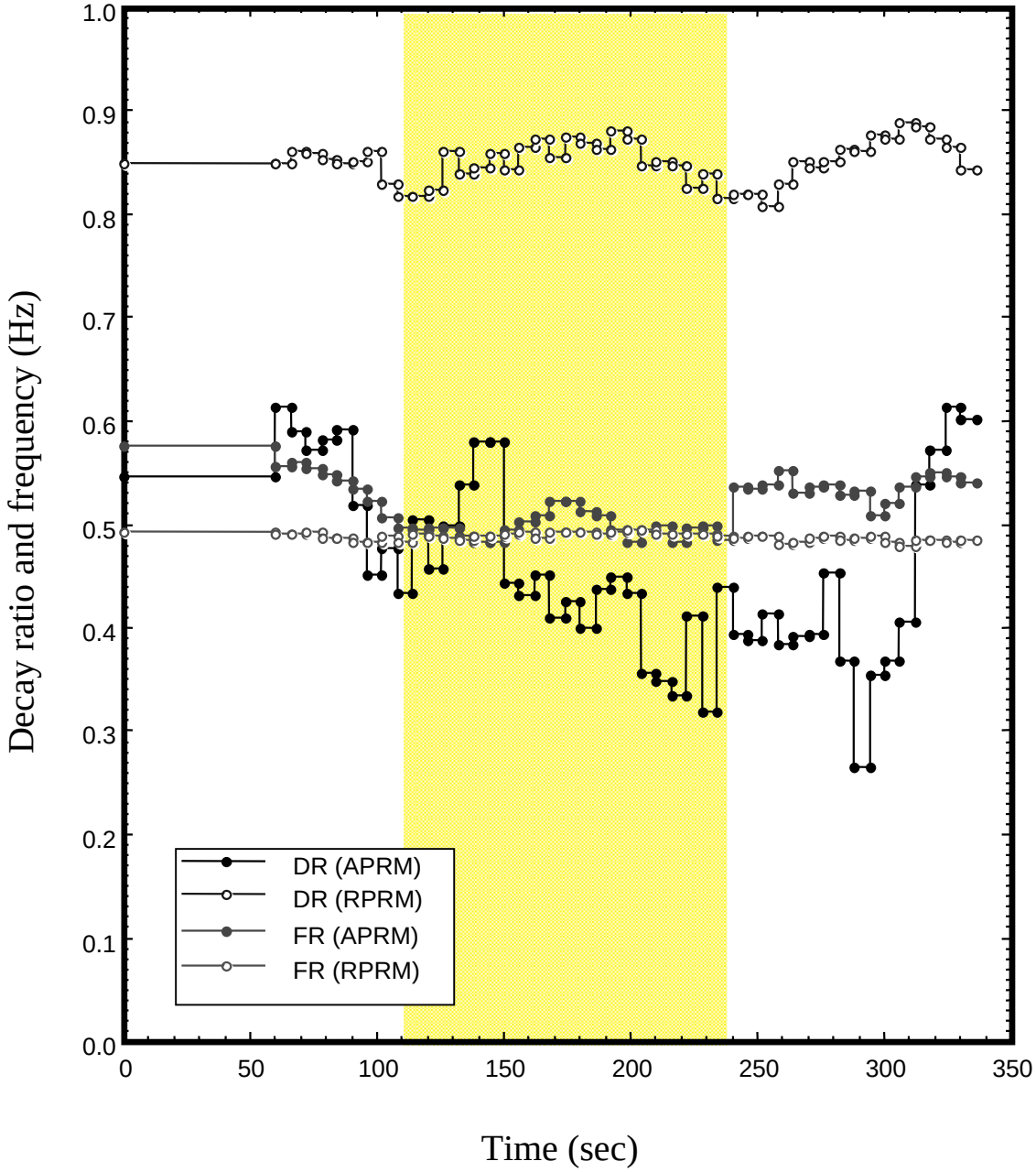

Figure 19. Estimated trend for Case 5

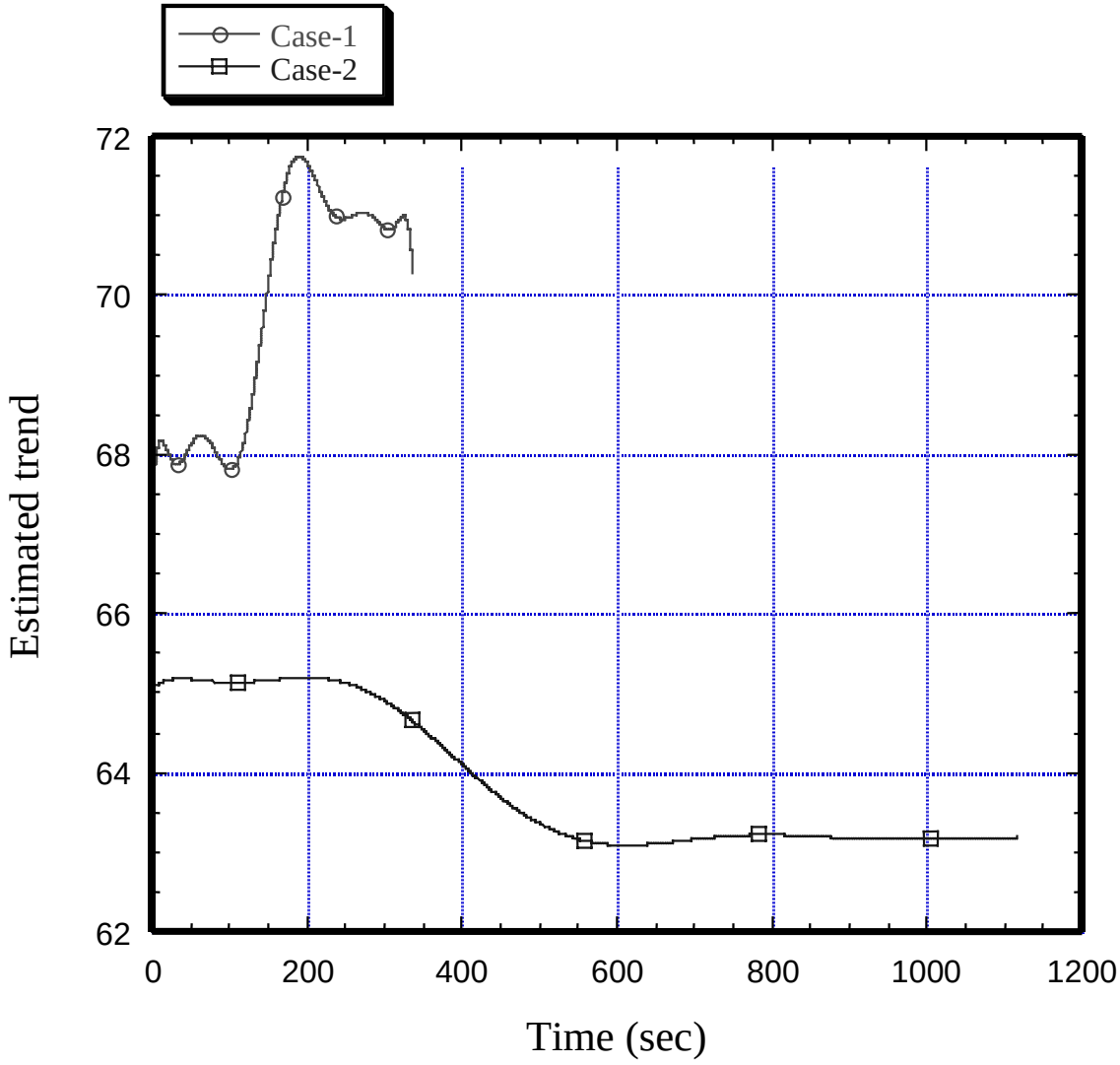

Figure 20. FFT analysed PSD of Case 5 data

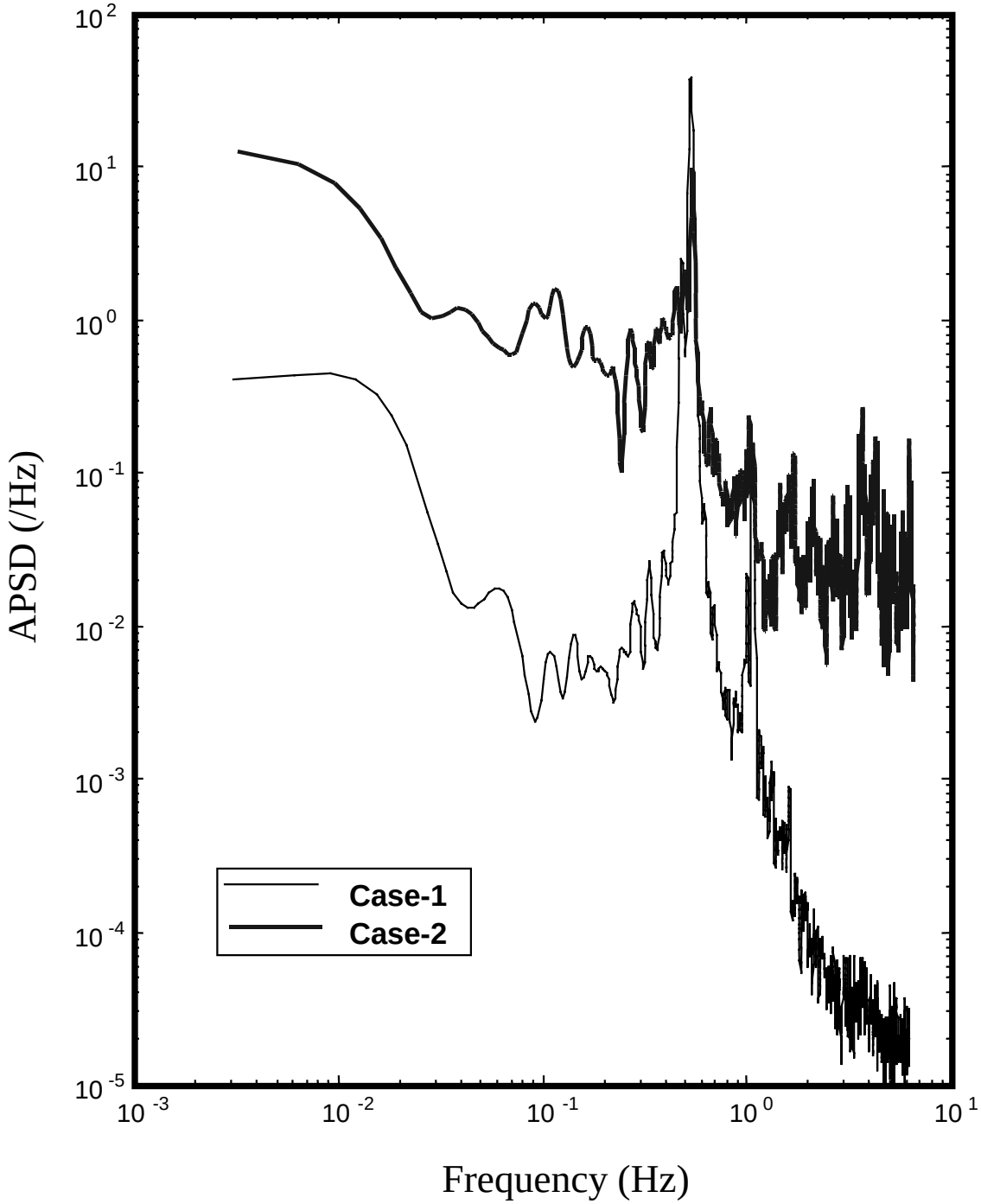

Figure 21. Results of Case 5

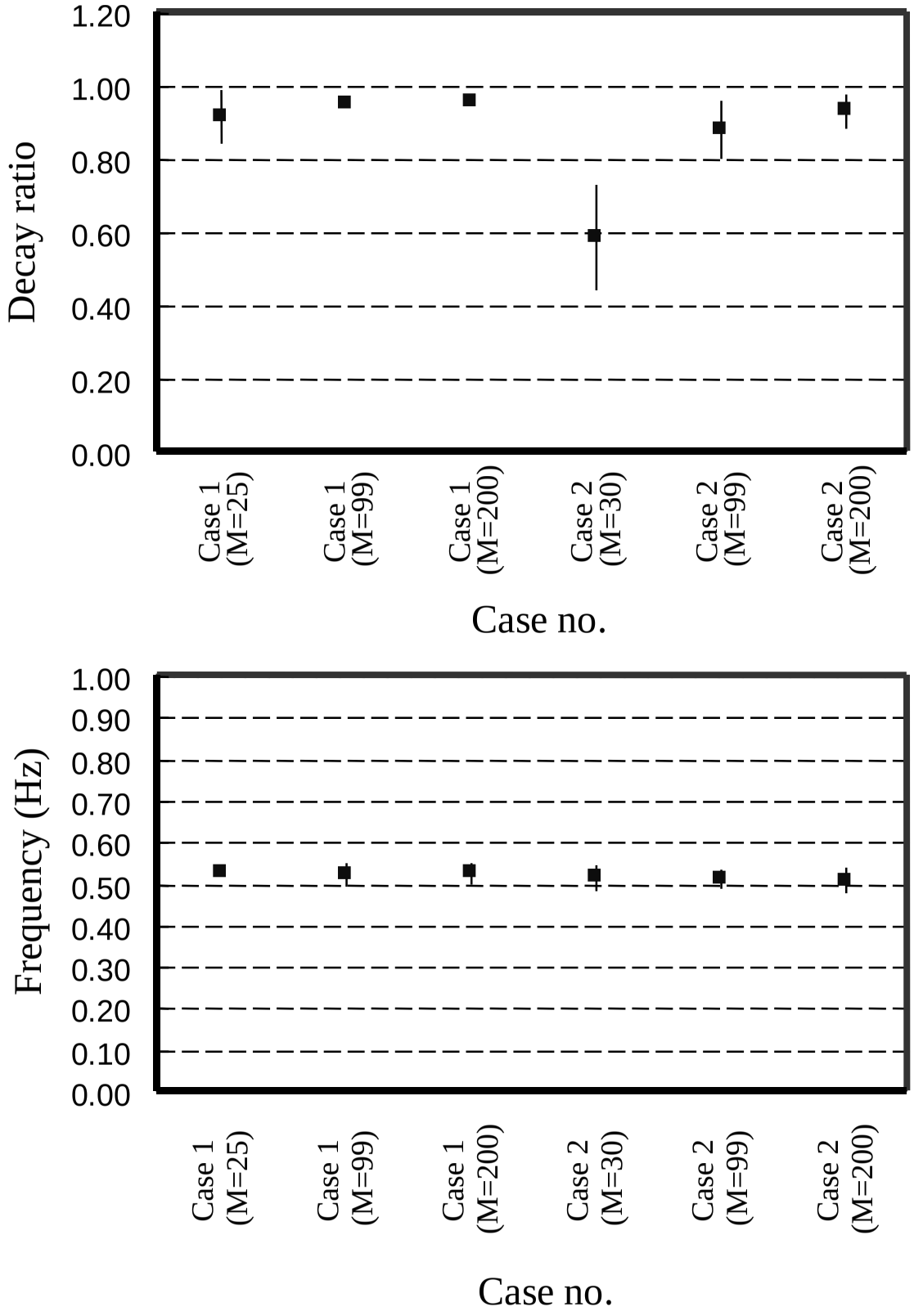

Figure 22. PSD of partial data interval

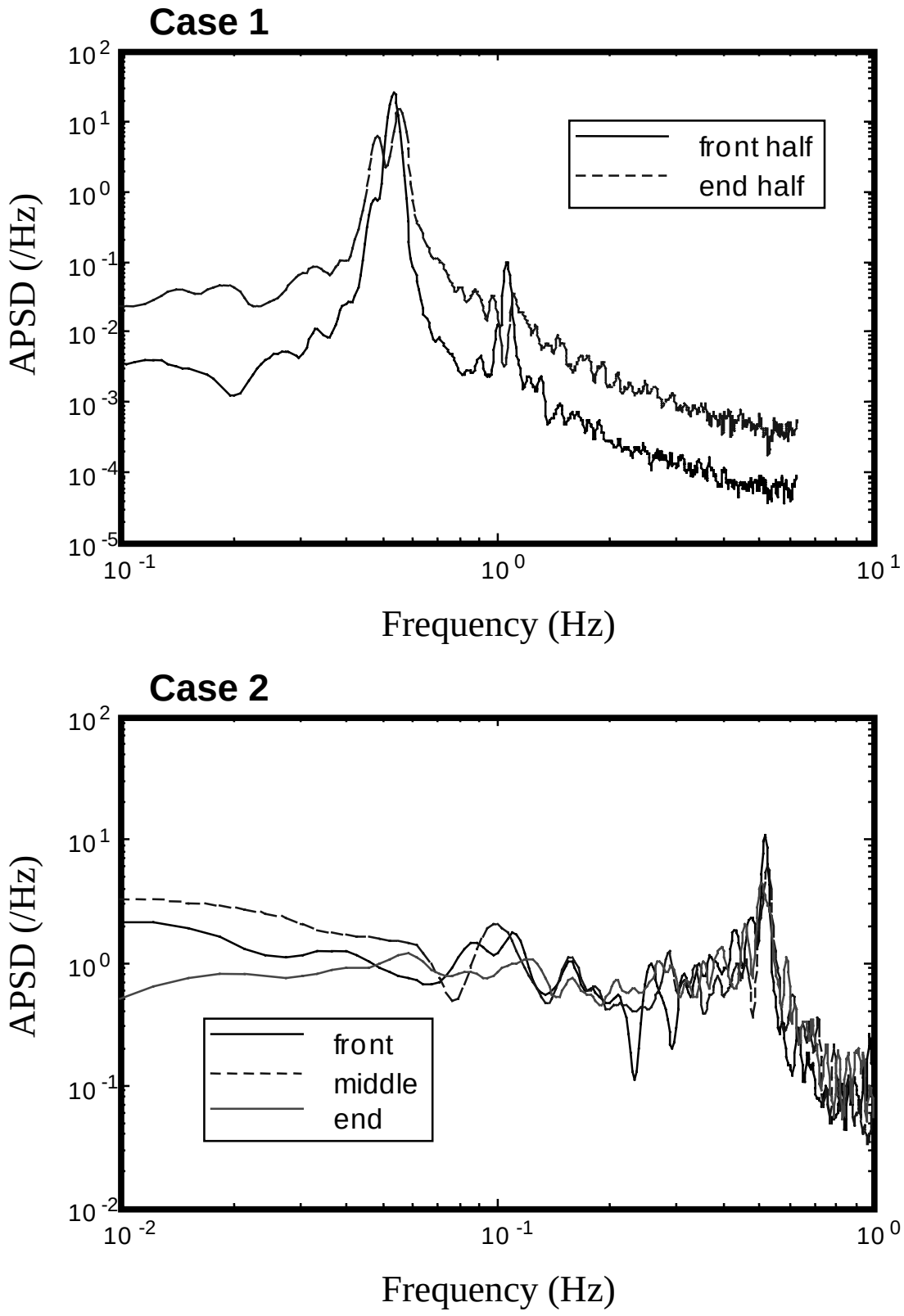

Figure 23. Change of dominant poles of s-plain

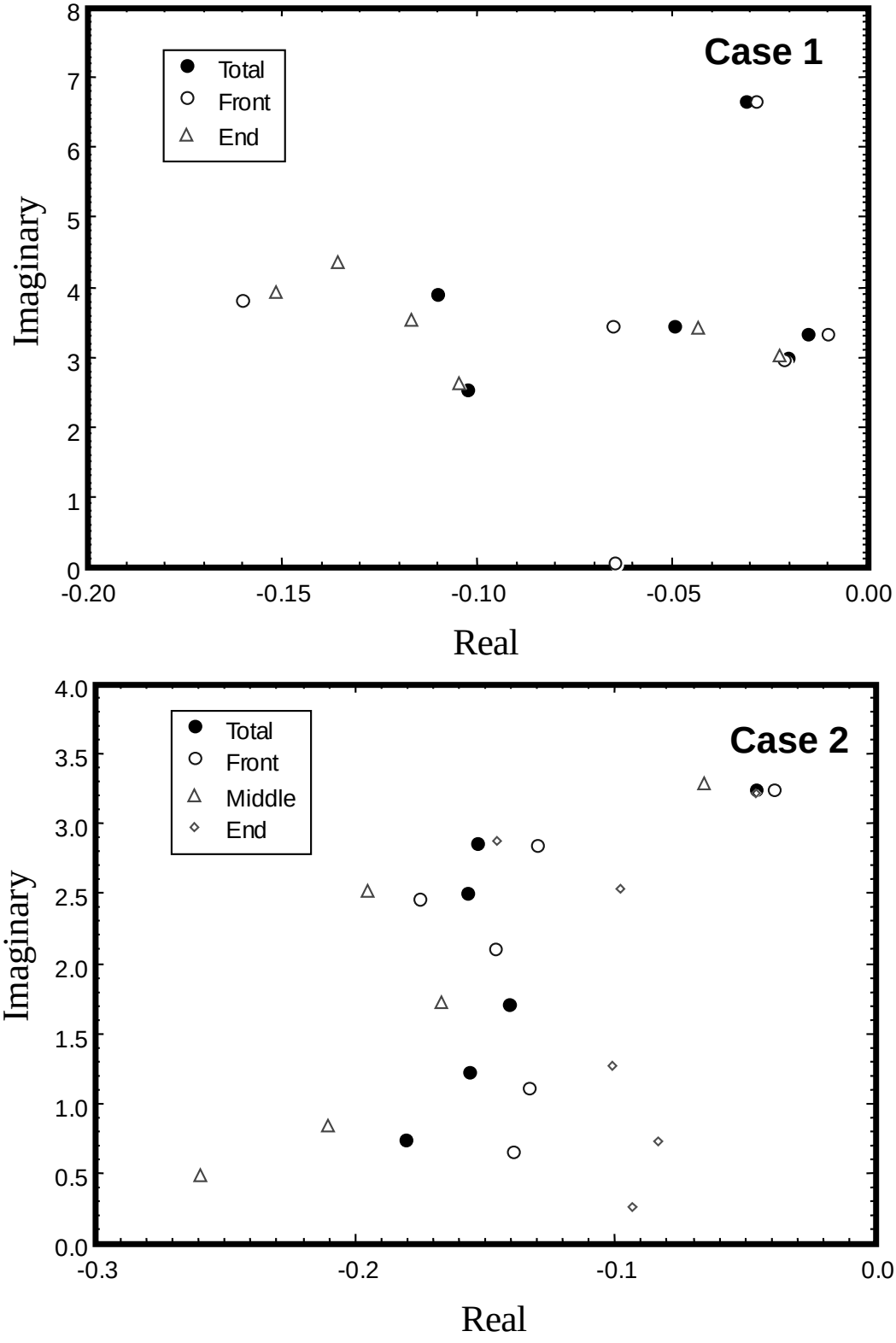

Figure 24. Results of Test 1 in Case 6

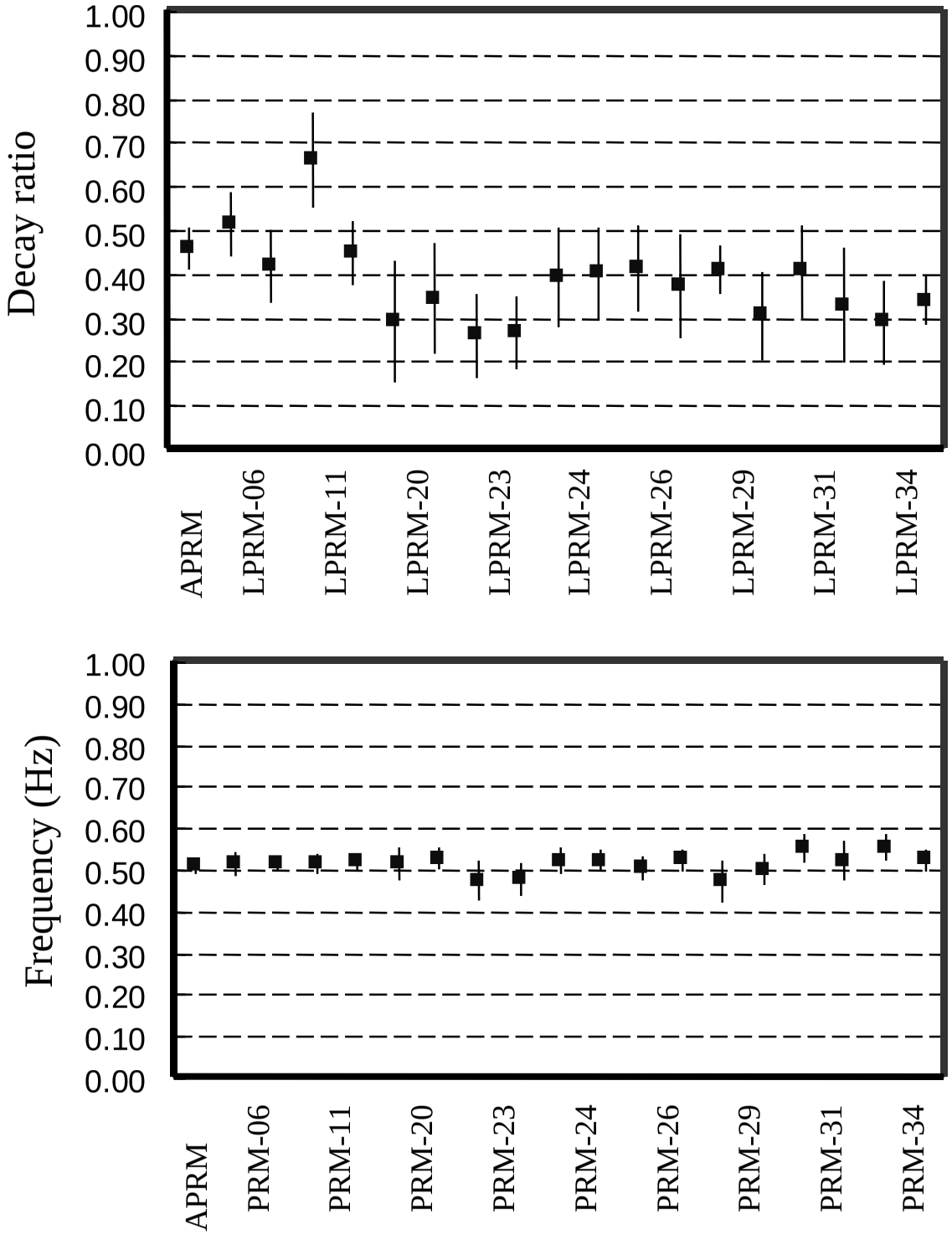

Figure 25. Results of Test 2 in Case 6

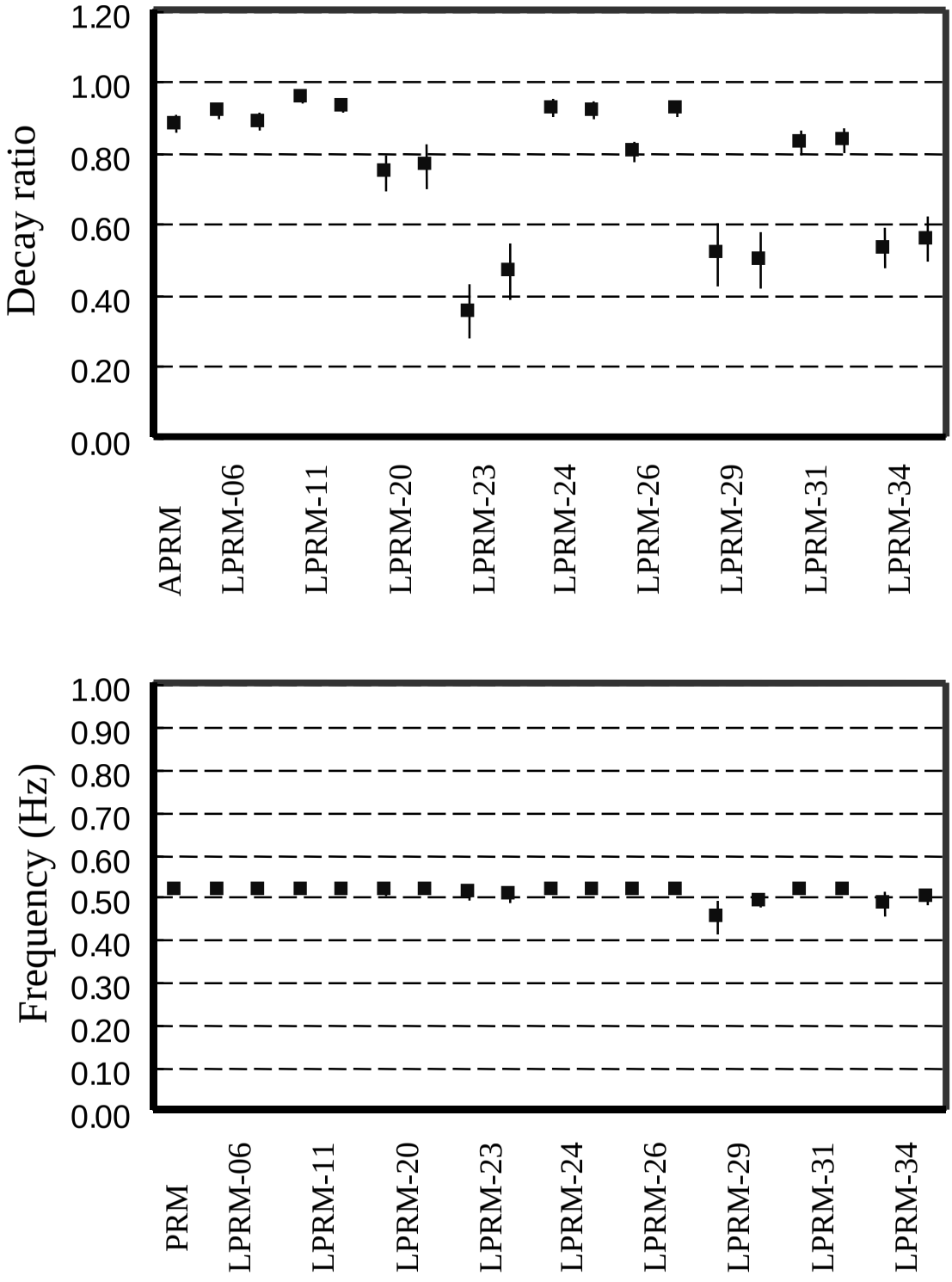

Figure 26. Phase delay from LPRM-11A

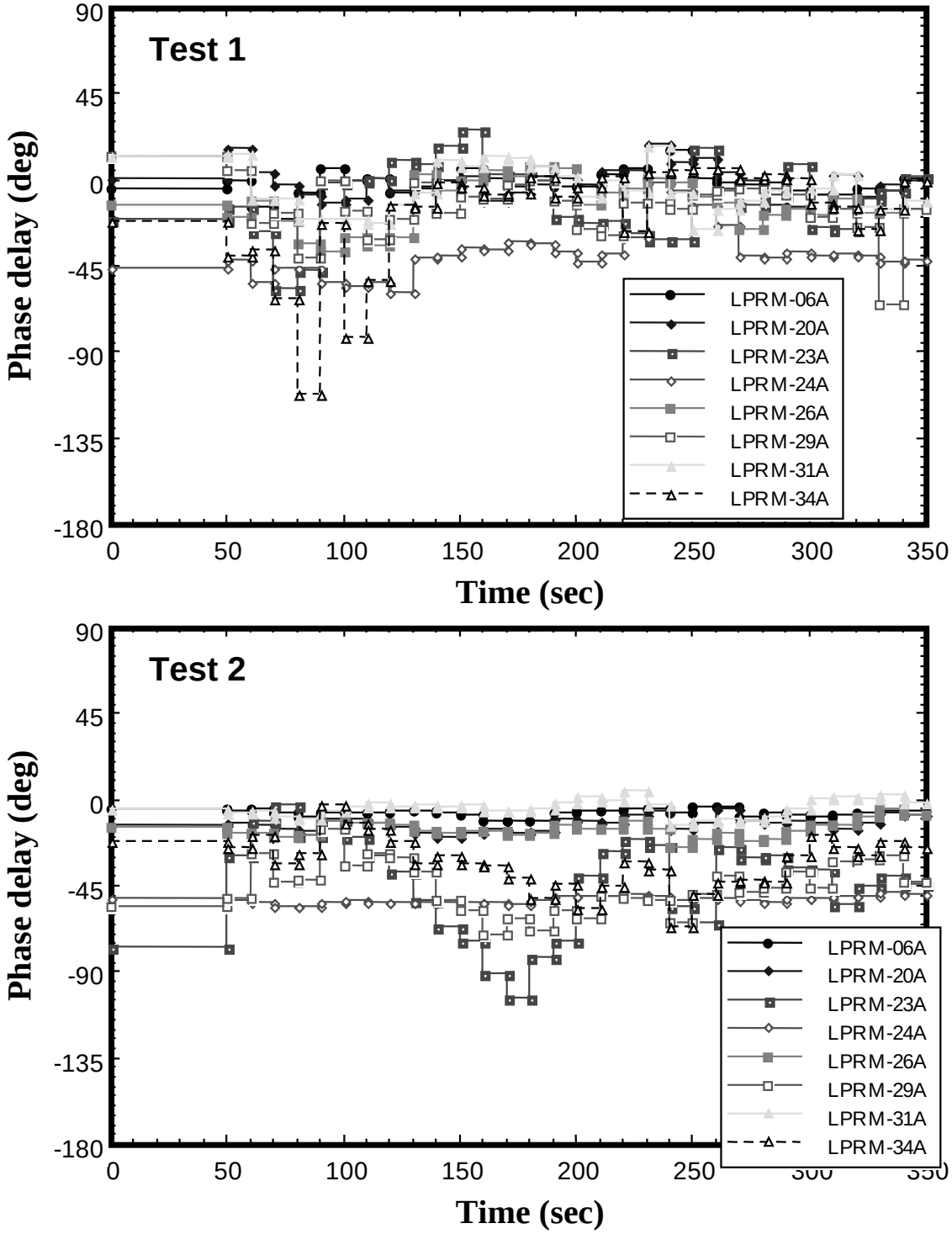

Figure 27(a). Noise source contribution of Test 2

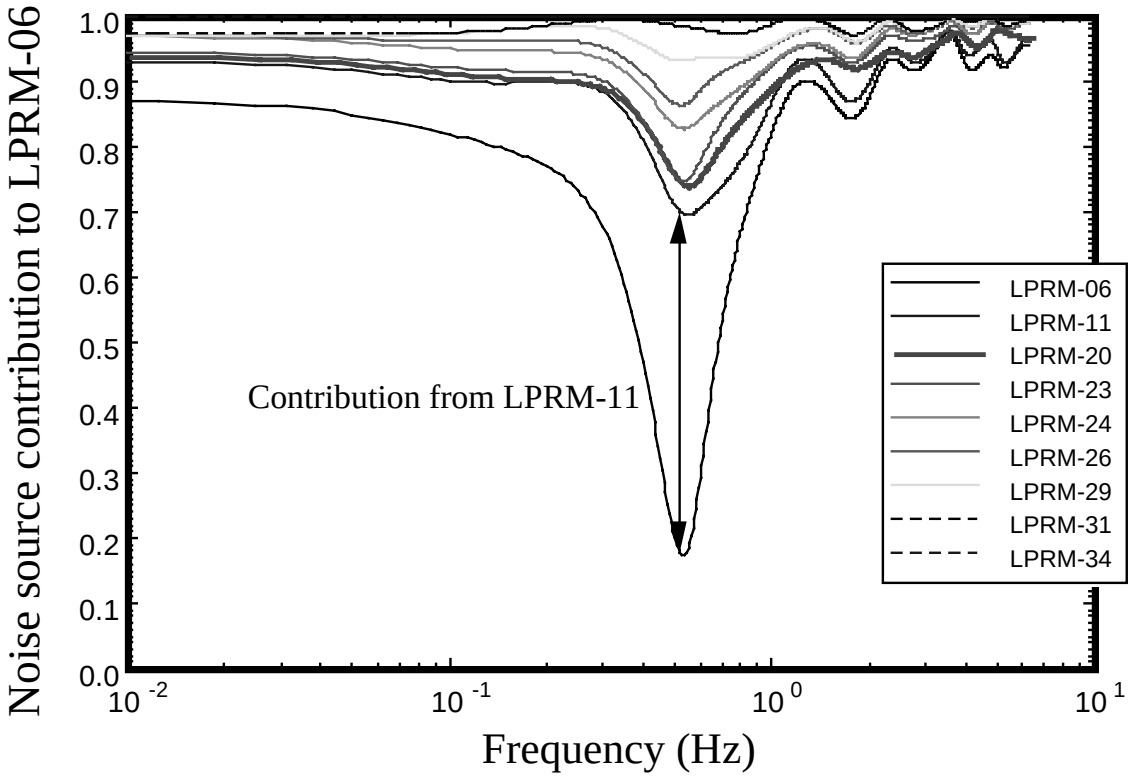

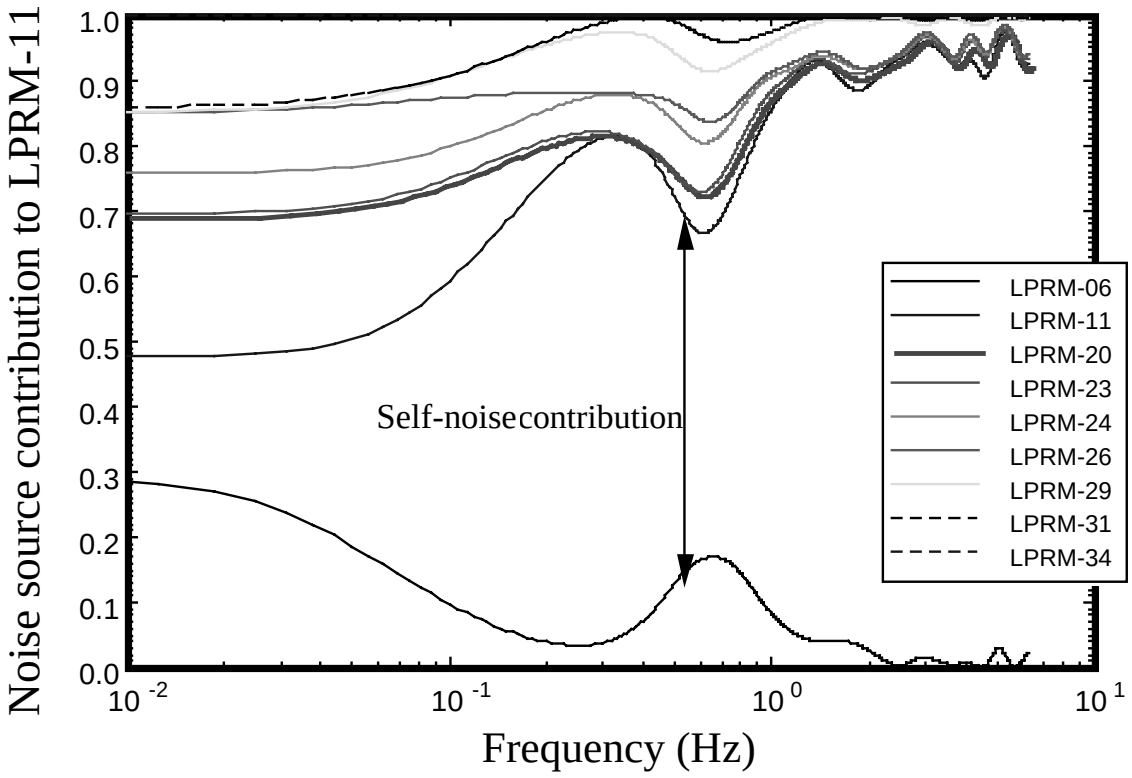

Figure 27(b). Noise source contribution of Test 2

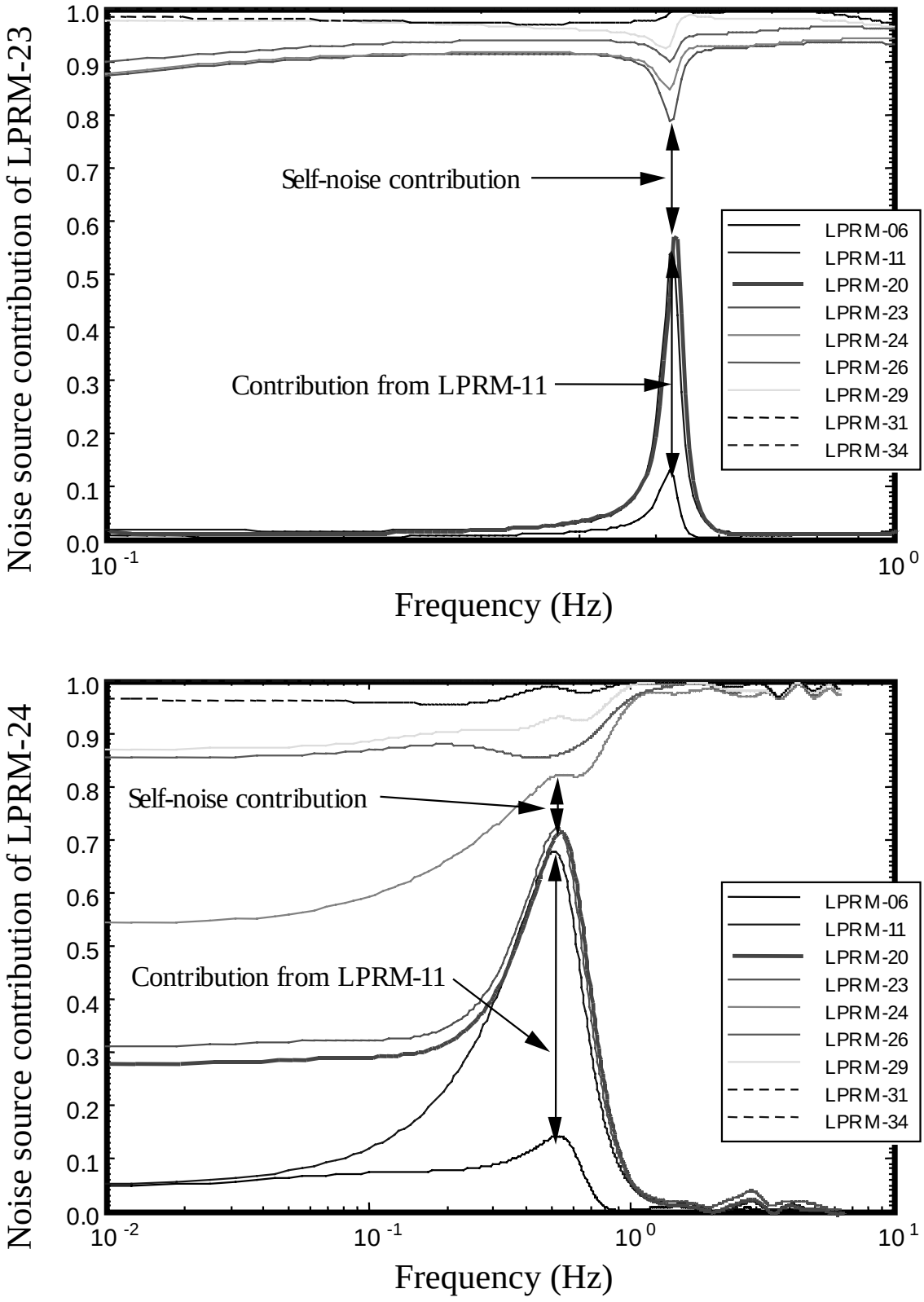

Figure 27(c). Noise source contribution of Test 2

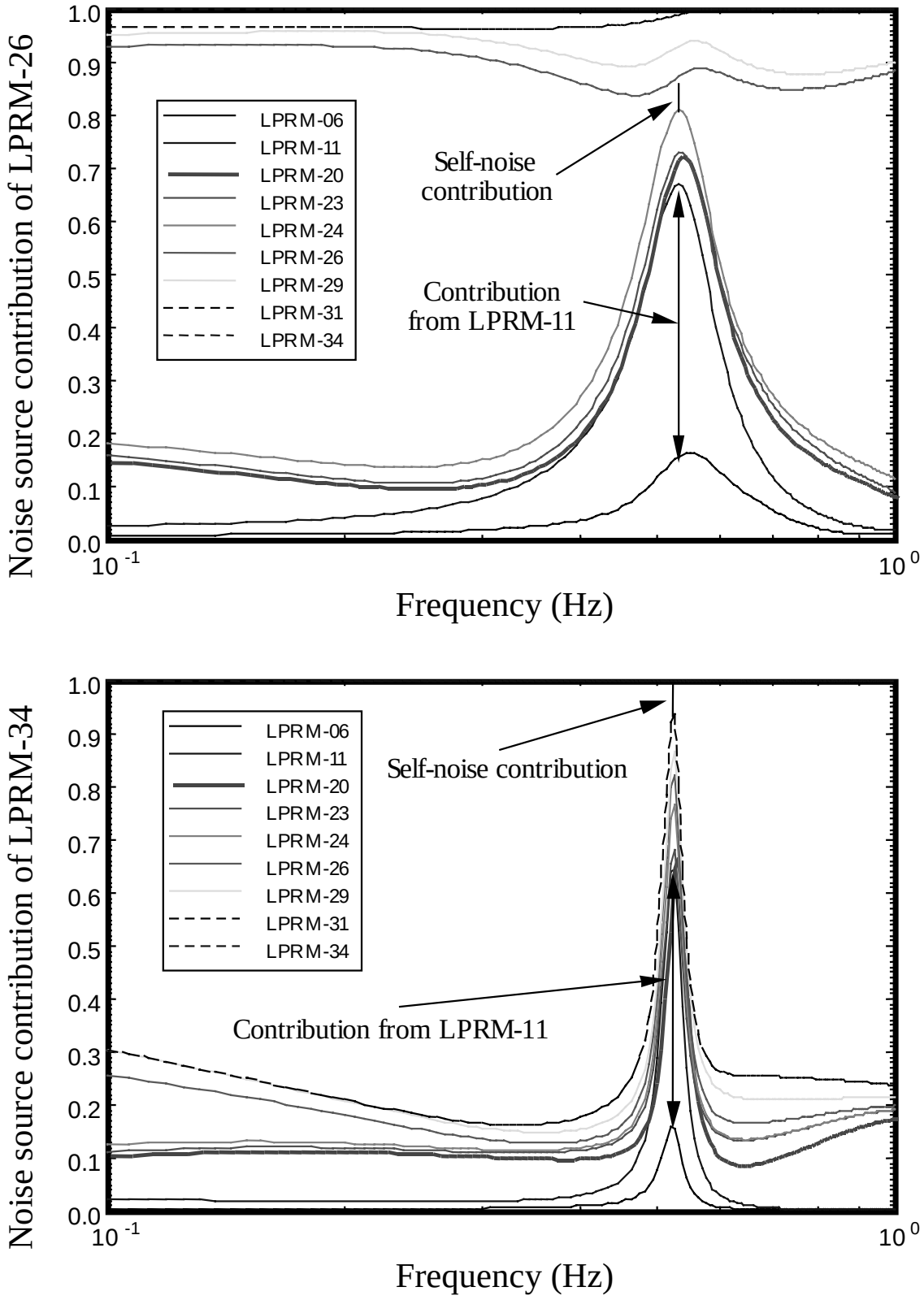

Annex 9

METHODOLOGIES AND RESULTS PRESENTED BY TU DELFT*

Introduction

In this report the preliminary results for the NEA benchmark on noise analyses of Forsmark data are given. Different methods for the determination of decay ratio and the oscillation frequency can be used. Within these methods choices are to be made on how to determine the stability parameters. Therefore, parameter studies on the influence of input parameters on the calculated stability parameters are very important to give an idea of the accuracy of the stability parameters. We have not performed such studies in the framework of this benchmark. Such results will arise as a consequence of intercomparison of the results of different participants to the benchmark. We have used a consistent methodology for all cases to enable such a comparison. In this report we will present the outcome of the calculations without discussing the results in detail. This discussion will be prepared for the preliminary meeting. In our opinion, during the discussion of the preliminary results, the participants to the benchmark should agree on intercomparison of specific further information (such as auto power spectral density, impulse responses, auto-correlation function, etc. for specific cases). The results presented in this report consist of the calculated decay ratios (DR), the oscillation frequencies (OF), and the time range that the impulse response as calculated by our auto-regressive (AR) model is fitted to a third order model. The uncertainties and the position of the poles of the transfer function have not yet been analysed. Moreover, more analyses need to be made in order to better understand the results.

Methodology

In-house developed software is used to analyse the time series. The time series are divided in records of 256 samples. These records are analysed by FFTCALC, a program which calculates auto and cross frequency spectra form discrete signal values by the Fast Fourier Transform method. A boxcar data window has been applied. The program SPEPLOT is used to calculate the auto and cross correlation functions. Then, an auto-regressive model is calculated using the SYSIDENT program. In the calculation a fixed model order has been used (= 80). From the AR matrices the system impulse response is calculated by the program ARRESP. This is done for 16 seconds. Next, this impulse response is fitted to a third order model:

$$f(t) = a\exp\left(-\frac{t}{b}\right) + c\exp\left(-\frac{t}{d}\right)sin(ex - f)$$

* W.J.M. de Kruijf
Interfaculty Reactor Institute
Delft University of Technology
Mekelweg 15, 2629 JB Delft
The Netherlands

in order to obtain the decay ratio and the oscillation frequency. The time range for which the impulse response is fitted depends on the behaviour of the impulse response. The longer the time range is in the results presented, the better the behaviour of the impulse response is with respect to the third order model. This indicates the accuracy of the decay ratio determined.

Results

Case 1

Table 1. Results of the decay ratio and the oscillation frequency for Case 1

Number	Time of fit (s)	Decay ratio	Osc. freq. (Hz)
1	1-4	0.57	0.47
2	1-5	0.46	0.48
3	1-8	0.60	0.51
4	1-6	0.78	0.51
5	1-6	0.36	0.51
6	1-6	0.53	0.48
7	1-10	0.66	0.55
8	1-4	0.57	0.53
9	1-5	0.50	0.41
10	1-5	0.32	0.45
11	1-5	0.29	0.47
12	0-16	0.66	0.47
13	1-6	0.51	0.42
14	1-16	0.71	0.49

Case 2

Table 2. Results of the decay ratio and the oscillation frequency for Case 2

Number	Time of fit (s)	Decay ratio	Osc. freq. (Hz)
Ll	1-6	0.23	0.45
S1l	1-4	0.34	0.45
S21	1-8	0.40	0.45
S31	1-4	0.27	0.45
S41	1-4	0.14	0.45
L2	1-12	0.54	0.54
S21	1-6	0.52	0.54
S22	1-8	0.56	0.54
S32	1-6	0.44	0.55
S42	1-4	0.49	0.50

Case 3

Table 3. Results of the decay ratio and the oscillation frequency for Case 3

Number	Time of fit (s)	Decay ratio	Osc. freq. (Hz)
1	1-4	0.30	0.45
2	1-4	0.39	0.40
3	0-4	0.20	0.46
4	1-4	0.36	0.48

Case 4

We have tried to extract the stability parameters of the out-of-phase mode from the LPRM signals by subtracting the relative variations in the signals of detectors nearly diagonal to each other. This is based on the assumption that the relative variation in the in-phase mode is equal for such positions. However, it seems as though the in-phase mode is dominating the results. More analyses are required.

Table 4. Results of the decay ratio and the oscillation frequency for Case 4

Number	Time of fit (s)	Decay ratio	Osc. freq. (Hz)
APRM	1-6	0.78	0.51
1-11	1-8	0.84	0.49
4-12	1-8	0.84	0.48
5-11	1-6	0.73	0.50
8-12	1-6	0.56	0.51
9-21	1-8	0.64	0.52
10-22	1-6	0.54	0.52
17-21	1-8	0.74	0.50
18-22	1-8	0.73	0.49

Case 5

Even though this is a transient, we have tried to treat it similarly to the other cases. For the first time series, this works well.

Table 5. Results of the decay ratio and the oscillation frequency for Case 5

Number	Time of fit (s)	Decay ratio	Osc. freq. (Hz)
1	1-16	0.85	0.53
2	1-3	0.80	0.52

Case 6

For Case 6, the same holds true as for Case 4. Again the in-phase oscillations seem to dominate the results since for the second time series the stability parameters of the APRM signal equals those obtained by subtracting relative variations in LPRMs almost diagonal to each other. For the first time series the results are inaccurate. More analyses are required to understand the behaviour.

Table 6. Results of the decay ratio and the oscillation frequency for Case 6

Number	Time of fit (s)	Decay ratio	Osc. freq. (Hz)
APRM-1	0-4	0.39	0.51
1-5	1-4	0.43	0.53
2-6	1-4	0.94	0.44
5-9	1-4	0.49	0.55
6-10	1-4	0.95	0.59
1-15	1-4	0.65	0.59
2-16	1-4	0.71	0.59
5-17	1-4	0.50	0.59
6-18	1-4	0.60	0.52
3-7	0-4	0.45	0.55
4-8	1-4	0.65	0.55
7-9	1-4	0.55	0.43
8-10	1-4	0.25	0.59
APRM-2	1-16	0.88	0.52
1-5	1-7	0.94	0.52
2-6	1-16	0.88	0.52
5-9	1-16	0.89	0.52
6-10	1-16	0.88	0.52
1-15	1-16	0.88	0.52
2-16	1-14	0.86	0.52
5-17	1-10	0.90	0.52
6-18	1-16	0.89	0.52
3-7	1-16	0.88	0.52
4-8	1-16	0.85	0.52
7-9	1-14	0.88	0.52
8-10	1-16	0.87	0.52

Annex 10

METHODOLOGIES AND RESULTS PRESENTED BY CSNNS*

The methodology used for the analysis of the time series for the experimental study of BWR oscillations at Forsmarks 1 and 2 nuclear power plant was the power spectrum estimation by the maximum entropy method. Although this is not the most proper method for the analysis of non-stationary signals, we are working in the analysis of these signals using a methodology for non-stationary signals based on the Short-Time Fourier Transform. The results using this methodology are not yet complete, but will be sent as soon as they are completed.

Maximum entropy method (MEM)

The maximum entropy method uses the transform of the complex frequency f plane to a new plane, called the Z transform plane or Z-plane, by the relation:

$$Z = exp(2 f_i \Delta) \tag{1}$$

where Δ is the sampling interval in the time domain. The Fast Fourier Transform (FFT) power spectrum estimate for any real sampled function $C_k = C(t_k)$ can be written, except for normalisation convention, as:

$$P(f) = \left| \sum_{k=-N/2}^{N/2-1} C_k Z^k \right|^2 \tag{2}$$

This is not the true power spectrum of the underlying function $C(t)$, but only an estimate, because the estimate is based on only a finite range of the function $C(t)$ which may have continued from $t = -\infty$ to $+\infty$, in the Z-plane of Eq. (2). The finite Laurent series offers, in general, only an approximation of a general analytic function of Z. In fact, a normal expression for representing the power spectra is:

$$P(f) = \left| \sum_{k=-\infty}^{+\infty} C_k Z^k \right|^2 \tag{3}$$

* Alejandro Nuñez-Carrera
Comision Nacional de Seguridad Nuclear y Salvaguardias
Dr. Barragan Num. 779
Col. Narvarte C.P. 03020
MEXICO D.F.
E-mail: cnsns1@servidor.unam.mx

This is an infinite Laurent series which depends on an infinite number of value C_k. Eq. (2) is just one kind of analytic approximation to the analytic function of Z represented by Eq. (3); in fact, that is implicit in the use of FFTs to estimate power spectra by periodogram methods. If we look at the approximation (3) more generally, we could do a rational function, one with a series of type (2) in both the numerator and denominator, after which we obtained:

$$P(f) \approx \frac{1}{\left|1+\sum b_k z^k\right|^2} = \frac{a_0}{\left|1+\sum_{k=1}^{M} a_k z^k\right|^2} \tag{4}$$

This equation brings in a new set of coefficients at which a_k can be determined from the b_k using the fact that lies on the unit circle. The b_k can be thought of as being determined by the condition that power series expansion of Eq. (4) agreea with the first M+1 terms of Eq. (3). The differences between the approximation (2) and (4), is the fact that Eq. (4) can have poles corresponding to the infinite power spectral density on the unit Z circle at real frequencies in the Nyquist interval $-f_c < f < f_c$. Such poles can provide an accurate representation for underlying power spectra which have sharp discrete lines or delta function. By contrast Eq. (2) can have only zeros, not poles, at real frequencies in the Nyquist interval, and must thus attempt to fit sharp spectral features with, essentially a polynomial. The approximation (4) goes under name of maximum entropy method (MEM) or auto-regressive model (AR).

Consider the auto-correlation at lag j of the sampled function C_k namely:

$$j = \left\langle C_j C_{i+j} \right\rangle \qquad j = \ldots\text{-3,-2,-1,0,1,2,3,}\ldots \tag{5}$$

The most natural estimate of (5) is:

$$C_j = C_{-j} \approx \frac{1}{N+1-j} \sum_{i=0}^{N-j} C_i C_{i+j} \qquad j = 0,1,2,\ldots,N \tag{6}$$

From $N+1$ data points, we can estimate the auto-correlation at $N+1$ different lag j.

According to the Wiener-Khinchin theorem, the Fourier transform of the auto-correlation is equal to the power spectrum. In the Z transform, the power transform is just a Laurent series in Z. The equation that is to be satisfied by the coefficients in Eq. (4) is thus:

$$\frac{a_0}{\left|1+\sum_{k=1}^{M} a_k z^k\right|^2} \approx \sum_{j=-M}^{M} j z^j \tag{7}$$

The approximately equal sign in Eq. (7) has a somewhat special interpretation. It means that the series expansion of the left-hand side is supposed to agree with the right-hand side term by term from Z^{-M} to Z^{M}. Outside this range of terms, the right-hand is zero, while the left-hand will still have non-zero terms. The number of coefficients M in the approximation on the left-hand side can be any integer up to N. The total number of auto-correlations available M is called the order or number of poles of the approximation.

The transfer function has complex poles, and the decay ratio for the system is defined as follows:

$$DR = \exp\left(\frac{-2\alpha}{w}\right) \tag{8}$$

where α is the real part of the pole and w is the imaginary part of the pole.

The decay ratio is related to the position of the least stable pole and is, therefore, a good measure of the stability of the system.

Results

Case 1

Table 1. Decay ratio and frequency results for Case 1

Data name	DR	DR uncertainty	Frequency	Frequency uncertainty
c1_aprm.1	0.600	0.024	0.458	0.002
c1_aprm.2	0.746	0.018	0.459	0.002
c1_aprm.3	0.731	0.025	0.476	0.008
c1_aprm.4	0.540	0.042	0.490	0.010
c1_aprm.5	0.463	0.057	0.494	0.009
c1_aprm.6	0.542	0.059	0.486	0.010
c1_aprm.7	0.700	0.020	0.521	0.011
c1_aprm.8	0.540	0.067	0.497	0.011
c1_aprm.9	0.719	0.017	0.402	0.002
c1_aprm.10	0.608	0.023	0.424	0.002
c1_aprm.11	0.516	0.026	0.424	0.002
c1_aprm.12	0.746	0.020	0.452	0.002
c1_aprm.13	0.466	0.025	0.408	0.001
c1_aprm.14	0.689	0.020	0.469	0.002

Case 2

Table 2. Decay ratio and frequency results for Case 2

Data name	DR	DR uncertainty	Frequency	Frequency uncertainty
c2_test.L1	0.488	0.057	0.442	0.005
c2_test.S11	0.239	0.057	0.444	0.010
c2_test.S21	0.478	0.055	0.448	0.009
c2_test.S31	0.430	0.030	0.441	0.009
c2_test.S41	0.476	0.034	0.428	0.012
c2_test.L2	0.622	0.033	0.516	0.006
c2_test.S12	0.602	0.032	0.520	0.010
c2_test.S22	0.688	0.036	0.516	0.010
c2_test.S32	0.452	0.050	0.516	0.011
c2_test.S42	0.553	0.041	0.509	0.014

Case 3

Table 3. Decay ratio and frequency results for Case 3

Data name	DR	DR uncert.	Freq. 1	Freq. 1 uncert.	Freq. 2	Freq. 2 uncert.	Dominant poles
c3_test.1	0.512	0.063	0.404	0.001			0.1180 ± 1.1073 0.1237 ± 1.6328 0.1331 ± 3.3487 0.1362 ± 1.3189
c3_test.2	0.447	0.063	0.312	0.001	0.408	0.001	0.1186 ± 0.9255 0.1485 ± 0.7142 0.1491 ± 0.1010 0.1491 ± 0.5361
c3_test.3	0.594	0.07	0.263	0.002	0.453	0.002	0.0863 ± 1.0401 0.1140 ± 0.0940 0.1188 ± 0.2615 0.1380 ± 0.5918
c3_test.4	0.794	0.038	0.260	0.002	0.472	0.002	0.0733 ± 1.9908 0.0741 ± 1.8454 0.0796 ± 1.6524 0.0816 ±1.4739

Case 4

Table 4. Decay ratio and frequency results for Case 4

Data name	DR	DR uncertainty	Frequency	Frequency uncertainty
c4_aprm	0.670	0.027	0.512	0.005
c4_lprm.1	0.861	0.021	0.503	0.014
c4_lprm.2	0.920	0.020	0.497	0.021
c4_lprm.3	0.882	0.011	0.494	0.020
c4_lprm.4	0.804	0.022	0.493	0.019
c4_lprm.5	0.826	0.018	0.512	0.016
c4_lprm.6	0.889	0.019	0.512	0.020
c4_lprm.7	0.830	0.020	0.512	0.016
c4_lprm.8	0.772	0.021	0.514	0.013
c4_lprm.9	0.777	0.025	0.520	0.011
c4_lprm.10	0.738	0.018	0.530	0.009
c4_lprm.11	0.793	0.022	0.532	0.017
c4_lprm.12	0.791	0.022	0.542	0.018
c4_lprm.13	0.735	0.031	0.518	0.015
c4_lprm.14	0.768	0.026	0.520	0.019
c4_lprm.15	0.777	0.026	0.518	0.014
c4_lprm.16	0.751	0.016	0.520	0.002

Table 4. Decay ratio and frequency results for Case 4 (*cont.*)

Data name	DR	DR uncertainty	Frequency	Frequency uncertainty
c4_lprm.17	0.840	0.020	0.506	0.018
c4_lprm.18	0.858	0.018	0.505	0.019
c4_lprm.19	0.771	0.031	0.507	0.001
c4_lprm.20	0.780	0.018	0.512	0.016
c4_lprm.21	0.746	0.030	0.533	0.020
c4_lprm.22	0.735	0.020	0.548	0.020

Case 5

Table 5. Decay ratio and frequency results for Case 5

Data name	DR	DR uncert.	Freq.	Freq. uncert.	Dominant poles
c5_aprm.1	0.793	0.017	0.535	0.005	0.1546 ± 3.2169 0.2163 ± 2.0738 0.2229 ± 1.5866 0.2231 ± 0.6531
c5_aprm.2	0.871	0.044	0.505	0.010	0.0418 ± 1.9059 0.0793 ± 1.5384 0.0839 ± 3.9270 0.0932 ± 3.4091

Case 6

Table 6. Decay ratio and frequency results for Case 6

Data name	DR	DR uncertainty	Frequency	Frequency uncertainty
c6_aprm.1	0.536	0.067	0.497	0.034
c6_lprm.11	0.540	0.042	0.552	0.010
c6_lprm.21	0.359	0.029	0.516	0.004
c6_lprm.31	0.592	0.031	0.523	0.006
c6_lprm.41	0.391	0.030	0.476	0.002
c6_lprm.51	0.633	0.034	0.526	0.010
c6_lprm.61	0.679	0.028	0.519	0.006
c6_lprm.71	0.666	0.035	0.513	0.007
c6_lprm.81	0.648	0.027	0.510	0.001
c6_lprm.91	0.424	0.050	0.520	0.010
c6_lprm.101	0.430	0.049	0.476	0.008
c6_lprm.111	0.505	0.060	0.529	0.012
c6_lprm.121	0.371	0.042	0.488	0.006

Table 6. Decay ratio and frequency results for Case 6 (*cont.*)

Data name	DR	DR uncertainty	Frequency	Frequency uncertainty
c6_lprm.131	0.278	0.064	0.527	0.011
c6_lprm.141	0.441	0.054	0.505	0.005
c6_lprm.151	0.275	0.065	0.530	0.009
c6_lprm.161	0.547	0.029	0.525	0.007
c6_lprm.171	0.245	0.059	0.523	0.010
c6_lprm.181	0.380	0.031	0.478	0.007
c6_aprm.2	0.821	0.020	0.520	0.010
c6_lprm.12	0.627	0.033	0.564	0.010
c6_lprm.22	0.355	0.028	0.519	0.005
c6_lprm.32	0.802	0.026	0.525	0.006
c6_lprm.42	0.834	0.019	0.516	0.002
c6_lprm.52	0.709	0.038	0.525	0.010
c6_lprm.62	0.835	0.021	0.522	0.006
c6_lprm.72	0.765	0.026	0.523	0.007
c6_lprm.82	0.859	0.024	0.520	0.001
c6_lprm.92	0.608	0.044	0.539	0.010
c6_lprm.102	0.542	0.029	0.494	0.009
c6_lprm.112	0.706	0.038	0.535	0.012
c6_lprm.122	0.909	0.022	0.516	0.006
c6_lprm.132	0.782	0.022	0.530	0.010
c6_lprm.142	0.761	0.018	0.523	0.005
c6_lprm.152	0.797	0.026	0.525	0.010
c6_lprm.162	0.843	0.020	0.525	0.007
c6_lprm.172	0.712	0.029	0.542	0.032
c6_lprm.182	0.614	0.045	0.504	0.008

ALSO AVAILABLE

NEA Publications of General Interest

1999 Annual Report (2000) *Free: available on Web.*

NEA News
ISSN 1605-9581 Yearly subscription: FF 240 US$ 45 DM 75 £ 26 ¥ 4 800

Geologic Disposal of Radioactive Waste in Perspective (2000)
ISBN 92-64-18425-2 Price: FF 130 US$ 20 DM 39 £ 12 ¥ 2 050

Radiation in Perspective – Applications, Risks and Protection (1997)
ISBN 92-64-15483-3 Price: FF 135 US$ 27 DM 40 £ 17 ¥ 2 850

Radioactive Waste Management in Perspective (1996)
ISBN 92-64-14692-X Price: FF 310 US$ 63 DM 89 £ 44

Nuclear Science

Shielding Aspects of Accelerators, Targets and Irradiation Facilities – SATIF 5 (2001) *In preparation*

Pyrochemical Separations (2001)
ISBN 92-64-18443-0 Price: FF 500 US$ 66 DM 149 £ 46 ¥ 7 230

Evaluation of Speciation Technology (2001)
ISBN 92-64-18667-0 Price: FF 525 US$ 70 DM 156 £ 49 ¥ 7 600

Core Monitoring for Commercial Reactors: Improvements in Systems and Methods (2000)
ISBN 92-64-17659-4 Price: FF 460 US$ 71 DM 137 £ 44 ¥ 7 450

Shielding Aspects of Accelerators, Targets and Irradiation Facilities (SATIF-4)(1999)
ISBN 92-64-17044-8 Price: FF 500 US$ 88 DM 149 £ 53 ¥ 10 300

3-D Radiation Transport Benchmarks for Simple Geometries with Void Regions
(2000) *Free on request.*

Benchmark Calculations of Power Distribution Within Fuel Assemblies
Phase II: Comparison of Data Reduction and Power Reconstruction Methods in Production Codes
(2000) *Free on request.*

Benchmark on the VENUS-2 MOX Core Measurements (2000) *Free on request.*

Calculations of Different Transmutation Concepts: An International Benchmark Exercise
(2000) *Free on request.*

Prediction of Neutron Embrittlement in the Reactor Pressure Vessel: VENUS-1 and VENUS-3 Benchmarks
(2000) *Free on request.*

Pressurised Water Reactor Main Steam Line Break (MSLB) Benchmark
(2000) *Free on request.*

International Evaluation Co-operation *(Free on request)*

Volume 1: *Comparison of Evaluated Data for Chromium-58, Iron-56 and Nickel-58* (1996)
Volume 2: *Generation of Covariance Files for Iron-56 and Natural Iron* (1996)
Volume 3: *Actinide Data in the Thermal Energy Range* (1996)
Volume 4: *^{238}U Capture and Inelastic Cross-Sections* (1999)
Volume 5: *Plutonium-239 Fission Cross-Section between 1 and 100 keV* (1996)
Volume 8: *Present Status of Minor Actinide Data* (1999)
Volume 12: *Nuclear Model to 200 MeV for High-Energy Data Evaluations* (1998)
Volume 13: *Intermediate Energy Data* (1998)
Volume 14: *Processing and Validation of Intermediate Energy Evaluated Data Files* (2000)
Volume 15: *Cross-Section Fluctuations and Shelf-Shielding Effects in the Unresolved Resonance Region* (1996)
Volume16: *Effects of Shape Differences in the Level Densities of Three Formalisms on Calculated Cross-Sections* (1998)
Volume 17: *Status of Pseudo-Fission Product Cross-Sections for Fast Reactors* (1998)
Volume 18: *Epithermal Capture Cross-Section of ^{235}U* (1999)

Order form on reverse side.

ORDER FORM

OECD Nuclear Energy Agency, 12 boulevard des Iles, F-92130 Issy-les-Moulineaux, France
Tel. 33 (0)1 45 24 10 15, Fax 33 (0)1 45 24 11 10, E-mail: nea@nea.fr**, Internet: www.nea.fr**

Qty	Title	ISBN	Price	Amount
			Total	

❑ Payment enclosed (cheque or money order payable to OECD Publications).

Charge my credit card ❑ VISA ❑ Mastercard ❑ Eurocard ❑ American Express

(N.B.: You will be charged in French francs).

Card No.	Expiration date	Signature
Name		
Address	Country	
Telephone	Fax	
E-mail		

OECD PUBLICATIONS, 2 rue André-Pascal, 75775 PARIS CEDEX 16
Printed in France.